

IMPULSE ELECTRICAL BREAKDOWN OF HIGH-PURITY WATER

by

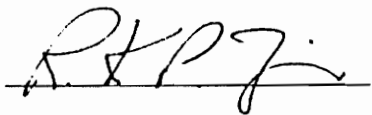
Victor H. Gehman, Jr.

Dissertation submitted to the Faculty of the
Virginia Polytechnic Institute and State University
in partial fulfillment of the requirements for the degree of
DOCTOR OF PHILOSOPHY

IN

PHYSICS

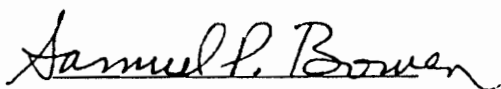
APPROVED



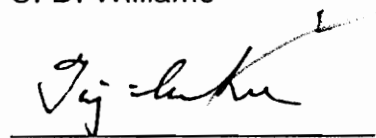
R. K. P. Zia, Chairman



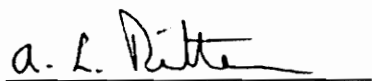
C. D. Williams



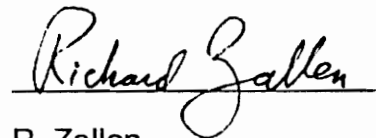
S. P. Bowen



T. K. Lee



A. L. Ritter



R. Zallen

May, 1995

Blacksburg, Virginia

Key Words: Electrical Breakdown, High-Purity Water, Dielectric

c.2

LD

5655

V856

1995

G446

c.2

IMPULSE ELECTRICAL BREAKDOWN OF HIGH-PURITY WATER

by

Victor H. Gehman, Jr.

R. K. P. Zia, Chairman

Physics

(ABSTRACT)

Experiments have been conducted on the electrical breakdown of high-purity water and water mixtures. The electrical regime of interest has been carefully defined and documented to consist of electrical impulses with approximately microsecond rise time and fall time greater than 65 microseconds, on approximately 81-square-centimeter-area planar electrodes with a dielectric gap of approximately one centimeter. The results of over 25,000 shots by a Marx generator have been distilled into database form in an Excel spreadsheet and analysis performed to try to find patterns or indirect evidence into the nature of the breakdown-initiation process.

An extensive review of all the experiments, which had been conducted over eight years by the Naval Surface Warfare Center and which had been designed to find the largest water-breakdown fields, was conducted with the intention of delineating the physical factors that led to breakdown. A variety of theoretical models of breakdown initiation were compared to the data, until it became clear that many of the breakdowns were dominated by impurities of various sorts. An extensive study of old and new experiments led to a more detailed understanding of the phenomenology of impurity-dominated water breakdown (such as the process of "conditioning" the electrodes and hysteresis) and the proposal of a number of new experiments to further characterize the

intrinsic role of electrode materials on determining high-electric-field dielectric breakdown in water.

Acknowledgments

My loving wife, Sharon Todd Gehman, and I met in 1973, became engaged in 1974, and married in 1976. For all that time, she has known of my personal dream to earn a Ph.D. in physics; she has constantly offered her support, encouragement, and prayers. Love like that has no name; words are an insufficient vehicle to offer thanks, but they're all I have. Thank You.

The first of our five children started to arrive in 1977. They have never known a father who wasn't spending much of his spare time pursuing an academic degree. They have been supporting and understanding.

My parents gave me love and a determination to excel to the best of my abilities. My brother Brian has always been the best.

I have had the great fortune to have been surrounded by many good people through out my life: starting with relatives, neighbors and friends in Lancaster, Pennsylvania, then Blacksburg, Virginia, and now Dahlgren and King George, Virginia. Again, thanks to my wife because I married into one of the noblest (and kindest) extended families - the Todd's. If I start naming people more specifically, I'm sure to leave someone out, and I don't want to hurt anybody's feelings. So, just let me say that I'm grateful to all of you.

My choices for professors to lead this research committee could not have been better. Sam Bowen and Royce Zia became personal friends and confidants as well as professional colleagues. They have put up with an unusually long process, because most of my work was carried out part time, but never complained. We faced the challenges of this research together, and I am a better scientist as a result.

While at Virginia Tech, other professors have assisted me including the other members of my committee: C. D. Williams, T. K. Lee, R. Zallen, and A. L. Ritter. Thanks also to all the graduate students who helped the rusty old man pass his prelims, especially Charles Potter, K. C. Ho and Peter Lo. Chris Pirie Thomas was always a source of help and inspiration. Judy Faw, Sherri Turner and the other department secretaries and staff were always kind and helpful.

Kenneth W. Chilton (Kenny) is the technician at the Naval Surface Warfare Center, Dahlgren Division (NSWCDD) who worked side-by-side with me throughout this process. The research could not have been accomplished without him. The early experiments were also assisted by L. W. (Sonny) Hardesty, who gave much valuable assistance. Kenny and Sonny taught me the advanced, applied course in working with high voltage (up to 500 kV), getting valid, repeatable results, and surviving. Drs. David B. Fenneman and Ronald J. Gripshover started the water experiments at NSWCDD, designed the initial apparatus, and have given generously of their time and counsel. Dr. Thomas L. Berger has been a source of advice, skill, and encouragement, as have other members of the Pulsed Power Systems and Technology Group. Stuart L. Moran has been the best Branch Head I could have asked for; he has constantly supported me. Eldridge Rowe and Nevin Rupert are two colleagues who became friends - they offered their own insights to this research and were always willing to be a sounding board for mine. Finally, I'd like to thank the management at NSWCDD for supporting me over the years, including a year of full-time study at Virginia Tech.

TABLE OF CONTENTS

Chapter One: Introduction	1
A. Overview of Pulsed Power.....	1
B. Water as a Dielectric	5
Chapter Two: Literature Review	8
A. Early Short-Stress-Time Experiments.....	8
B. Long-Stress-Time Experiments	11
C. Area Effect.....	25
Chapter Three: Experimental Apparatus	26
A. Liquid Purification System	26
1. Ionic Purity	27
a. Plastic Piping and Surfaces.....	27
(1) Piping	27
(2) Pump	28
(3) Test Cell	28
b. Deionization Beads.....	29
(1) Description	29
(2) Providers	29
c. Deaeration Column.....	30
(1) Vacuum & Partial Pressure of Water.....	30
(2) Definition of % Deaeration.....	31
(3) Design of Column.....	31
(4) Cold Trap.....	32
d. Chiller	33
(1) Rationale	33

(2) Design of Heat Exchanger.....	34
(3) Operation.....	34
(4) Problems	35
2. Non-ionic Purity.....	36
a. Rationale	36
b. Activated Charcoal	36
c. Microfilters	37
d. U. V. Oxidation	37
B. Electrical-Impulse Generator	40
1. Design.....	40
a. Marx Generator.....	40
b. Charging Resistor.....	41
c. Diode	41
2. Operation	43
3. Problems	43
C. Electrical Diagnostics	44
1. Dividing-Resistor Probe	44
2. Capacitive-Divider Probe	45
3. Shielded Rooms and Absorber	46
4. Shielded Data Cables	46
5. Oscilloscopes.....	47
6. Tau Meter	47
Chapter Four: Filters, Contaminants, Conditioning, and Dielectric Breakdown	48
A. Introduction.....	48
B. Analysis of Data From the Industrial-Filter Experiments.....	49

C. Analysis of Data From the Modern-Filter Experiments	55
D. Experimental Procedures to Condition a Gap for Maximum	
Electrical-Breakdown Strength	57
1. Standard Conditioning.....	57
2. Other Conditioning Suggestions	59
3. Experimental Results	61
Chapter Five: Conditioning and Dielectric Breakdown	75
A. Experimental Basis For a Conditioning Theory of Dielectric Breakdown	
in Pure Water	75
1. Early Short-Time-Constant Experiments	75
2. Ethylene Glycol & Water Experiments	77
3. Long-Time-Constant Water Experiments	78
B. Other Salient Experimental Features That Theory Must Explain.....	79
1. Spurious Breakdowns	79
2. Water Flow and Total Liquid Volume	80
3. Time Scale of Conditioning Shots	82
4. Thermal Cycling Effects on Breakdown.....	82
C. Statistical Tests of Average Breakdown Fields	83
D. Can Bubbles Be a Source of "Conditioning"?	107
1. Historical Interest	107
2. Electric-Field Enhancement Causes Bubbles	108
3. Time-Scale and Energy Considerations.....	108
E. Can Aggregated Dielectric Inclusions Explain "Conditioning" ?.....	110
1. Flow Clues to Location of Critical Inclusions.....	110
2. Are Low ϵ Inclusions Attracted to the Electrode Surface?.....	111

3. Van der Waal Forces and Binding Energy for Inclusions.....	112
4. Distribution of Inclusion Sizes - Growth Dynamics.....	113
5. Conditioning Breakup of Inclusions.....	116
Chapter Six: Conclusions	139
Appendix A: Water Breakdown Database	150
Vita.....	181

LIST OF FIGURES

1.1	Sketch of the pulsed-power concept.....	3
1.2	Pulsed-power circuit.....	4
3.1	The sketch of the older, industrial-grade water-treatment apparatus for the electrical-impulse, water-breakdown experiment.	38
3.2	The sketch of the more modern water-treatment apparatus for the electrical-impulse, water-breakdown experiment.	39
3.3	An electrical sketch of the electrical-impulse, water-breakdown experiment.	42
4.1	Plot of the mean breakdown field for copper demonstrating the efficacy of industrial-grade filters.	50
4.2	Breakdown data for copper electrodes with industrial-grade particulate filters and a Barnstead organic filter.	51
4.3	Breakdown data for tungsten electrodes with industrial-grade particulate filters and a Barnstead organic filter.	53
4.4	Breakdown data for stainless-steel electrodes with industrial-grade particulate filters and a Barnstead organic filter.	54
4.5	Breakdown data for tungsten electrodes with modern Barnstead particulate and organic filters.....	56
4.6	Breakdown data for stainless-steel electrodes with modern Barnstead particulate and organic filters.....	58
4.7	Test run of 9/3/93.....	62
4.8	Test run of 9/9/93.....	64
4.9	Test run of 9/10/93.....	66
4.10	Test run of 9/23/93.....	67

4.11	Test run of 9/24/93.....	69
4.12	Test run of 10/5/93.....	71
4.13	Test run of 10/6/93.....	73
5.1	Plot of the mean breakdown field plus or minus the 95% confidence interval for stainless-steel electrodes with no filters.	90
5.2	Plot of the mean breakdown field plus or minus the 95% confidence interval for aluminum electrodes with no filters.	92
5.3	Plot of the mean breakdown field plus or minus the 95% confidence interval for 304 stainless-steel, 2024 aluminum electrodes with no filters.	94
5.4	Plot of the mean breakdown field plus or minus the 95% confidence interval for pure gold, pure lead, and mixed electrodes with no filters...	96
5.5	Plot of the mean breakdown field plus or minus the 95% confidence interval for stainless-steel electrodes with filters.	98
5.6	Plot of the mean breakdown field plus or minus the 95% confidence interval for aluminum 5083-alloy electrodes with filters.	100
5.7	Plot of the mean breakdown field plus or minus the 95% confidence interval for a series of experiments on copper demonstrating the efficacy of various filter combinations.	102
5.8	Plot of the mean breakdown field plus or minus the 95% confidence interval for tungsten and other copper electrodes with filters.	104
5.9	Plot of the mean breakdown field plus or minus the 95% confidence interval for graphite, nickel, and silver electrodes with filters.....	106
5.10	Schematic of the general idea of dustball size, distribution and conditioning effects.	118

5.11	The plot of approximate energy (arbitrary units) versus $1/E$ for all the experiments in the database.	120
5.12	Same plot for copper electrodes with filters.	121
5.13	Same plot with filters for all electrode materials.....	122
5.14	Same plot for filters and graphite electrodes.	123
5.15	Same plot for all unfiltered breakdown experiments.	124
5.16	Same plot for filters and stainless-steel electrodes.	125
5.17	Same plot for no filters and stainless-steel electrodes.	126
5.18	Same plot for tungsten electrodes.	127
5.19	Log-log plot of the approximate energy vs. $1/E$	129
5.20	Same plot, but for filters with stainless-steel electrodes.	130
5.21	Plot of "true" energy versus $1/E$ for all shots in the water database. ...	133
5.22	Plot of the log of "true" energy versus $1/E$ for tungsten electrodes.....	134
5.23	Schematic representation of a more developed idea about the mechanism of conditioning.....	136
6.1	Conceptual diagram of the hysteresis region for the breakdown probability as a function of electric field	146

LIST OF TABLES

5.1	Stainless-steel electrodes, no filters.	89
5.2	Aluminum electrodes, no filters.	91
5.3	Mixed 304 stainless-steel, 2024 aluminum electrode sets, with no filters.	93
5.4	Pure gold, pure lead and mixed electrodes, no filters.	95
5.5	Stainless-steel electrodes, with filters.	97
5.6	Aluminum 5083-alloy, with filters.	99
5.7	A series of experiments on copper demonstrating the efficacy of various filters.	101
5.8	Other miscellaneous copper data and tungsten data, with filters.	103
5.9	Other electrode sets.	105
6.1	Electric-field breakdown results by material for unfiltered water.	141
6.2	Comparison of electric-field breakdown results for filtered versus unfiltered water.	142
A.1	Database of Experiments on Electrical Breakdown in Water.	150

I. CHAPTER ONE: INTRODUCTION

A. OVERVIEW OF PULSED POWER

The central idea to all of pulsed power is to take energy from a source, store it for a relatively long time, and switch it into a load (i.e., application) within a much shorter time than the storage time. In this way power amplification is achieved via time compression. There are many interesting future applications that require very high peak power, but moderate-to-high average power, and thus are prime candidates to use pulsed-power technology. Some of the more interesting are : inertial-confinement fusion, pulsed cleanup of biofouling, pulsed plasma reactors to clean up hazardous waste, electromagnetic propulsion, pulsed radar, charged-particle beams, free-electron lasers, high-power microwaves, nuclear-event simulators, active-RF jamming, and acoustical jamming.

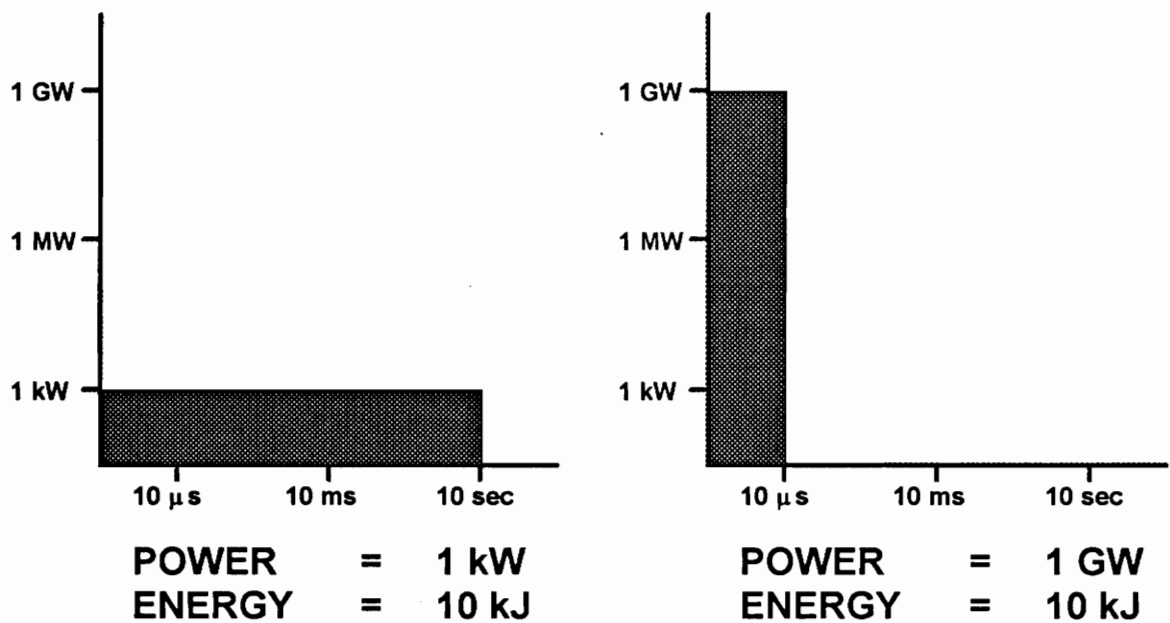
In Figure 1.1, we present a tutorial example whereby a 1-kW power source delivers 10 kJ to an energy store over ten seconds. When the energy is held without loss and then switched perfectly into a load within ten microseconds, a power amplification of 10^6 is achieved and the 1-kW source is capable of producing a 1-GW pulse. Of course, energy is neither delivered nor stored losslessly and switches do not work perfectly. Research on each aspect of the pulsed-power circuit is active.

In Figure 1.2, we present a simplified pulsed-power circuit in the form of a block diagram. The prime-power block is the constant power source. It charges an energy store over a relatively long period of time and then the energy is

switched out of the energy store at a specific time. Often the energy goes through a pulse-conditioning stage to achieve some desired characteristic, for example to produce a flat-top voltage pulse with fast rise and fall times. Typically, this is achieved with a pulse forming line (PFL) in a real device. Finally, the energy is delivered to the load and the duty cycle of the device may start again.

An important fact to realize is that the energy store and/or the pulse conditioner are usually the largest and heaviest components for high-peak-power machines, and therefore the costliest. Reducing the size and weight of these components is one of the more important tasks required to make pulsed-power machines practical for future applications.

INTRODUCTION TO PULSED POWER



- * **SAME ENERGY**
- * **POWER AMPLIFICATION OF 10^6 ACHIEVED BY TIME COMPRESSION**

Figure 1.1: Sketch of pulsed-power concept.

PULSED POWER TECHNOLOGY BLOCK DIAGRAM

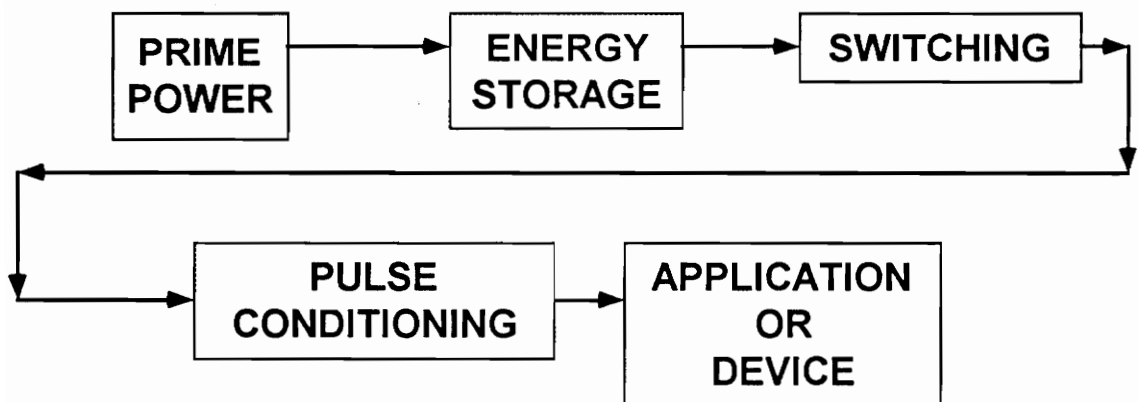


Figure 1.2: Pulsed-power circuit.

B. WATER AS A DIELECTRIC

Water is a useful dielectric for two parts of the block diagram in Figure 1.2; namely, energy storage and pulse conditioning. In fact, these two functions are often combined into one stage of real pulsed-power devices. Water is useful because it has a high dielectric constant (78 at room temperature) and excellent frequency response. This means that the effective dielectric constant of water does not decrease appreciably for frequencies up to 1 GHz. This is important because more useful energy recovery times for water are in the 10- to 100-ns regime rather than 10 μ s as depicted in Figure 1.1. A high dielectric constant, ϵ , is important because the energy density is proportional to ϵ . We wish to keep energy density as high as possible, because that will mean the volume of water needed to store the energy will be minimized. Also, the higher the dielectric constant, the shorter the length of the PFL (length $\propto 1/\sqrt{\epsilon}$). Again, the shorter the PFL, the less mass, volume and cost.

Another valuable characteristic for water as a dielectric liquid is electrical breakdown strength. Energy density varies as the square of the breakdown strength, which considerably affects size, weight, and cost. Within the pulsed-power community, there is a hope that the breakdown strength of water can be significantly improved over the present value. Because of the great impact on energy density, increasing electrical breakdown strength is of the highest priority for water researchers in the pulsed-power community and it is the objective of our thesis.

Water can be purified using commercially available deionizers down to the part-per-billion regime for ionic impurities. Since ordinary water resistivity is controlled by impurity ions, this means that water resistivity can be increased by orders of magnitude by deionization (e.g., 10 k Ω -cm distilled water improved to 18.3 M Ω -cm) If good deaeration is achieved, the intrinsic time constant, τ (which is equal to the product of dielectric constant times resistivity) can be as large as 650 microseconds at temperatures just above freezing. Since a large τ leads to slow voltage decay and less energy loss, it is important, in order to achieve minimal loss, for a PFL to be designed with as large a τ as possible.

Finally, there are other reasons why water is an excellent dielectric liquid. Water is self repairing; after a breakdown it recovers its electrical breakdown strength. Water is certainly non-flammable and non-toxic. Water is cheap, has an acceptable viscosity, and is relatively easy to purify using commercial techniques developed by the semiconductor-manufacturing industry.

The superiority of water is well accepted in the pulse-power community. In fact, almost every large pulsed-power machine, that we know, uses water as a dielectric liquid. Therefore, the focus of this thesis, increasing the breakdown strength of high-purity water, is important to pulsed power and the future applications listed above.

In addition to our empirical investigation of factors that control the breakdown strength of water, we have examined some models for the process. The experimental results which we consider most intriguing are the beneficial effects of filters on breakdown strength and the time dependence of the conditioning process (explained later in Chapter Four). This data is best explained by a population of non-ionic contaminants in a thin stagnant layer of

water next to the electrode surface. In our model, the presence of non-ionic contaminants causes breakdown to occur at a lower value of the electric field than for absolutely pure water. Filters remove contaminants from the bulk water quickly, but only slowly from the stagnant layer. High-voltage shots to the water capacitor breakup the impurities into smaller pieces. We hypothesize that smaller impurities require larger electric field to initiate a breakdown, which means breaking up impurities increases the voltage holdoff of the water capacitor. We further hypothesize that this process is the key to conditioning. The effect of filters on contaminants is that they improve breakdown strength, but only if they are used for some time and constantly. Shutting down overnight allows new contaminants to leach into the water from pipes and other surfaces. As a result, the benefits of conditioning are lost overnight, and a new cycle of filtered flow and conditioning shots are needed before breakdown strength is restored to a high value.

II. CHAPTER TWO - LITERATURE REVIEW

A. EARLY SHORT-STRESS-TIME EXPERIMENTS

Experiments on the breakdown strength of water started at the Naval Surface Warfare Center (NSWC) in the latter part of the 1970's and formed the basis for our later work. The motivation for the Navy to investigate high-purity water as a dielectric liquid arose out of the desire to reduce the volume and weight required for pulsed-power systems that could power any one of several applications (e.g., particle-beam weapons, free-electron lasers, inertial-confinement fusion devices, etc.). The heaviest and largest components of a typical high-peak-power machine was its energy store or its pulsed forming line (PFL). These devices often used water as a dielectric, although energy density must be kept low to avoid breakdown across the water gap. Since energy density increases as the square of the electric field in the water, increasing the breakdown strength was chosen as a logical avenue to pursue increased energy density.

This early work at NSWC built upon experiments carried out by J. C. Martin¹, Ian Smith^{2 3}, and P. D. A. Champney⁴ at the Atomic Weapons Research Establishment. Their aim was, among other things, to develop better flash x-ray

¹J.C. Martin, "Comparison of Breakdown Voltages for Various Liquids Under One Set of Conditions", Note 1, *Pulsed Electrical Power Dielectric Strength Notes*, PEP 5-1, Vol. 1, Notes 1-23, Air Force Weapons Lab TR 73-167, April 1973.

²Ian Smith, "Impulse Breakdown of Deionized Water", Note 4, *Pulsed Electrical Power Dielectric Strength Notes*, PEP 5-1, Vol. 1, Notes 1-23, Air Force Weapons Lab TR 73-167, April 1973.

³Ian Smith, "Further Breakdown Data Concerning Water", Note 13, *Pulsed Electrical Power Dielectric Strength Notes*, PEP 5-1, Vol. 1, Notes 1-23, Air Force Weapons Lab TR 73-167, April 1973.

⁴P.D.A. Champney, "Impulse Breakdown of Deionized Water with Asymmetric Fields", Note 7, *Pulsed Electrical Power Dielectric Strength Notes*, PEP 5-1, Vol. 1, Notes 1-23, Air Force Weapons Lab TR 73-167, April 1973.

devices. They are the first, as far as we are aware, to measure intrinsic high-voltage properties of water and other materials using modern devices. Other researchers from that period include T. H. Martin⁵, who envisioned pulsed power for inertial confinement fusion, A. R. Miller⁶ who helped create several large devices, and J. P. VanDevender⁷.

During this time a figure-of-merit for the breakdown performance of water came into use. At NSWC, it was given the designation M in honor of

J. C. Martin:

$$M = E_{\max} * t_{\text{eff}}^{1/3} * A^{1/10},$$

where M was Martins number (higher is better), E_{\max} was the maximum electric field in the water, t_{eff} was the effective time duration of the electric stress and was defined as the time interval for which the field exceeded 63% E_{\max} , and finally A was the area of the electrode which experienced 90% or more of the field. For electric field in MV/cm, time in μs , and A in cm^2 , M was a measure for an electrode system that ranged between 0.3 and 0.6, but mostly remained nearer the 0.3 mark.

Subsequently, D. B. Fenneman and R. J. Gripshover repeated these experiments while meticulously purifying, deionizing, and deaerating the water. Careful documentation of all aspects of their apparatus considerably facilitated our work. This had not always been done in previous work. Their result^{8 9} was

⁵T. H. Martin, "Pulsed Power For Fusion", *Proceedings International Pulsed Power Conference*, Lubbock, Texas, Nov. 1976, IEEE Catalog No. 76 CH1147-8 Reg. 5.

⁶A.R. Miller, "Low Impedance Capacitors Using Pressurized Water as a Dielectric", *Proceedings of the 5th Symposium on Engineering Problems of Fusion Research*, p. 471, IEEE, New York, 1974.

⁷J. P. VanDevender, "Short Pulse Electrical Breakdown Strength of H_2O ", *Proceedings International Pulsed Power Conference*, Lubbock, Texas, Nov. 1976, IEEE Catalog No. 76CH 1147-8 Reg. 5.

⁸D. B. Fenneman and R. J. Gripshover, "Experiments on Electrical Breakdown in Water in the Microsecond Regime", *IEEE Trans. Plasma Sci.*, vol. PS-8, no. 3, pp. 209-213, Sept. 1980.

impressive, namely, an approximately two-fold increase, consistently, in the Martin's number to consistent performance of 0.58 for steel and brass, 0.55 for copper and 0.41 for aluminum.

The fact that electrode materials had an effect on breakdown performance was considered interesting. It reinforced theories that the electrode-water interface was the key to breakdown behavior. Our first effort in water breakdown was to use ion bombardment of the electrode surface to attempt to affect breakdown¹⁰. Our hypothesis was the ion bombardment might eliminate micro-whiskers or other small imperfections on the electrode surface that might produce field enhancement. Unfortunately the process didn't improve the Martin's number for either copper or stainless steel electrodes. Possible reasons for the result are: (1) small surface inhomogeneities causing electric-field enhancement are not part of the breakdown mechanism, (2) ion flux was too low or (3) the energy of the ions was too low .

However, as a side issue, we also tested the effect of polished stainless-steel surface versus the accepted surface treatment of bead blasting (i.e., glass peening). While the breakdown strength was slightly worse for polished results, we did notice two other interesting phenomena. First, upon post-test examination, bead-blasted stainless-steel surfaces have breakdown craters arranged in a random fashion, but breakdown craters of polished stainless steel are grouped together in a few clusters. Despite this dramatic difference, the breakdown strength was almost the same. Second, post-test microscopic

⁹D. B. Fenneman and R. J. Gripshover, "Experiments on Electrical Breakdown in Water in the Microsecond Regime", *Proc. 2nd IEEE Int. Pulsed Power Conf.*, pp. 122-126, June 12-14, 1979.

¹⁰V. H. Gehman, Jr. and D. B. Fenneman, "Experiments on Water-Capacitor Electrode Conditioning by Ion Bombardment", *1980 Fourteenth Pulsed Power Modulator Symposium*, Orlando, Florida, IEEE 80CH 1573-5, pp. 154-160, June 3-5, 1980.

examination of the polished stainless steel revealed large numbers of twins near the breakdown craters in the grains of the metal. This indicates considerable stress in the region of the electrode near the breakdown crater.

This was some of the last short-stress-time work. Focus shifted to long stress time for two reasons: (1) it was more relevant to a new class of machines proposed for pulsed-power applications, and (2) electric breakdown strength was found to be stress-time independent for time longer than about 65 μ s.

B. LONG-STRESS-TIME EXPERIMENTS

Fenneman and Gripshover also performed experiments with longer charging times. One motivation is that a long charging time could allow a new type of pulsed-power machine to be developed, specifically where a new kind of prime-power source (e.g., compulsator, brushless rotary flux compressor-BRFC, etc.) charges the PFL directly. This would eliminate several stages of previous machines. The key connection was the faster prime power interacting directly with the PFL. If charge times as short as 100 μ s could be achieved, then pure water could be charged and then discharged in the standard way over a time period of 10-100 ns. This would result in power amplification on the order of 1,000 to 10,000 times. If the new prime-power sources couldn't achieve as short a time as 100 μ s, then more conservative charging times of 1 to 100 ms (which would result in power amplification on the order of 100,000 times) would require a different dielectric than pure water, which is limited to an ultimate intrinsic time constant of about 650 μ s. However, ethylene glycol and water mixtures can

accommodate these longer charging times, as NSWC researchers demonstrated in a series of ground-breaking papers^{11 12 13 14}.

Further, the effect of charge injection on electrical breakdown strength was also investigated. NSWC researchers had discovered charge injection in cooled glycol-water mixtures^{13 14}, and the result had been confirmed using Kerr electro-optics at the Massachusetts Institute of Technology (MIT) in collaboration with Markus Zahn, et al.^{15 16}. Zahn discovered the different materials injected either positive or negative excess charge or sometimes both. Positive charges are injected if the electrodes are both made of stainless steel or copper. However, a copper electrode will inject negative charges when combined with a stainless-steel electrode. Aluminum injects negative charge, but brass is a bipolar injector. The injected ions have mobilities that are close to the literature values for the hydronium and hydroxyl ions and that identification became the working assumption. Perhaps the most significant fact about charge injection was that the electric field was lower at a charge-injecting electrode and higher at a non-injecting electrode.

Because charge injection would limit the charging time of a PFL and might affect the breakdown strength by altering the electric field at the electrode

¹¹D. B. Fenneman and R. J. Gripshover, "The Electrical Performance of Water Under Long Duration Stress", *Proc. 1980 Fourteenth Pulsed Power Modulator Symposium*, Orlando, Florida, IEEE 80CH 1573-5, pp. 150-153, June 3-5, 1980

¹²D. B. Fenneman, "Water Capacitors for Pulsed Power Applications", *Proc. Symp. on High-Energy-Density Capacitors and Dielectric Materials*, Washington, D. C., National Academy Press, pp. 156-165, 1981.

¹³D. B. Fenneman and R. J. Gripshover, "High Power Dielectric Properties of Water Mixtures", *Proc. 4th IEEE Pulsed Power Conf.*, pp. 302-307, June 6-8, 1993.

¹⁴D. B. Fenneman, "Pulsed High-Voltage Dielectric Properties of Ethylene Glycol/Water Mixtures", *J. Appl. Phys.*, Vol. 53, No. 12, pp. 8961-8968, Dec. 1982.

¹⁵M. Zahn, S. Voldman, and T. Takada, "Charge Injection and Transport in High-Voltage Water Glycol Capacitors", *J. Appl. Phys.*, Vol. 54, No. 1, pp. 315-325, Jan. 1983.

¹⁶M. Zahn and T. Takada, "High Voltage Electric Field and Space-Charge Distributions in Highly Purified Water", *J. Appl. Phys.*, Vol. 54, No. 9, pp. 4762-4775, Sep. 1983.

surface, we investigated¹⁷ the effect of standard bead-blasted surfaces and differing surface treatments on charge injection for 304 stainless steel, electrolytic tough-pitch copper (CDA 110), 70-30 brass and 7075 aluminum electrodes. In order to conduct our analysis of charge injection (since we didn't have the Kerr electro-optics of MIT), we digitized the voltage waveforms and then modeled them with a computer program to determine the amount and mobility of the injected charge. As expected we found that electropolishing and passivating (EP) the surface of 304 stainless-steel electrodes reduces the amount of charge injection by 2-10 times as compared to bead-blasted (BB) surfaces. We found that the effect wears off over the course of a year but can be reapplied. Furthermore, we confirmed that 304 stainless steel is a unipolar positive injector by examining mixed (EP and BB) electrode sets. Unexpectedly, anodized aluminum did not inject less charge than BB aluminum but did have a 20% greater breakdown strength. We also observed charge injection in the brass electrodes, confirming the MIT results.

With the copper electrodes in this experiment ¹⁷ we tried a more exotic process. A cuprous oxide layer was grown on the electrode by annealing in a controlled-gas furnace. We chose cuprous oxide because it was p-type semiconductor and we hypothesized that this coating might reduce the gradient of the electric field from the electrode into the dielectric, which might improve the breakdown strength. Copper oxide did inhibit charge injection as compared to bead-blasted copper. A limited number of breakdown tests showed a slight decrease in breakdown strength for cuprous oxide (about 126 versus 129 kV/cm;

¹⁷V. H. Gehman, Jr., D. B. Fenneman, and R. J. Gripshover, "Electrode Surface Effects on Unipolar Charge Injection in Cooled Liquid Dielectric Mixtures", *4th IEEE Pulsed Power Conference*, Albuquerque, New Mexico, June 6-8, 1983.

the next paper would have more dramatic results as we learned about the aging characteristics of copper). Using mixed electrode sets, we found that making the copper oxide electrode the anode yielded about the same charge injection as using two copper oxide electrodes. However, making the copper oxide electrode the cathode gave a charge-injection amount roughly midway between two pure bead-blasted copper electrodes and two cuprous oxide electrodes. This ambiguous result is reminiscent of the MIT result, where Zahn found that copper is usually a unipolar positive injector, except when combined in a mixed electrode set with stainless steel. This puzzling result has never been explained nor are we sure that it is important.

Finally, in this comprehensive paper ¹⁷ we found that we could inhibit charge injection which would lead to the desirable result of allowing longer charging times. We expressed this result numerically as a new quantity called action density, which was the energy density of the dielectric liquid multiplied by a normalized, high-voltage-measured intrinsic time constant. In this regard, electropolished and passivated stainless steel was best, anodized aluminum was better than bead-blasted aluminum because of the 20% increase in breakdown strength, and cuprous oxide was better than copper.

Since our results with cuprous oxide appeared promising, we expanded our work on this material and its effect on breakdown strength¹⁸. Before discussing this work, we report the remarkable discovery that the breakdown strength of copper electrodes will improve if they were simply immersed in glycol and water for an extended period. Thus, fresh copper (immersed only a short time and

¹⁸V. H. Gehman, Jr., R.K. Hutcherson, Jr., D. B. Fenneman, and R. J. Gripshover, "Effects of Cuprous Oxide Coated Electrodes on the Breakdown Voltage of Liquid Dielectric Mixtures", *1984 Sixteenth Power Modulator Symposium*, Arlington, Virginia, June 18-20, 1984.

freshly bead blasted) has a breakdown strength of about 135 kV/cm for the 2.5-inch diameter electrodes, while aged copper (immersed over a month) has a breakdown strength of 143 kV/cm. Also surprising was that polished copper had the highest breakdown strength of all (153 kV/cm), which is not what we expected based on polished stainless-steel work described previously.

Returning to cuprous oxide layers, our annealing procedure was difficult because cuprous oxide is not thermodynamically favored until the temperature of the copper was within about 50 C of the melting point. Therefore we had to heat and cool for long periods of time under inert argon gas and react for short times with a partial pressure of oxygen. Our research sources indicated that the resistivity of the cuprous oxide would depend greatly on the preparation conditions and could vary from 100 to 10^{10} ohm-centimeters. The measurement of surface resistivity is not straightforward because we have a conducting substrate. We could not confirm that a resistivity in the target range of a 1000 ohm-cm or less was ever achieved. Layers with the desired thickness in the micron range were not obtained, instead thickness varied between 0.002-0.007 **inches**. Consequently, breakdown shots would severely damage the oxide layer. Cuprous oxide did inhibit charge injection but it also had low breakdown strength (96-105 kV/cm). Faced with many sources of uncertainties, e.g., whether charge injection was important to increasing breakdown strength, whether our layers were too thick or resistive, how to test for different explanations, etc., this line of approach was eventually abandoned.

In the same work¹⁸, another important issue was addressed. For rep-rated machine (with a frequency of operation of many times a second), it may be more relevant to introduce another threshold for defining breakdown. We term the new

value as the 1% breakdown threshold. Specifically, in previous studies, breakdown tests in sets of ten shots at each voltage setting were used and the highest groupings of ten shots without a breakdown were defined as the 10% breakdown threshold. However, for some classes of pulsed-power machines more reliability might be needed. It would be interesting to know the highest value of the electric field that would holdoff 100 shots without breaking down. This we define as the 1% breakdown threshold. The two thresholds were assumed to provide similar results. Sincerny¹⁹ explicitly investigated the inherent performance of pure water under high repetition rate (many Hz) and found a slight, but acceptable, decrease in the breakdown strength. Although our apparatus is not designed to achieve Sincerny's repetition rates, we did repeat experiments at several cycles per minute. We found that in cooled glycol and water, for 2.5-inch diameter copper electrodes: the 1% breakdown threshold is 153 kV/cm which is surprisingly better than the 10% value (143 kV/cm). Since the former set of data were taken with aged electrodes, while the latter were not, our conclusion is that the aging process is more important. In experiments we describe below, the breakdown strength of copper are found to depend on other factors as well as immersion time.

Because we continued to see different breakdown and charge-injection behavior for different electrode materials, in our next effort²⁰ we measured and compared two alloys of stainless steel (304 vs. 310) and two alloys of aluminum (7075 vs. 5083) in a water (40%)/glycol (60%) mixture. Stainless steel contains

¹⁹P. S. Sincerny, "Electrical Breakdown Properties of Water for Repetitively Pulsed Burst Conditions", *Proc. 3rd IEEE Int. Pulsed Power Conf.*, pp. 222-225, June 1-3, 1981.

²⁰V. H. Gehman, D. B. Fenneman, and R. J. Gripshover, "Effects of Alloys and Surface Treatments on Electrical Breakdown Strength of Water and Water Mixtures", 5th IEEE Pulsed Power Conference, Arlington, Virginia, June 10-12, 1985.

chromium, among other elements, which forms a passive surface layer of chromic oxide. We suspected that this passive surface layer would affect charge injection and breakdown. We chose 310 stainless steel because it had a higher chromium content than 304 and might be expected to inject less charge. For bead-blasted surfaces, the action density, for a given value of electric field, was greater for 310 than 304, implying that the 310 indeed injected less charge. However, when both alloys were given a commercial passivation treatment designed to increase the inert layer of the surface of the steel, the action density for the two alloys was about the same and reduced compared to the bead-blasted surface, which implied that charge injection was equivalent for the two alloys when the surface was passivated. Clearly, the passive surface layer of stainless steel was responsible for inhibiting charge injection, because whenever the passive layer was strengthened, either by commercial treatment or simply by using an alloy with a higher chromium content, charge injection was reduced. We also found that 310 had a higher breakdown strength than 304 for both bead-blasted and commercially passivated surfaces.

Electrodes made of two aluminum alloys (7075 and 5083) were tested initially. The latter was chosen because it is a more corrosion resistant alloy, and like stainless steel, our goal was to find out if corrosion resistance was a key to reduced charge injection and increased breakdown strength. We also compared aluminum electrodes with a standard bead-blasted surface to a commercially prepared anodized surface. Using a similar strategy to the stainless-steel experiments, we chose an anodized surface because it increases the thickness and integrity of the native aluminum-oxide surface for aluminum alloys. Unfortunately, the results were not conclusive. The amount of action density for

a given electric field was the same for 7075 aluminum, regardless of whether the surface was bead blasted or commercially anodized. This implies that charge injection was unchanged. Yet, we observed that the breakdown strength for anodized 7075 was greater than for bead-blasted 7075 (i.e., 150 kV/cm versus 125 kV/cm). The breakdown results did not follow charge-injection behavior. When we tested the 5083 aluminum electrodes results were even more confusing. The first breakdown measurements gave 192 kV/cm, but could not be repeated. Subsequent measurements decreased to 150 kV/cm and then to 100 kV/cm. We removed these electrodes from the test cell, bead blasted them again, and measured a different breakdown strength of 130 kV/cm, which then fell off to 100 kV/cm again. This was the first time we had observed such unstable breakdown behavior for bead-blasted electrodes. We anodized the 5083 aluminum electrodes and then measured a holdoff strength of less than 80 kV/cm. Clearly, we could not assign a logical explanation for these results with respect to alloys or surface treatments.

Our next effort²¹ carried out jointly with researchers at MIT, was an extensive review on the subject of water and water/glycol. Topics included specific pulsed-power machines, design of a pulse forming line (PFL), the physical and chemical properties of water and ethylene glycol and water mixtures (e.g., dielectric constant, resistivity, Kerr constant, freezing-point suppression). We reviewed the high-voltage properties of these liquids including: empirical relations for breakdown, polarity effects on breakdown, surface effects, area effects, pressure effects, repetition-rate effects, and water switching. There were extensive

²¹M. Zahn, Y. Ohki, D. B. Fenneman, R. J. Gripshover, and V. H. Gehman, "Dielectric Properties of Water and Water/Glycol Mixtures for Use in Pulsed Power System Design", *Proceedings of the IEEE*, September 1986, pp. 1182-1221.

charge-injection calculations followed by experimental results including the identification of stainless steel as a unipolar positive charge injector, copper as a usually unipolar positive injector except in the presence of stainless steel when it injects negative charge, aluminum as a unipolar negative injector, and brass as a bipolar charge injector. Furthermore, promising results of increased breakdown strength were presented for electrodes with bipolar charge injection versus electrodes with no charge injection that had lower breakdown strength.

In a conference²² hosted by NSWEC to discuss the issues facing energy-storage technology, we reported our findings on water breakdown²³, including the effect of stress time on breakdown and breakdown values for various electrode materials. We introduced results of new experiments that confirmed the MIT observations that a bipolar charge-injecting polarity (i.e., 2024 aluminum negative and 304 stainless steel positive) was initially stronger than the reverse polarity where no charge injection takes place. However, immersion in high-purity water had an effect on the breakdown. Over time the aluminum electrodes developed a dark film (presumably an oxidized coating) that prevented charge injection. More interestingly, the breakdown strength for both polarities gradually increased and became equal. We also presented our latest theoretical speculation about breakdown initiation including (1) enhanced dissociation of the water molecule and enhanced mobility for ions in high electric fields, (2) decreased dielectric constant at high electric field and near the

²²V. H. Gehman, editor, *Record Of Workshop on Electrical Breakdown in Water-Based Dielectrics*, Dahlgren, Virginia, October 24, 1986

²³V. H. Gehman, "Past and Present Research Concerns For Water-Based Energy Storage Devices", *Workshop on Electrical Breakdown in Water-Based Dielectrics*, Dahlgren, Virginia, October 24, 1986.

electrode surface, and (3) the effect of the electron energy level near the electrode surface and the electrochemical double layer.

M. Buttram asserted ²⁴ the goal for water researchers should be 200 kV/cm. Reviewing the data on area effects on water breakdown, he stated that beneficial effects from pressure seem to disappear when electrode area reaches a square meter. M. Zahn reviewed ²⁵ the capabilities of Kerr electro-optical measurements, the effects of charge-injection on breakdown strength for short immersion times, and postulated that measuring the zeta potential would provide information on the trapped charge in the double layer. J. Bockris claimed ²⁶ that the electrochemical model for smooth electrodes predicts a breakdown strength of 300 kV/cm. Though it is unclear what are the assumptions or the mathematical analysis which led to this claim, he concluded that breakdown improvement might be possible by experimenting with: (1) semiconductor coatings, (2) pressure greater than 1000 atmospheres, (3) atomically smooth electrodes, (4) aprotic solvents (e.g. benzene), (5) dilute ice films at low temperatures. Unfortunately, this line of approach was not pursued due to insufficient support. Consequently, these ideas played no further role in our investigation. They are included for completeness.

We next reported ²⁷ on efforts to build a nearly full-scale demonstration PFL using water/glycol technology. We were able to attain long intrinsic time

²⁴M. Buttram, "High Permittivity Fluids For Large Pulsed Power Systems", *Workshop on Electrical Breakdown in Water-Based Dielectrics*, Dahlgren, Virginia, October 24, 1986

²⁵M. Zahn, "Charge Injection Effects and Kerr Electro-Optic Measurements of High Voltage Phenomena in Water", *Workshop on Electrical Breakdown in Water-Based Dielectrics*, Dahlgren, Virginia, October 24, 1986

²⁶J. O'M. Bockris, "Electrochemical Aspects of Electrical Breakdown in Water", *Workshop on Electrical Breakdown in Water-Based Dielectrics*, Dahlgren, Virginia, October 24, 1986

²⁷T. L. Berger, V. H. Gehman, D. D. Lindberg and R. J. Gripshover, "A 2.5 Gigawatt Liquid Dielectric Coaxial Pulse Forming Line", *Proceedings of the 6th IEEE International Pulsed Power Conference*, Arlington, Virginia, June 29-30 and July 1, 1987.

constants as confirmed by the Tau Meter²⁸ and high-voltage measurements. Unfortunately, the observed breakdown strength in the PFL was significantly less than expected. This apparatus was built before we suspected that non-ionic impurities were important. We made liberal use of Tygon® tubing, which may suffer from plasticizer migration in high-purity water or water/glycol, as we later discovered²⁹. This problem may have contributed to our difficulties with breakdown strength.

We also gave³⁰ extensive details of the breakdown strength in pure water (as opposed to glycol/water mixture) using stainless steel and aluminum alloys. The use of pure water represents a shift in strategy. We hoped that, in a simpler dielectric medium, the phenomenon of breakdown may be more easily understood, giving us some insight on how to attack the problem in the more complex medium of glycol-water mixtures. Using 304, 310, 316, and 430 stainless steel, and 2024, 5083, 6061, and 7075 aluminum, we found substantial differences in breakdown strength for the alloys. We confirmed our earlier observation that a bipolar-injecting electrode set (specifically, negatively charged 2024 aluminum and positively charged 304 stainless steel) is better than the reverse polarity at early times. However, these benefits disappear in time as corrosion film grows on the aluminum electrode. Both polarities improve with time but the non-injecting polarity (aluminum positive and stainless steel negative) improves more. Eventually both polarities have about the same

²⁸D. B. Fenneman, L. F. Rinehart, and L. W. Hardesty, "Apparatus For And A Method Of Measuring The Intrinsic Time Constant Of Liquids", United States Patent Number 4,516,077, May 7, 1985.

²⁹John Copley, Private Communication based upon discussions with Kigre, Inc., circa late 1980's.

³⁰A. R. McLeod and V. H. Gehman, "Water Breakdown Measurements Of Stainless Steel and Aluminum Alloys For Long Charging Times", *Proceedings of the 6th IEEE International Pulsed Power Conference*, Arlington, Virginia, June 29-30 and July 1, 1987.

breakdown strength. Lastly, we noted that, for electrode sets made of the same material, aluminum alloys achieve higher breakdown strength with immersion time in contrast with stainless-steel electrodes, which are more stable in time.

On the theoretical front, we reported some work on breakdown initiation³¹. The interface between the electrode and the water was assumed to be the weak link. We reviewed a paper by Sharbaugh³² on liquid breakdown, who reviewed the breakdown mechanisms of electron avalanche and bubble theories, the latter explaining much of the experimental results for dielectric fluids. Bockris³³ had written a paper that indicated the dielectric constant of water was significantly lower (6 vs. 78) near the interface. This implied that the field strength in a high-voltage experiment would be considerable higher near the interface (~10 MV/cm) than in the bulk water (~150 kV/cm). Booth³⁴ considered whether the high electric field might reduce the dielectric constant. We also considered other phenomena which might play a role in breakdown initiation, such as enhanced dissociation of water, higher ionic mobility, and the oxidation and reduction of water at the interface due to high electric fields, and the recombination of excess hydronium and hydroxyl ions just outside a high field region (the enthalpy of recombination is 13,300 cal/mol vs. 11,600 cal/mol for evaporation). We stated that these effects could cause local heating at the interface, which might produce a low-density region where enhanced electron

³¹V. H. Gehman, T. L. Berger, and R. J. Gripshover, "Theoretical Considerations Of Water Dielectric Breakdown Initiation For Long Charging Times", *Proceedings of the 6th IEEE International Pulsed Power Conference*, Arlington, Virginia, June 29-30 and July 1, 1987.

³²A. H. Sharbaugh, J. C. Devins, and S. J. Rzed, "Progress In The Field Of Electrical Breakdown In Dielectric Liquids", *IEEE Trans. Electr. Insul.*, Vol. EI-13, No. 4, pp. 249-276, August 1978.

³³J. O'M Bockris, M. A. V. Devanathan, and K. Muller, "On The Structure Of Charged Interfaces", *Proc. Roy. Soc. (London)*, A274, 55, 1963.

³⁴F. Booth, "The Dielectric Constant Of Water And The Saturation Effect", *Jour. Chem. Phys.*, Vol. 19, No. 4, 391, April, 1951.

conduction or other mechanisms could cause a streamer to grow. We stated the intent of looking at gold electrodes because they might not have oxide layers to influence breakdown. We also stated the hypothesis that reducing non-ionic contaminants may have a profound effect on breakdown. Clearly, we had many potential culprits that might be breakdown initiators^{35 36}. Unfortunately, it is impossible to investigate all possibilities.

The conclusions of the most recent study³⁷ of charge-injecting electrodes are as follows. After 23 days of immersion, the surfaces have changed so that both polarities (injecting and non-injecting) have the same breakdown strength. This result remained constant for nine months. We also examined gold electrodes and found they have reasonably good breakdown strength (170 kV/cm). Had oxide layers been the controlling factor, then we would have expected these electrodes to give the significantly better performance. Either oxide patches did not play a major role in breakdown, or our gold-coated electrodes developed oxide patches, so that using gold cannot avoid oxides. We also used gold-lead electrode combinations to see if double layers³⁷ are an improvement. However, no difference in breakdown strength for different polarity was observed. We also included breakdown measurements on lead electrodes (150 kV/cm) for completeness, but the results were not interesting. On the other hand, dramatic improvements in breakdown strength were found when particulate and organic

³⁵V. H. Gehman and R. J. Gripshover, "Water-Based Dielectrics For High-Power Pulse Forming Lines", *NATO Advanced Study Institute on The Liquid State And Its Electrical Properties*, poster session, Sintra, Portugal, July 5-17, 1987.

³⁶V. H. Gehman, T. L. Berger and R. J. Gripshover, "Water-Based Dielectrics For Energy Storage And Pulse Forming Lines", *19th International SAMPE Technical Conference*, Arlington, Virginia, October 1987.

³⁷V. H. Gehman, L. B. Atwell, D. A. Dorer, and R. J. Gripshover, "Determination Of Electrical Breakdown Strength For Various Materials In Pure Water", *IEEE 1988 Eighteenth Power Modulator Symposium*, pp. 385-388, 20-22 June 1988.

filters were employed. Particulate filters alone increased the breakdown strength of 304 stainless steel from 140 kV/cm to 180 kV/cm. Both kinds of filters improved the breakdown strength of copper electrodes from 135 kV/cm to about 200 kV/cm, which is the best performance to date.

Finally, we report attempts at a more quantitative theory³⁸. We hypothesized that, under the influence of high electric fields, ions would be emitted from the electrode surface. The ions would bull their way through the water molecules (due to higher mass and momentum) creating short-lived low-density regions, known as proto-streamers, which usually collapse before they can grow. But, if other ion emissions would occur while the proto-streamer is still in existence, there was a possibility (described by Poisson statistics) that the proto-streamer could grow long enough to reach a critical length. Our definition for the critical length involved the formation of daughter charged particles as a charge carrier transited the proto-streamer and impacted on the end. As soon as that happened, we reasoned that growth of the streamer was assured. Our theory predicted the right time scale for breakdown, the correct shape of the breakdown distribution curve, and an approximately correct ordering of electrode materials, but could not predict the effects of filters.

³⁸S. P. Bowen and V. H. Gehman, "Microscopic Theory Of Dielectric Breakdown In Liquids", *NSWC Technical Note 88-289*, October, 1988.

C. AREA-EFFECT

For the sake of completeness we quote the work of M. Buttram, et al, at Sandia national Laboratory. In a series of papers^{39 40 41 42} they reported a study of the effect of electrode area on breakdown strength over a wide regime and drew conclusions about breakdown statistics. Among other reasons, their papers are notable for confirming that a weak area effect on breakdown strength exists from 81 cm² to 10,000 cm².

³⁹F. Zutavern and M. Buttram, "Area And Time Dependence Of The Breakdown Of Water Under Long Term Stress", *Proc. 1983 Conf. on Elec. Insul. and Dielec. Phenomena*, pp. 251-256, October, 1983.

⁴⁰M. Buttram and M. O'Malley, "Area Effects In The Breakdown Of Water Under Long-Term Stress", *Sandia Report SAND83-1016*, 1982.

⁴¹F. Zutavern, M. Buttram, and M. O'Malley, "Dielectric Breakdown Distributions Of Large Dielectric Constant Liquids", *Proc. 1984 16th Power Modulator Symp.*, pp. 273-279, June 1984.

⁴²M. Buttram, "Area Effects In The Breakdown Of Water Subjected To Long-Term (~100 μs) Stress", *Proc. 15th Pulsed Power Modulator Symp.*, pp. 168-173, June 3-5, 1980.

III. CHAPTER THREE: EXPERIMENTAL APPARATUS

Our experimental apparatus for measuring the breakdown strength of water capacitors has evolved from the late 1970's when Drs. Fenneman and Gripshover first started this work at NSWCCD. They documented the initial system in detail.^{43,44} Rather than recount the entire history of the evolution of the apparatus, we will present a general description with emphasis on two important improvements in the water-purification system over the original system. First, we discovered that consideration of non-ionic impurities was important and introduced crude particulate and organic filters. This increased the electrical breakdown voltage. Second, we found that employing more state-of-the-art particulate and organic filters gave even bigger improvements to breakdown strength.

A. LIQUID-PURIFICATION SYSTEM

This system pumps the high-purity water to and from the test cell while it maintains a desired range of temperature, removes dissolved gas (principally air) from the water, and removes ionic and non-ionic impurities.

⁴³D. B. Fenneman and R. J. Gripshover, "Experiments on Electrical Breakdown in Water in the Microsecond Regime", *IEEE Trans. Plasma Science*, PS-8, September 1980, p. 209.

⁴⁴D. B. Fenneman, "Pulsed High-Voltage Dielectric Properties of Ethylene Glycol/Water Mixtures", *J. Appl. Phys.*, 53(12), December 1982, p. 8961.

1. IONIC PURITY

Achieving and controlling ionic purity requires four things. First, non-metallic materials wherever practical because pure water will leach ions from exposed metal. Second, a mechanism (i.e., deionizer beads) for removing impurity ions (e.g., Na^+ and Cl^-) from the water. Third, a deaeration system because dissolved CO_2 in water forms carbonic acid, and air bubbles in water can lead to interfaces with different dielectric constants which lowers breakdown strength. Fourth, heat regulation because once water is pure to the parts-per-billion level, the conductivity is controlled by the auto-dissociation of the water molecule which is exponential with temperature.

a) PLASTIC PIPING AND SURFACES

(1) PIPING

We use polyvinyl chloride (PVC) pipe for the water-purity system. It is relatively inexpensive, easy to assemble, durable, and is much better in terms of ion infiltration than metal pipe. At the time of our first experiments, it was pretty much considered the material of choice. However, time has passed and current practice for ultrapure-water systems calls for either polypropylene (PPP) or polyvinylidene fluoride (PVDF) piping, because of their superior performance in leaching few impurities (ionic and non-ionic) into water. Our problem is that these alternate materials are expensive and much harder to assemble. Furthermore, we use a Plexiglas test cell because we wish to observe the breakdown arc. Plexiglas is also a less desirable alternative than either PPP or

PVDF. There would seem to be little benefit to painstakingly and expensively replacing our PVC pipe with PVDF while keeping the Plexiglas test cell. We don't know of a source for transparent PVDF or PPP in sizes adequate for our test cell. This would probably be a custom manufacturing order and almost certainly more expensive than our limited research budget can afford.

(2) PUMP

To assist in maintaining ionic purity, we use centrifugal pumps with plastic-coated impellers. The pumps must be carefully chosen because we run a deaerated system. This means the pump has only the height of the water column above the pump inlet to form the input pressure for the pump. For this reason, we raise the deaeration column, which is just before the pump inlet, as high off the floor as possible.

(3) TEST CELL

The test cell is made from a cylindrical Plexiglas tube approximately 12-inches in diameter, 18-inches long with walls about 0.25-inches thick. End caps are made from circular, 304-stainless-steel plate that have O-ring grooves milled near the edge. The wall of the tube serves to compress the O-rings into the grooves. Water and gas ports are drilled through the end caps. Threaded solid Plexiglas rods are placed outside the wall of the test cell and are attached with screws to the end plates to provide the compressive force required to hold the end caps and tube together. The tube serves as a pressure vessel with the

deaeration port located on top. The circular-shaped planar electrodes are supported from threaded rod attached to the end caps. Water flows directly through the electrode gap via a PVC pipe extension that extends into the test cell.

b) DEIONIZATION BEADS

(1) DESCRIPTION

Deionizer beads⁴⁵ are polymers (e.g., Barnstead resins are Styrene-divinylbenzene copolymers) that have ion-exchange sites throughout the structure. Simply stated, the polymers are designed so that the free energy of the system decreases if anions or cations in the water exchange places with the hydrogen and hydroxyl ions on the polymer sites. The net result is to replace impurity ions with water molecules.

(2) PROVIDERS

Commercial off-the-shelf systems can provide ionic purity routinely down to the part-per-billion regime. Culligan, Barnstead, and Millipore are among the best known and respected companies, but there are many other choices. Early on in our work (see Figure 3-1) we used a large mixed-bed deionizer tank from Culligan, but found that this technique led to large organic-carbon contamination in our water system, because the large, dark, wet deionization tanks were

⁴⁵*The Water Book 1993-1994*, published by Barnstead-Thermolyne, Dubuque, Iowa, pp. 16-17.

breeding grounds for bacteria. In our modern filter set-up (see Figure 3-2), we have opted for replaceable Barnstead filter cartridges, placed immediately after a macroreticular cartridge that removes gross quantities of chlorine and organics. This combination of cartridges provides the optimum in ionic purity when combined with the deaeration system described below.

c) DEAERATION COLUMN

(1) VACUUM & PARTIAL PRESSURE OF WATER

The partial pressure of water depends on temperature; for instance, it is 4.579 mm of Hg at 0 C, 9.209 mm of Hg at 10 C, and 23.756 mm of Hg at room temperature 25 C.⁴⁶ Thus, a vapor pressure will be present above the surface of water at these pressures. If there is no dissolved gas in the water, the vapor pressure will equal the partial pressure alluded to above. If there is dissolved gas present in the water then the vapor pressure above the water surface will be higher than just the partial pressure of water at that temperature. Measuring the vapor pressure above the water surface then provides a convenient way of detecting dissolved gases in the water. We use a vacuum pump to gradually deaerate the water and measure the vapor pressure to determine the degree of deaeration.

⁴⁶Weast, Robert C., Editor-in-Chief, *CRC Handbook of Chemistry and Physics 1984-1985, 65th Edition*, Chemical Rubber Publishing Company, 1984, ISBN 0-8493-0465-2, pp. D-192 and D-193.

(2) DEFINITION OF % DEAERATION

If the pressure above the water surface is atmospheric pressure (760 torr at STP), we define that to be 0% deaeration. If the pressure above the water surface is the vapor pressure of water, we define that to be 100% deaeration.

This leads us to the formula:

$$\% \text{ DEAERATION} = \left(\frac{P_{atm} - P}{P_{atm} - P_{H_2O}} \right) \times 100\%$$

where P is the measured pressure, P_{atm} is the atmospheric pressure (varies daily), and P_{H_2O} is the partial pressure of water (a function of temperature).

Therefore, we monitor the atmospheric pressure before each experiment, and continually monitor the pressure in the deaeration column and the temperature of the water. This allows us to compute the deaeration in the water. Typically, the deaeration of the water is greater than 98%.

(3) DESIGN OF COLUMN

The column is a tall Plexiglas tube, capped with Plexiglas end plates (see Figures 1 and 2). Vacuum and water-inlet ports are threaded through the top cap, while the water outlet port is located a few inches from the bottom and is threaded through the cylindrical wall. Starting near the top and continuing down the length of the tube are a series of horizontal Plexiglas plates that only partially span the diameter of the tube. Water cascades from plate to plate in a thin sheeting action to facilitate gas bubbling out from the water.

Plexiglas was chosen early in the experimental program because it is non-metallic and would not affect the ionic purity. With what we know now, we should replace it with a more inert material. However, we need the column to be transparent because we manually adjust the water flow valves to maintain the liquid level in the column. Transparent PVC tubing is available (Excelon®), but not in sufficiently large diameter - at least not in stock from our sources. PVDF would be preferred over PVC in any case, but also is not available from our sources. A special order would be expensive and we have not had the funds for this purchase.

(4) COLD TRAP

We use a mechanical pump to provide vacuum for the deaeration column. To retard the back flow of pump oil into the water (which would make our organic-contamination problem worse) and to reduce the amount of water vapor that gets into the pump oil (which would degrade the pump), we have installed a home-made cold trap. The trap features a simple cylindrical cold wall to trap water vapor and pump oil. The wall is chilled by a methyl alcohol - dry ice slurry, so the temperature is only about -78.2 C.

We realize that a more convoluted cold wall and a colder wall (e.g., chilled by liquid nitrogen at -195 C) would have been more efficacious. However, funding limitations precluded these improvements.

d) CHILLER

(1) RATIONALE

As the ionic-impurity level falls to parts-per-billion regime, the chief source for electrical conductivity becomes the hydronium and hydroxyl ions arising from the autodissociation of water. Since the dissociation is exponential in temperature, we need to control the temperature of pure water to control the conductivity.

Furthermore, early water-breakdown experiments demonstrated that water breakdown depends on $t_{eff}^{1/3}$ for times in the microsecond regime, where t_{eff} is the time water is exposed to greater than 63% of the maximum electric field stress, But D. B. Fenneman⁴⁷ discovered that water breakdown slowly loses its time dependence, finally becoming constant for t_{eff} greater than $65 \mu\text{s}$. Since the stress time in our apparatus is a function of the RC time constant, and since the RC time constant is identically equal to the product of the resistivity times the dielectric constant, we need to control conductivity to control which breakdown regime we are in. We chose early in the thesis to operate in the time-independent regime; therefore, we purify the water and maintain the temperature that keeps the RC time constant greater than $162 \mu\text{s}$ ($RC > 162 \mu\text{s} \Rightarrow t_{eff} > 65 \mu\text{s}$, in fact we usually operate around $RC > 300 \mu\text{s}$).

⁴⁷Private communication

(2) DESIGN OF HEAT EXCHANGER

Unfortunately, a heat exchanger requires a good heat-transfer material and for this project's budget that meant metal (more exotic materials like diamond are a possibility but hardly practical in large macro-scale experiments). We compromised by choosing 316 stainless steel as a metal which we hoped would infiltrate few ionic impurities into the water and still be affordable and available. Therefore the PVC piping feeds directly into a 316 stainless-steel pillow (two pieces of metal welded together around long-path water channels). The pillow is immersed in a cooling fluid: either methanol and dry ice slurry or ice water. The cooling fluid is contained in a home-made ice chest, at one time a modified Coleman cooler and later a PVC box with Styrofoam insulation. It is low-tech but reliable and rugged.

(3) OPERATION

The purified water constantly flows through the pillow. During the deaeration stage we don't introduce a cooling fluid into the ice chest. After the desired levels of deaeration and resistivity are achieved we carefully introduce the cooling fluid. Manual addition of dry ice or water ice allows us to control temperature. We usually operate around 10 C.

(4) PROBLEMS

Because the control and feedback system is the operator, there is chance of freezing the water in the pillow. When this happens flow stops; the pump undergoes extreme stress; and system grinds to a halt. The operator switches off the pump and frantically tries to bail the cooling water out of the ice chest and replace it with hot water. By the time this is done and water flow is restored, enough pressure or temperature transients have occurred to flush impurities out of every crack and crevice in the piping system. The experiment is almost always over for the day, with an extended period of conditioning extending into the next day required before another experiment can be attempted.

For this reason, we have had ample incentive to discover and stick to good operating practices. Most importantly, we must choose a rugged pump, because it has to operate with little inlet suction head, and still pump about a gallon per minute, while being able to tolerate sudden blockages and the pressure spikes they entail. We've found that swimming-pool pumps with plastic-coated impellers do well. Next, we found that using ice and water as a cooling fluid works better than dry ice and methanol, although it is slower. Ice and water gives a nice controlled approach to 10 C.

2. NON-IONIC PURITY

a) RATIONALE

Non-ionic impurities would probably have significant dielectric mismatch with water, which could result in enhanced electric fields in dielectric contaminant layers. As explained in later chapters, when we added filters designed to reduce non-ionic impurities, we noticed significant improvements in the breakdown strength of water. This fact plus another observation led us to seriously consider the effects of non-ionic contaminants: a laser company (KIGRE) in a private communication⁴⁸ to one of our colleagues mentioned the Tygon tubing was a problem if installed in high-purity water systems used to cool lasers. They believed that the Tygon tubing gave off impurities into the water which impaired the laser cooling.

b) ACTIVATED CHARCOAL

Activated charcoal or high-efficiency synthetic carbon in combination with mixed-bed ion-exchange resin are the main ingredients in the commercial filters we used. A key factor for successful use of these filters is to maintain a roughing cartridge (sometimes referred to as a macroreticular filter) ahead of the high-efficiency organic filters.

⁴⁸Copley, John, Private Communication with Kigre, Inc. including a page copied from a company document.

c) MICROFILTERS

A filter removes bacteria and particulates. In early tests, see Figure 3.1, we used industrial polypropylene 30-micron prefilter followed by a 0.5-micron final filter. As we learned more about the proper use of commercial water-purification systems, we replaced the industrial-grade filters with a 0.2-micron filter specifically designed for high-purity water, see Figure 3.2.

d) UV OXIDATION

Ultraviolet light can oxidize organic impurities and convert them into carbon dioxide. UV can also serve to kill bacteria and prevent their growth as a pollutant in the water system. In early experiments we occasionally used UV illumination. In our later experiments when the importance of controlling impurities became clear, we routinely used UV illumination.

WATER TREATMENT SYSTEM INDUSTRIAL FILTERS

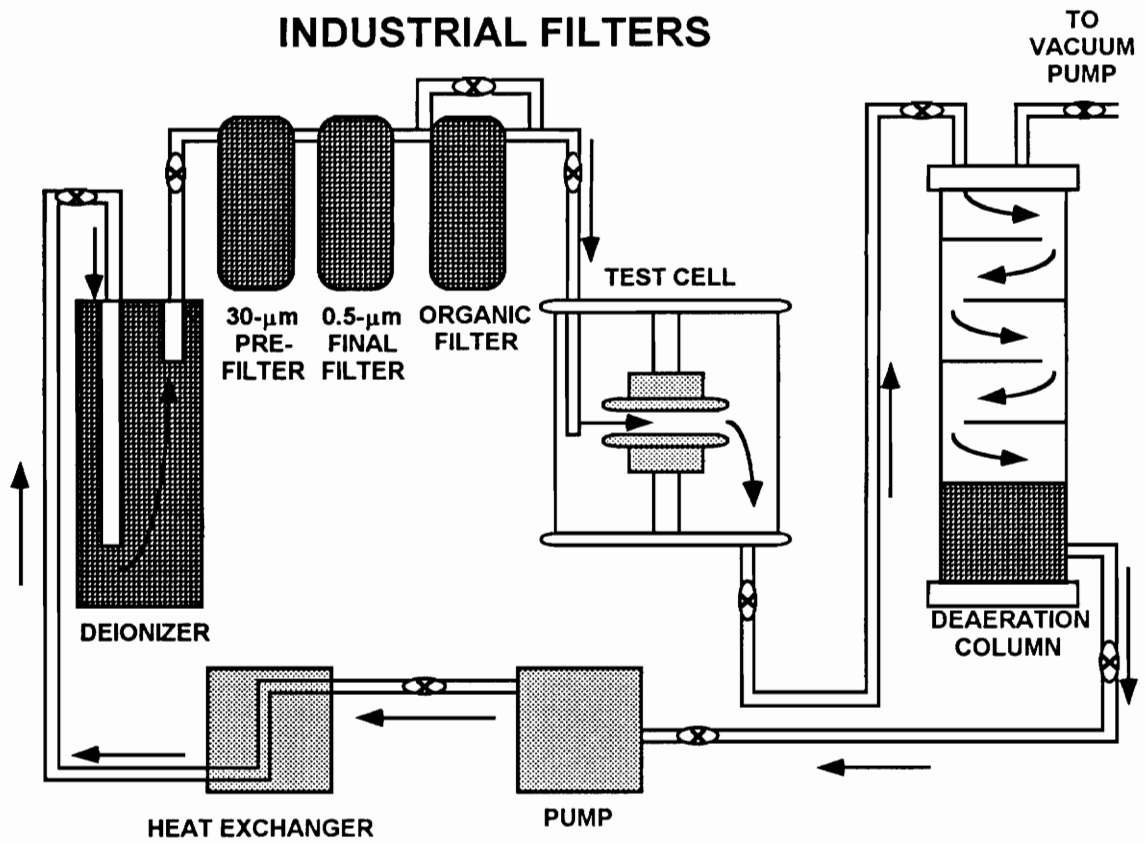


Figure 3.1 The sketch of the older, industrial-grade water-treatment apparatus for the electrical-impulse, water-breakdown experiment.

WATER TREATMENT SYSTEM MODERN LABORATORY FILTERS

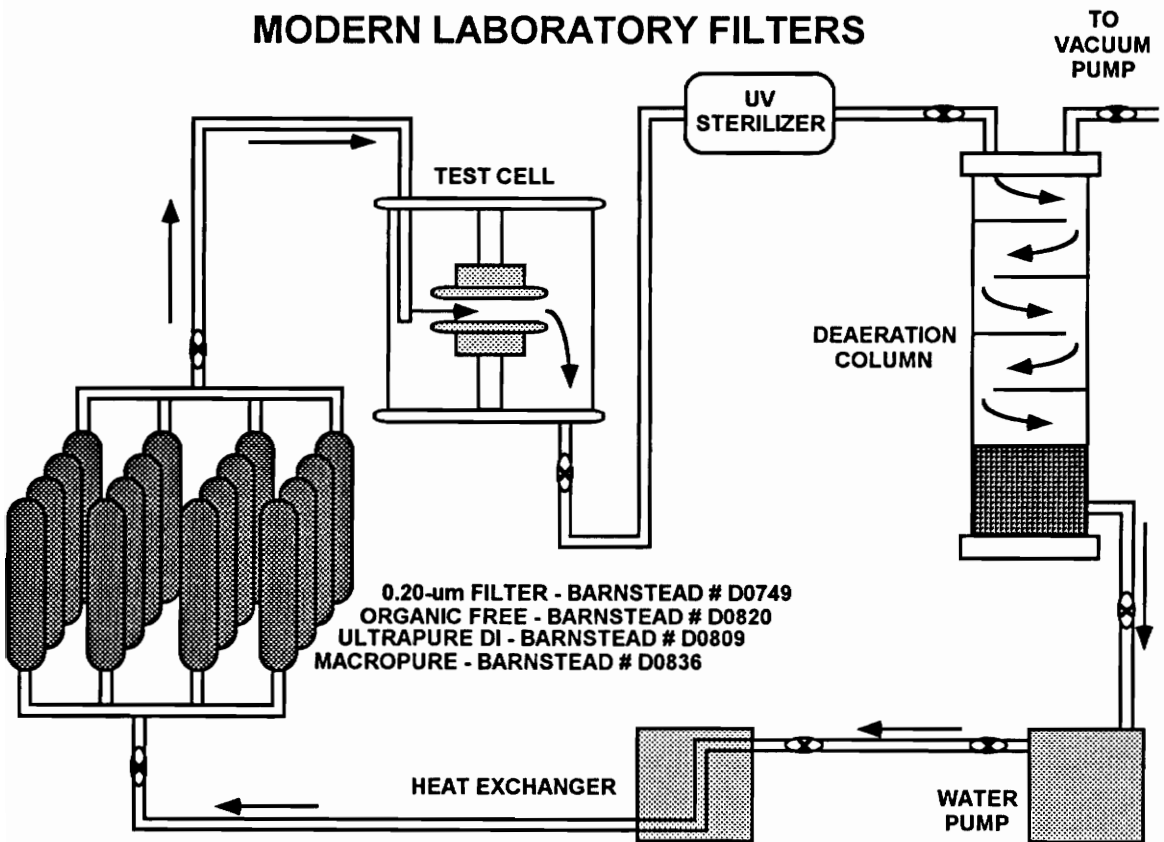


Figure 3.2 The sketch of the more modern water-treatment apparatus for the electrical-impulse, water-breakdown experiment.

B. ELECTRICAL-IMPULSE GENERATOR

The Marx generator is described more thoroughly in other publications^{1,2,49}. We will cover the highlights in this section. Basically, we used the Marx system (see Figure 3.3) to provide fast-rising (about 2 microseconds) pulses to the water test cell. High-voltage diodes then held the voltage across the water gap and did not allow the voltage pulse to decay through the Marx. Thus, fast pulses were imposed across a water gap and then either decayed with the time constant of the water or broke down the water gap by creating a conductive plasma channel between the electrodes that eliminated the potential difference across the cell in less than a nanosecond.

1. DESIGN

a) MARX GENERATOR

A Marx generator (named for Erwin Marx) is a pulse device that allows a number of capacitors to be charged in parallel over a relatively long period of time, then discharged in series to add the voltage of each capacitor to its successor to "erect" a final voltage pulse equal to the sum of the potentials for each individual capacitor. Usually, each capacitor is part of a stage, hence our ten-stage Marx consists of ten capacitors. This type of device is used because electrical-insulating problems increase in difficulty in a nonlinear fashion (i.e., 200-kV insulation is much more than ten times as difficult as 20-kV insulation). Therefore, during the long charging time only the lower voltages

⁴⁹Frank C. Creed, *The Generation And Measurement Of High Voltage Impulses*, Center Book Publishers, 1989, ISBN 0-944954-00-6, pp. 13-51.

need to be handled, while the high-voltage pulse is over quickly. The fast appearance and disappearance of the pulse simplifies the electrical problem. Thus, our Marx is charged at voltages up to 50 kV, which can easily be handled by standard electrical practices. However, our Marx produces discharge pulses up to 500 kV, but the pulses only last for tens of microseconds in the Marx.

b) CHARGING RESISTOR

To control the current and rise time of the voltage from the Marx across the test cell, a liquid ballast resistor is introduced (see Figure 3.3). It consists of a Plexiglas tube with metal end plates filled with a copper-sulfate solution. The copper-sulfate concentration is controlled to maintain a resistance of approximately 7 k Ω .

c) DIODE

The internal impedance of the Marx generator produces an intrinsic time constant of approximately 20 μ s. However, we wish to operate with electrical stress times across the test cell of hundreds of μ s. Therefore, we install a high-voltage diode (see Figure 3.3) in series after the ballast resistor but before the test cell. This holds the voltage on the test cell.

ELECTRICAL PARAMETERS FOR
THE EXPERIMENTAL APPARATUS

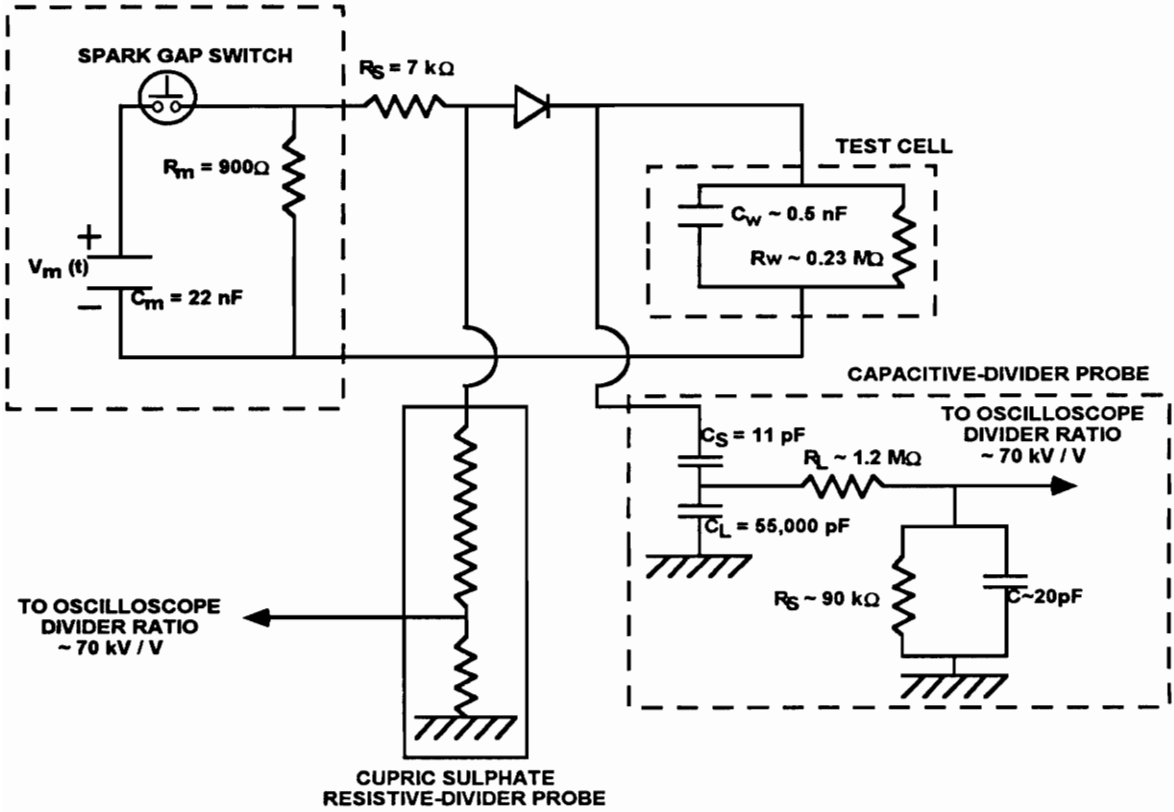


Figure 3.3 An electrical sketch of the electrical-impulse, water-breakdown experiment.

2. OPERATION

When defining a standard conditioning curve for a pair of electrodes in the test cell, we would start at a low voltage to avoid breakdown. Run 10 shots at that voltage. If there were no breakdowns, we would increase the Marx voltage by 20 kV, thereby increasing the voltage across the test cell by about 10 kV with the other 10 kV dissipated in the charging resistor, and shoot another ten times. If there was no breakdown again, we would increase the Marx another 20 kV and continue on in this pattern until we encountered a breakdown. The series of ten shots where we first encountered a breakdown would be completed. We would then continue to increase the Marx voltage by 20 kV and do series of ten shots until we obtained 100% breakdown. At that point, time permitting, we would pause to take readings on the water, then significantly lower the Marx voltage and repeat the procedure.

3. PROBLEMS

The Marx does not reliably erect below about 120 kV; nor can the shielded room containing the Marx holdoff more than about 450 kV before arcing occurs between a high-voltage conductor and grounded screening of the shielded room. This defines the operating range for voltage. The electrode gap must be adjusted, by experience or trial and error, to breakdown within that range. The Marx we're using has been refurbished many times and must be observed on each shot to guarantee that it erects to the proper voltage. Finally, all parameters essential to the experiment (water quality, voltage sources and

electrical probes) must be operating properly throughout the several hours it takes to conduct a single experiment.

C. ELECTRICAL DIAGNOSTICS

To record voltage with time we use a high-bandwidth oscilloscope. Unfortunately, the oscilloscope is limited in voltage measurement to a range from millivolts to tens of volts; whereas we wish to measure hundreds of kV. Therefore, we use voltage-divider probes between the oscilloscope and the high-voltage event.

1. DIVIDING-RESISTOR PROBE

The concept behind the dividing-resistor probe⁵⁰ seen in Figure 3.3 is simple. A very high-impedance-to-ground path is established such that insignificant current flows through the path. Then an oscilloscope is attached to a certain point in the path where the ratio of resistance between the oscilloscope and the high voltage to the resistance between the oscilloscope and ground is sufficiently high (typically 70,000 to 1). Then for each volt measured on the oscilloscope, there were 70 kV present in the high-voltage portion of the circuit.

Our probe is actually two probes in series. The higher-voltage probe is a dividing-resistor made from a water and copper sulfate solution in a tube. This

⁵⁰Ibid. pp. 107-111.

divides the voltage by a factor of about a hundred. Then another dividing-resistor probe is attached in series using high-voltage resistors. The second probe is quite stable over time, but the copper sulfate solution in the first probe can plate out to the sides of the tube resulting in varying levels of voltage division. This probe is inherently very fast because there is only stray capacitance in series with it, but the copper sulfate problem means we have to calibrate the probe before each use.

2. CAPACITIVE-DIVIDER PROBE

The concept for the capacitive-divider probe⁵¹ is also simple. A high-impedance path between high voltage and ground is used again, only this time the impedance is established using capacitive elements. The scope is attached between two capacitors but this time circuit theory requires the large-capacitive element to be between the oscilloscope and ground and the small-capacitive element to be between the oscilloscope and the high voltage. In our setup the voltage-divider ratio is about 5,000 to 1.

As this does not reduce the voltage signal sufficiently, we then add a small dividing-resistor probe in series between the capacitive probe and the oscilloscope. This produces the desired 70,000 to 1 voltage-divider ratio, but the combination of the capacitive probe with a dividing-resistor probe slows the response of this hybrid device to about ten microseconds. This disadvantage is

⁵¹Ibid. pp. 105-107.

offset by the reduced variability in the capacitive probe (because there is no copper sulfate problem) as compared to the dividing-resistor probe.

For these reasons, at the beginning of each day's test we calibrate the dividing-resistor probe by firing a 200-kV shot into an open circuit and observing the reflection. Then we could match the peak response of the capacitive probe to the dividing-resistive probe for each shot of the day and gain two reliable views of voltage versus time: the dividing-resistor probe which is fast but needs to be calibrated every day, and the capacitive probe which is more stable but has a slower response.

3. SHIELDED ROOMS AND ABSORBER

Repeatability is obviously desired for quantified analysis. Even with the voltage source and probes properly operating, electrical noise could still ruin the experiment if it gets into the probe. Unfortunately, the impulses emitted by the Marx are inherently noisy over a wide range of the radio-frequency (RF) spectrum. We isolate the oscilloscope in its own shielded room and the experiment in another. We also install RF absorber in the experiment room to absorb noise.

4. SHIELDED DATA CABLES

As part of our attempt to shield our oscilloscope signals from noise, only high-quality coaxial cables (e.g., Helix solid-shield coaxial cable) and

connectors (e.g., BNC connectors) are used to transfer the voltage signal from the probes in the experiment's screened room into the oscilloscope's screened room.

5. OSCILLOSCOPES

Our experiments are inherently single shot. We use high bandwidth (400 MHz) analog oscilloscopes to capture the voltage signal. We can capture two signals (capacitive and resistive probes) by using the dual beam Tektronix Model 7844 oscilloscope. There are now digitizers with the single-shot performance needed for this measurement (like the Tektronix RTD720 and the Lecroy 7200), but we started to use analog oscilloscopes in the late 1970's when they were the only tool capable for this job.

6. TAU METER

There is an NSWC invention called the Tau Meter which constantly monitors the RC time constant of the water. The big advantages for this device are that we are more interested in the time constant than the resistivity and it is not temperature compensated. We use this device to monitor ionic purity and check the results of commercial water purity meters that are temperature compensated and only display resistivity.

IV. CHAPTER FOUR: FILTERS, CONTAMINANTS, CONDITIONING AND DIELECTRIC BREAKDOWN

A. INTRODUCTION

As a result of the research (described in Chapter 2) conducted by others over many years and ourselves since 1980, we concluded that:

1. Breakdown initiates at or near an electrode surface.
2. Electrode materials affect the breakdown strength.
3. Increasing water (ionic) purity improves breakdown performance.

Then around 1987, we hit upon the idea of using filters to study breakdown. We knew from the semiconductor industry that there were non-ionic contaminants in water that were not affected by standard mixed-bed deionizers. We also knew from the high-power laser community⁴⁸ that Tygon® tubing released plasticizers into high-purity water and this caused problems in water-cooled lasers. Removing the Tygon tubing was a natural first step, but we also wanted to eliminate the non-ionic contaminants. At first, we used industrial-grade filters in PVC housings with a 30- μm prefilter and a 0.5- μm final filter. There was no other documentation or certification for these devices. Next we added a more laboratory-grade organic filter (using activated charcoal) from Barnstead, but we didn't use the conventional prefilters used with this organic cartridge (at the time we were unaware of the recommended order for filter sets as specified by Barnstead). Still the beneficial effects on breakdown were quite remarkable, as can be seen in Figure 4.1.

The mean breakdown strength increased and the scatter reduced as we increased the quality of filtration. The scatter improvement seems to be associated with the particulate filters; we didn't observe further improvement in scatter with the addition of the organic filter. However, the average breakdown value did increase when we added the organic filter. Still, the news was not all good as we shall discuss in the next section.

B. ANALYSIS OF DATA FROM THE INDUSTRIAL-FILTER EXPERIMENTS

Figure 4.2 presents the time-ordered breakdown data for copper electrodes with industrial-grade particulate filters and the Barnstead organic filter. Unfortunately, after the extraordinarily consistent results of 3/11/88, the breakdown performance becomes erratic, starting with the next set of runs on 3/22-23/88. We're still not sure which filter set is responsible for this behavior, because at the time we needed to search for higher-breakdown-strength results for our sponsor. Therefore, we were intent to try other electrode combinations with this filter set and did not concentrate on the scientific issue as to why the breakdown strength varied.

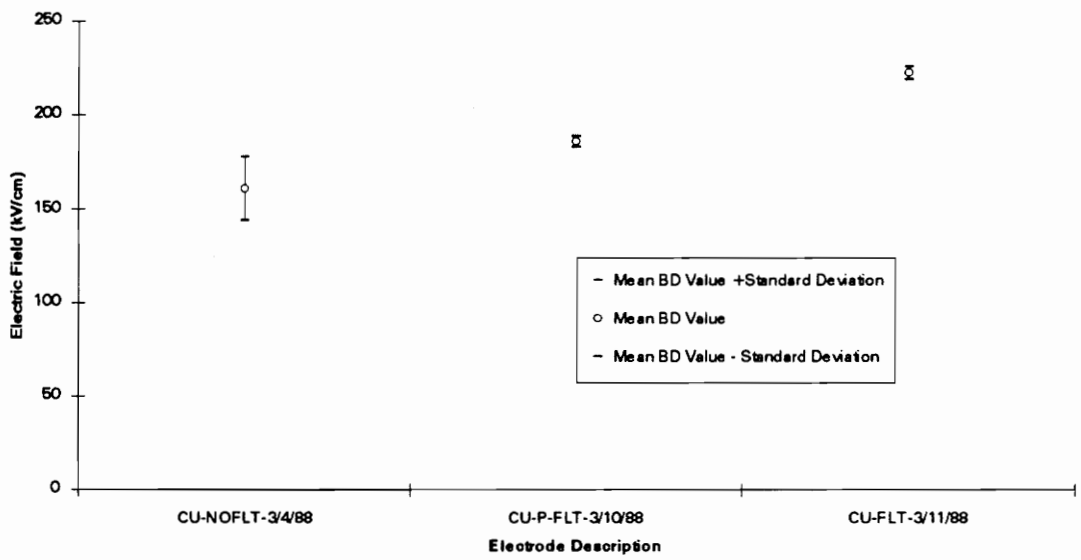


Figure 4.1 Plot of the mean breakdown field plus or minus the 95% confidence interval for a series of experiments on copper demonstrating the efficacy of various industrial-grade filter combinations. On the left is no filters, in the center is only particulate filters, and on the right is the combination of particulate plus organic filter.

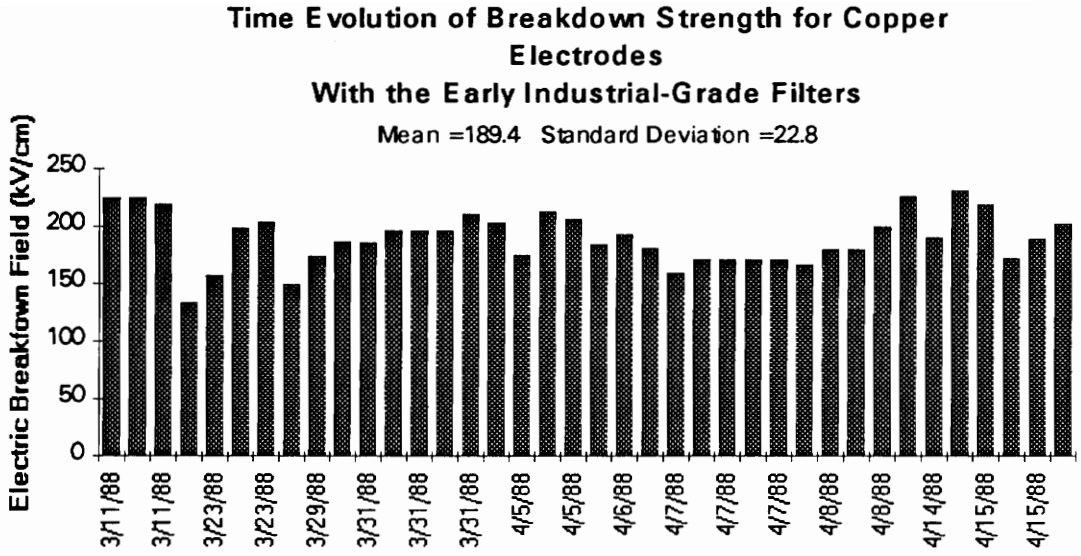


Figure 4.2 Breakdown data for copper electrodes with industrial-grade particulate filters and a Barnstead organic filter. Note the erratic behavior after the initial runs on 3/11/88.

The ratio of the standard deviation to the mean for the copper electrodes is 12%. The ratio for the tungsten data (shown in Figure 4.3) is 13%. In both cases the variation in breakdown strength was considered too large to reliably conclude that filtration was the cause for improved breakdown performance.

Stainless-steel electrodes led to considerably more consistent results, even with the industrial-grade filters.. In Figure 4.4, the ratio of the standard deviation to the mean is only about 4%. This is a somewhat surprising result, but then the sample size is small and inhomogeneous (there were three different alloys in the data set), so the results may not be statistically significant.

By this time we had developed (other supporting reasons are given in Chapter 5) a hypothesis for water breakdown. We believe a semi-trapped layer of water exists near the surface of the electrode, wherein contamination (e.g., dielectric particles, metal flakes, metal-oxide particulates) is the weak link in the electrical-breakdown process. This would explain why filtration would beneficially affect breakdown. The difference in variance between stainless steel and the other electrode materials (copper and tungsten) could be explained if, for some reason, the principal source for the contaminants of the semi-trapped layer of water was the electrode and not other parts of the apparatus, and if stainless steel gave off a more-uniform distribution of contaminants, or if different electrode materials attracted and retained different amounts of contaminants from the fluid. If this hypothesis is correct, and if better filters could gradually reduce the contaminant concentration in the semi-trapped layer, then better

Time Evolution of Breakdown Strength for Tungsten Electrodes With the Early Industrial-Grade Filters

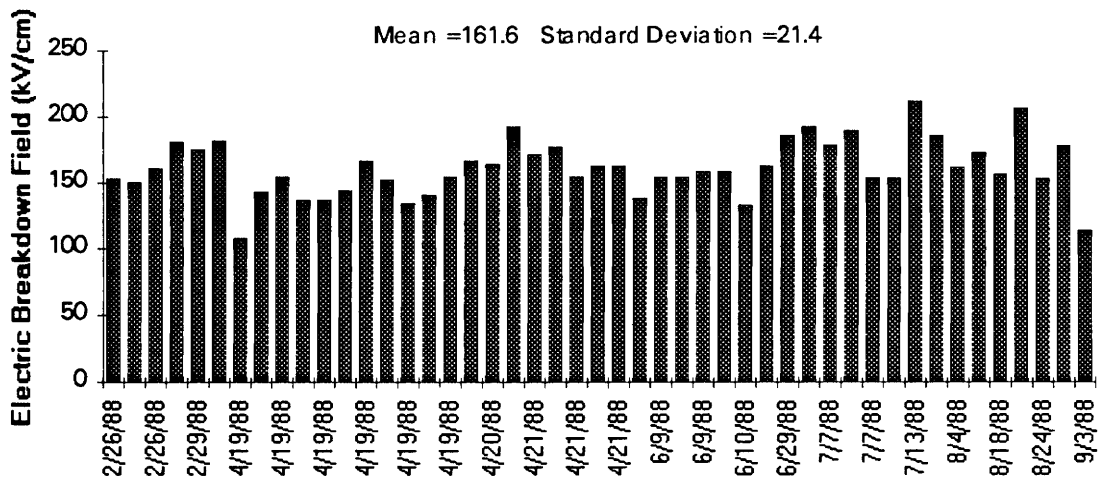


Figure 4.3 Breakdown data for tungsten electrodes with industrial-grade particulate filters and a Barnstead organic filter. Note the erratic behavior.

Time Evolution of Breakdown Strength for Various (304, 430, 316) Stainless-Steel Electrodes With the Early Industrial-Grade Filters

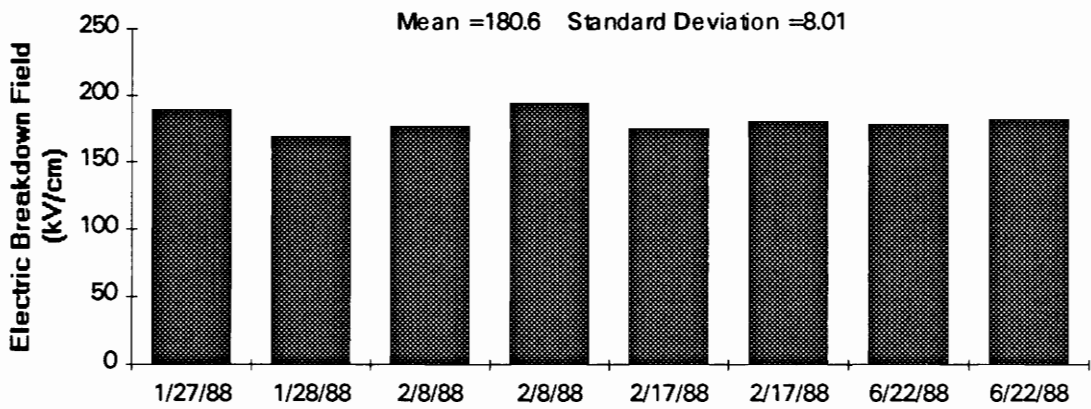


Figure 4.4 Breakdown data for stainless-steel electrodes with industrial-grade particulate filters and a Barnstead organic filter. Note the consistent breakdown behavior.

filtration methods should improve breakdown performance. The next section addresses this subject.

C. ANALYSIS OF DATA FROM THE MODERN-FILTER EXPERIMENTS

Finally in 1993 we were able to pursue the hypothesis of the previous section by purchasing modern Barnstead filters. As explained in Chapter 3, a bank of four identical filters was used: first, a macroreticular filter (Barnstead number DO836) which serves as a prefilter for the organic and deionization filters; second, a mixed-bed deionization cartridge (Barnstead number DO809); third, an "organic-free" cartridge (Barnstead number DO820) with activated charcoal to remove organic contaminants; and finally a 0.2-micron particulate filter (Barnstead number DO749). With this filter bank, we were almost equivalent to state-of-the-art water systems used in the semiconductor industry. However, we still had significant parts of our apparatus that were not made of either polypropylene (PPP) or polyvinylidene fluoride (PVDF) - materials that minimized contamination of high-purity water. Specifically, our test cell was made of Plexiglas (methyl methacrylate) and our piping was polyvinyl chloride (PVC).

Figure 4.5 presents the data for tungsten electrodes. The ratio of the standard deviation to the mean is 6%, which is about half the value with the older filters. We believe that the lowering of the standard-deviation-to-mean ratio and the increase in electric-breakdown strength of 35% proves that better

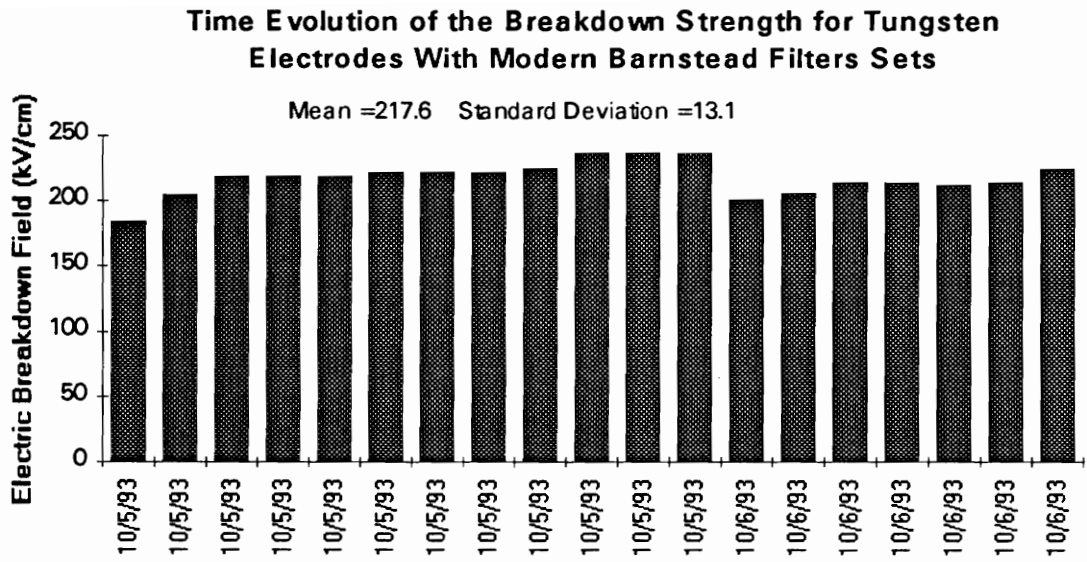


Figure 4.5 Breakdown data for tungsten electrodes with modern Barnstead particulate and organic filters. Note the more consistent breakdown behavior as compared to Figure 4.3.

filtration beneficially affects holdoff performance. We believe that the breakdown strength is controlled by water impurities, not by the inherent electrical properties of water, itself.

Figure 4.6 presents the data from the stainless-steel electrodes. The ratio of the standard deviation to the mean is about 9%, which is more than the 4% measured previously, but there is a larger sample size to the set. Thus, this change in variance may not be significant. The breakdown strength is about the same as the older filters but significantly less than tungsten electrodes with modern filters. Therefore, we are not seeing the intrinsic breakdown strength of water in this experiment. Rather, the results are consistent with the hypothesis that stainless steel gives off a more uniform distribution of particles than tungsten. Perhaps smaller than the 0.2-micron filter can effectively remove. Perhaps, so numerous as to reduce the breakdown strength compared to tungsten. Of course, this conclusion can only be supported by circumstantial evidence in the absence of direct imaging or other measurements of the hypothesized contaminant population.

D. EXPERIMENTAL PROCEDURES TO CONDITION A GAP FOR MAXIMUM ELECTRICAL-BREAKDOWN STRENGTH

1. STANDARD CONDITIONING

It's well known within the water-breakdown community that water will

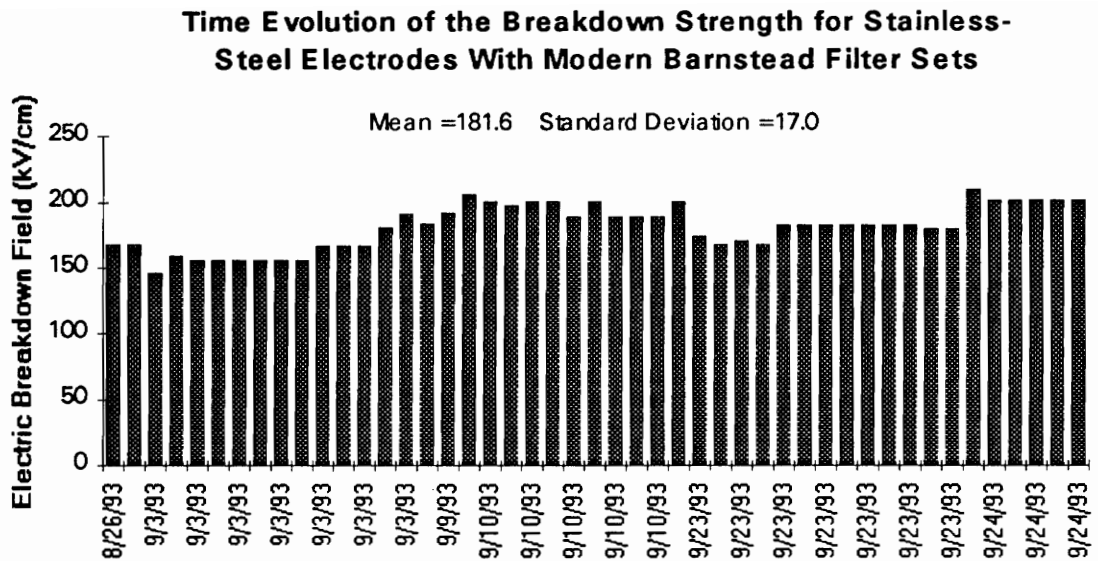


Figure 4.6 Breakdown data for stainless-steel electrodes with modern Barnstead particulate and organic filters. The variation in breakdown strength is larger than for Figure 4.4, but the mean breakdown strength is about the same.

ultimately holdoff higher voltage if the gap is first subjected to lower voltage and then gradually increasing voltage pulses. We have found that starting at the lowest reliable triggering setting on our Marx generator (about 120 kV) for ten shots and then working upward at increments of 20 kV with ten shots at each increment yields repeatable high breakdown strength for a given electrode-gap combination. (Because of losses in the charging resistor and in the Marx generator, the actual voltage across the water gap is only about 70 kV when the Marx erects at 120 kV.) Thus, if you don't follow the conditioning curve and go immediately to a target voltage, the probability of breakdown is increased.

The conditioning curve also exists for the opposite direction. If you go to a voltage well above the breakdown strength, and then proceed to drop the voltage gradually, you will have to go well below the normal holdoff voltage to avoid an arc in the gap. However, for the discussion in this chapter, we're concerned only with the ascending part of the curve. In the following figures, the heavy line presents the standard-conditioning results on the ascending part of the conditioning curve.

2. OTHER CONDITIONING SUGGESTIONS

At the oral presentation of the thesis topic, Dr. Zia raised a question that had never been tested. What if you just went to a 50% voltage (one that would normally be about 50% probability of breakdown after a standard-conditioning treatment) on a gap and kept testing at that same voltage? We refer to this procedure as initial-breakdown (IB) conditioning. We didn't know at the time, but

our hypothesis on contamination-controlled breakdown suggested an explanation and a prediction. If the conditioning shots affected the contaminant population, then conditioning should affect breakdown strength. Specifically, if conditioning shots broke up larger pieces of contaminant into smaller pieces, or if conditioning shots expelled the contaminants from the semi-trapped layer out into the bulk water to be swept away and into filters, then conditioning would increase voltage holdoff. Larger contaminants presumably lead to a higher probability of breakdown because the voltage potential across the larger piece is higher. The only unknown is the relative effectiveness of conditioning shots that are breakdowns (as the first part of the IB conditioning probably would be) as opposed to non-breakdowns (standard conditioning).

Making the reasonable assumption that breakdown conditioning shots would contribute at least some energy into reducing the amount or size distribution of the contaminant population, we hypothesized that the IB conditioning process should result in a series of breakdowns, gradually succeeded in time by non-breakdowns to about the same probability-of-breakdown numbers found after standard conditioning. Indeed this is what we found with one important complication.

The maximum improvement for increasing breakdown strength is not seen by the IB conditioning unless sufficient time is allowed between breakdown shots, although non-breakdown shots can be as close together, in time, as possible (given the restriction of the charging time for the Marx generator). To obtain maximum improvement in voltage holdoff, the time between breakdown

conditioning shots must be at least one minute; more time does not seem to gain any advantage, but less time results in lower holdoff. We believe that if the breakdown shots are too close together during IB conditioning, then breakdown for shot number "N" is influenced by the bubbles and other residual effects of breakdown for shot number "N-1", and is not really affecting the contaminant population in the same way as for shots with a greater time interval.

Dr. Sam Bowen suggested yet another conditioning pattern to test our hypothesis on contaminants. If we were to go to a voltage level where the probability of breakdown was one, even had a standard conditioning curve been done, we would expect a long series of breakdowns. Then, if sufficient change to the contaminant population had been effected, a return to a lower voltage level (e.g., a 50% breakdown electric field) should result in about 50% non-breakdowns. Once again the uncertainty is what percentage of the energy of the breakdown conditioning shot affects the contaminants. We call this total-breakdown (TB) conditioning.

3. EXPERIMENTAL RESULTS

Figure 4.7 shows the standard conditioning curve and the increase in breakdown strength brought about by the IB conditioning, especially when one-minute intervals are maintained between breakdowns. For short time intervals the breakdown voltage couldn't be increased beyond 156 kV/cm. But use of one-minute intervals produced a zero-breakdown sequence of ten shots at 178 kV/cm. We did the standard conditioning curve first, then proceeded with the

Comparison of Standard Conditioning Versus Initial Breakdown Conditioning For 304 Stainless-Steel Electrodes

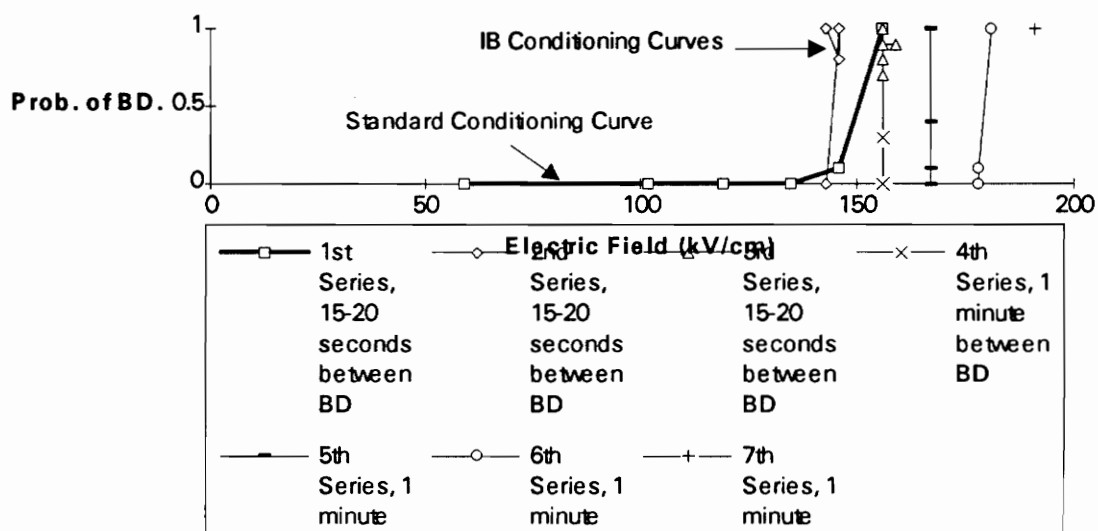


Figure 4.7 Test run of 9/3/93. Note the heavy line depicting the standard conditioning curve. Also note that the IB-conditioning curves are of two types: those where only a short time (i.e. 15-20 seconds) elapsed between breakdowns; and those where a longer time (i.e., 1 minute) was allowed between breakdown. Some of the lines are not vertical because the applied voltage strays slightly about the set point due to variations in the charging circuitry.

IB conditioning shots. In general, during IB conditioning the first tens of shots (each set is usually composed of ten shots) would be breakdowns, followed by mixed sets of breakdowns and non-breakdowns, followed by sets of non-breakdowns. Also, usually one-minute delay sequences required significantly fewer sets of breakdowns before achieving non-breakdown sets. Finally a subjective observation, we ordinarily would have done a second standard-conditioning treatment on this day, and often the second treatment would have achieved a higher breakdown voltage perhaps as good as achieved with the IB conditioning. Therefore, the IB conditioning produced results at least comparable to standard conditioning. These results agree with our prediction and are consistent with our hypothesis of conditioning shots affecting contaminants in the quasi-static water layer next to the electrode surfaces.

Figure 4.8 depicts the next run with 304 stainless-steel electrodes. We changed the procedure for cooling the water down to operating temperature by substituting an ice/water slurry for the dry ice/methanol slurry. This is slower procedure, but results in more stable resistivity behavior. Presumably, less-dramatic temperature variations bring out fewer contaminants that may be hidden in crevices, seams, or other locations within the purification system. We mention this detail because it may explain the fact that the standard-conditioning treatment achieved a significantly higher breakdown voltage this day, 169 kV/cm without a breakdown. However, the IB conditioning still produced an improved voltage holdoff, 192 kV/cm, with a minimal number (5) of breakdown conditioning shots before achieving a set of non-breakdown shots. Again, this agrees with our prediction.

Comparison of Standard Conditioning Versus Initial Breakdown Conditioning For 304 Stainless-Steel Electrodes

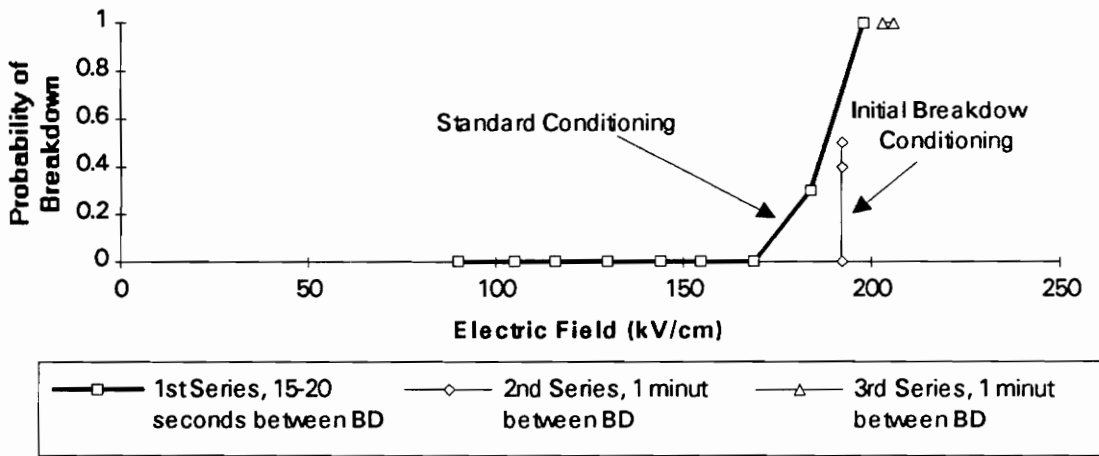


Figure 4.8 Test run of 9/9/93. Note the heavy line depicting the standard conditioning curve. Also note that the standard-conditioning curves allowed only a short time (i.e. 15-20 seconds) to elapse between breakdowns; while a longer time (i.e., 1 minute) was allowed between breakdowns for the IB-conditioning curves.

We continued to use the ice/water slurry to control water temperature from then on. The next day's results are shown in Figure 4.9. Here the standard conditioning achieved the highest holdoff yet at 187 kV/cm. The IB conditioning could only achieve 189 kV/cm - essentially the same. Still, the IB conditioning equaled the standard conditioning which still agrees with our prediction.

At this point we changed from testing the IB-conditioning strategy to TB conditioning. We still used the same 304 stainless-steel electrodes; and we still did a standard-conditioning treatment before the new procedure was tested. However, now we went well above 100% breakdown value to condition. Hence, all TB-conditioning shots are breakdowns. In between the total breakdown conditioning we would drop down to a lower-voltage regime and test for voltage holdoff. The graphs are messy, but we'll try to describe the highlights and significance of the data depicted in the next two figures.

Figure 4.10 is the first test of TB conditioning. Perhaps due to the nearly two-week interval from the previous tests, standard conditioning achieved only 162 kV/cm holdoff before starting to have breakdowns. Series 2 was breakdown conditioning around 190 kV/cm followed by series 3 at 170 kV/cm (which achieved a slightly lower probability of breakdown than the standard conditioning). We went back to 195 kV/cm for a breakdown series of 10 shots labeled series 4, followed by an attempt (series 5) to achieve voltage holdoff at

Comparison of Standard Conditioning Versus Initial Breakdown Conditioning For 304 Stainless-Steel Electrodes

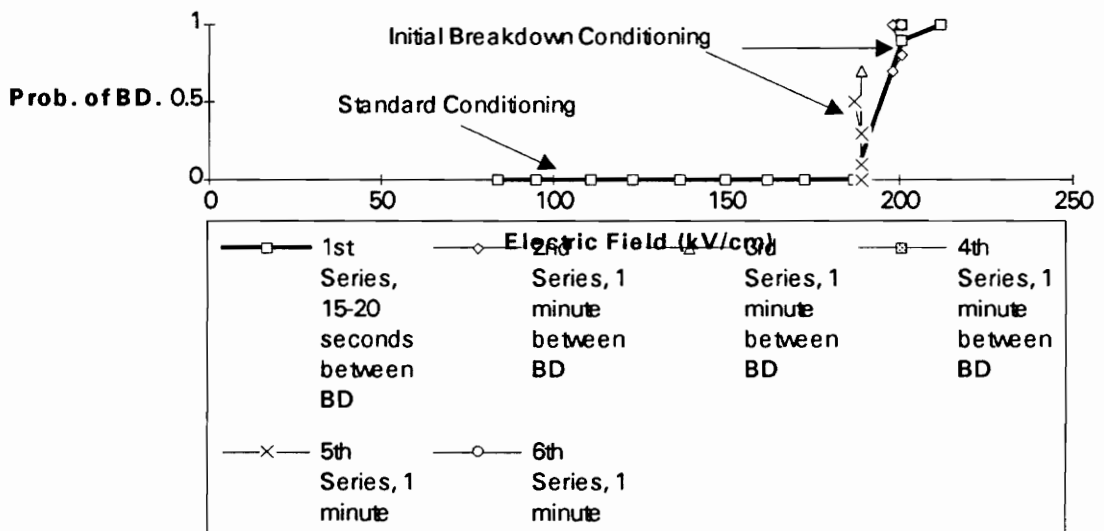


Figure 4.9 Test run of 9/10/93. Note the heavy line depicting the standard conditioning curve. Also note that the IB-conditioning curves use a longer time (i.e., 1 minute) between breakdown. Some of the lines are not vertical because the applied voltage strays slightly about the set point due to variations in the charging circuitry.

Comparison of Standard Conditioning Versus Total Breakdown Conditioning For 304 Stainless-Steel Electrodes

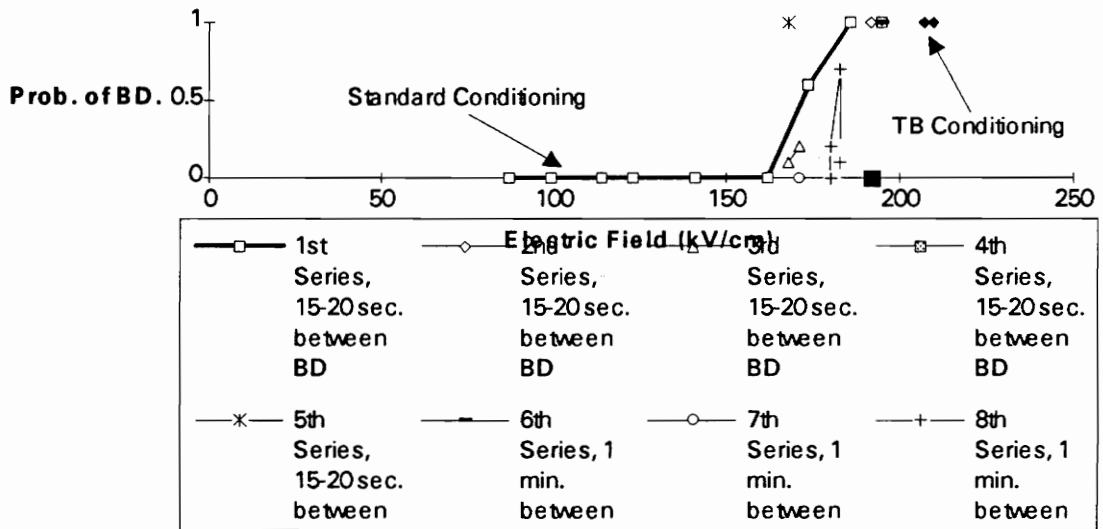


Figure 4.10 Test run of 9/23/93. Note the heavy line depicting the standard conditioning curve. This is the first attempt at TB conditioning. Also note that the TB-conditioning curves are of two types: those where only a short time (i.e. 15-20 seconds) elapsed between breakdowns; and those where a longer time (i.e., 1 minute) was allowed between breakdown. Some of the lines are not vertical because the applied voltage strays slightly about the set point due to variations in the charging circuitry.

168 kV/cm which surprisingly failed. Up to this point we had been allowing only the minimum amount of time between breakdowns (15-20 seconds), and were not improving voltage holdoff significantly. We concluded that, just as with IB conditioning, a longer pause between breakdowns was needed. Consequently, we allowed one minute between breakdowns from now on. Series 6 was ten conditioning shots at 195 kV/cm, followed by three successful searches for voltage holdoff at 171 kV/cm (series 7) and 180 kV/cm (series 8) and 192 kV/cm (series 9). We attempted to continue with voltage holdoff at 210 kV/cm (series 10), but failed. Nevertheless, TB conditioning achieved significantly better results than standard conditioning, just as IB conditioning did.

Figure 4.11 is our attempt to compare the results of different time intervals between breakdowns (45 seconds versus 60 seconds). This experiment was performed the day after Figure 4.10, and as we noted previously, sometimes the standard conditioning achieves higher voltage holdoff on successive days of testing. That is the case here, where standard conditioning achieves 190 kV/cm before breakdowns start.

We then conditioned at 202 kV/cm with 45 seconds between breakdowns, but observed no voltage holdoff. When we switched to one minute between breakdowns, we observed some improvement (breakdown probability fell to 0.7 at one point). Unfortunately, we were unable to spend any more time on this effort, because we wanted to get on with testing tungsten electrodes. The

Comparison of Standard Conditioning Versus Total Breakdown Conditioning For 304 Stainless-Steel Electrodes

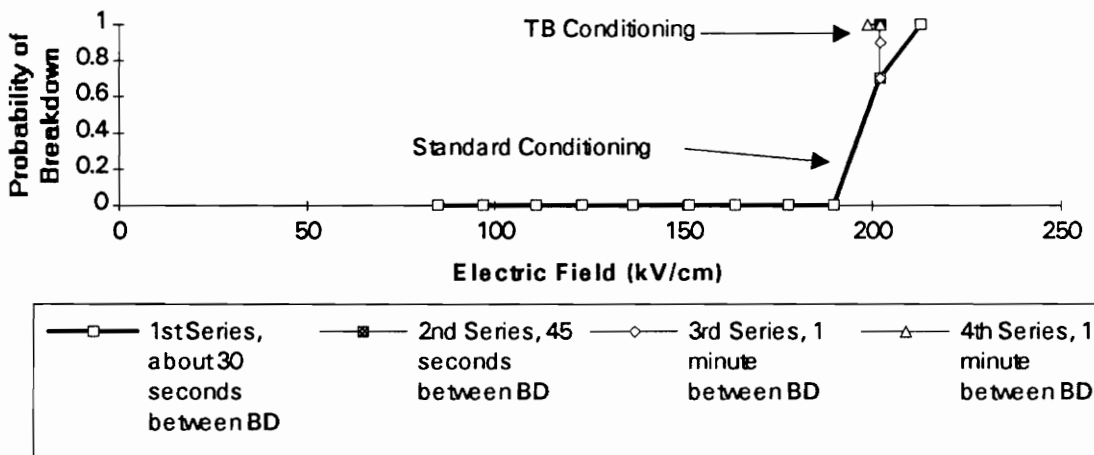


Figure 4.11 Test run of 9/24/93. Note the heavy line depicting the standard conditioning curve. We want to determine if there is any difference in TB conditioning when 45 seconds elapsed between breakdowns or a longer time (i.e., 1 minute) is allowed between breakdowns. Some of the lines are not vertical because the applied voltage strays slightly about the set point due to variations in the charging circuitry.

results have to be considered preliminary. A more complete investigation into the dependence of breakdown strength on time-interval-between breakdown conditioning shots should be carried out.

Figure 4.12 presents the first attempt at IB conditioning on tungsten electrodes. Based upon past experience, we initially felt that standard conditioning achieved a fairly high holdoff value of 167 kV/cm before breakdowns started. We felt that significant improvement might not occur. However, the second series achieved voltage holdoff immediately at 176 kV/cm as did the third series at 193 kV/cm. We finally had to work our way through some breakdowns in the fourth series, achieving voltage holdoff at 208 kV/cm. Series 5 went through many sets of ten shots where the probability of breakdown was between 0 and 1, but finally achieved voltage holdoff at 225 kV/cm. Finally, series 6 could not produce zero breakdowns but did have low probability of breakdown at 237 kV/cm.

IB conditioning worked far better than expected on tungsten electrodes. Our predictions for breakdown behavior were correct. Except for the standard-conditioning curve, all conditioning shots were separated by one minute. We wanted to examine the effect of a shorter time interval (back to 15-20 seconds) on breakdown strength. We also wanted to see if we could attain high voltage holdoff if we shortened the standard-conditioning step. Unfortunately, funding and operating supplies were depleted, so we decided to combine both of these experiments into one last run.

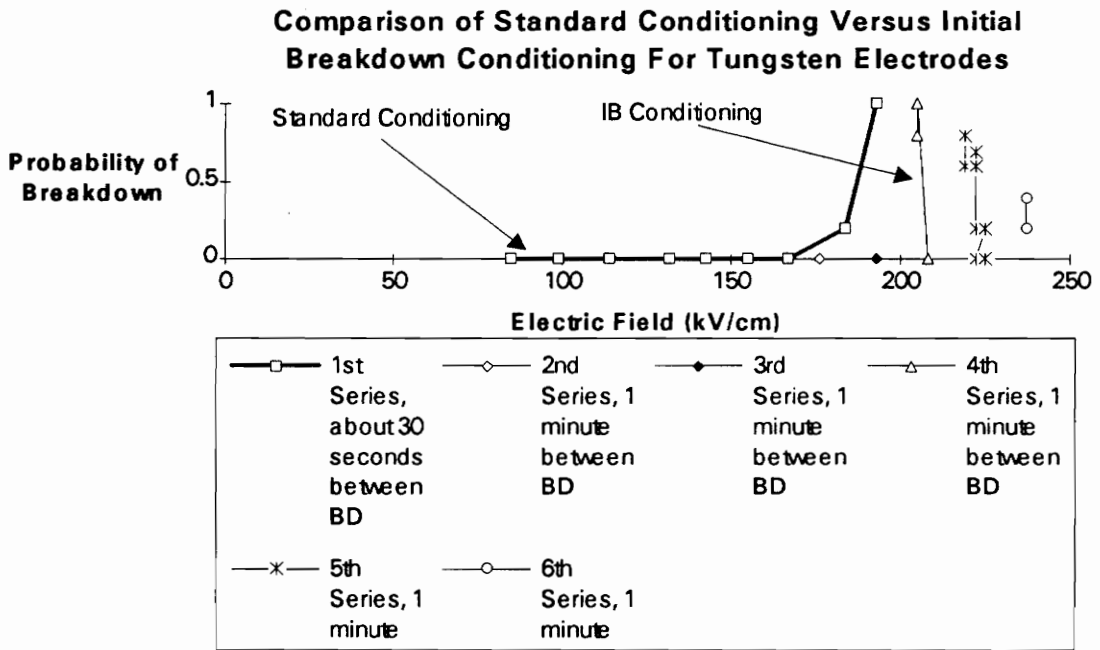


Figure 4.12 Test run of 10/05/93. Note the heavy line depicting the standard conditioning curve. This was the first attempt at IB conditioning on tungsten electrodes. Also note that 1 minute was allowed between breakdown for the IB conditioning curves. Some of the lines are not vertical because the applied voltage strays slightly about the set point due to variations in the charging circuitry.

Figure 4.13 shows the results of our last experimental run. Based upon the previous day's experience, we chose around 190 kV/cm as the starting point. We achieved no breakdowns at 187 kV/cm and all breakdowns at 201 kV/cm in the first series. During the second series, we conditioned with breakdowns at 201 kV/cm, but couldn't get voltage holdoff. Upon closer examination of the apparatus, we noticed bubbles in the purification loop. We eliminated the bubbles (by adjusting the pressure difference between the deaeration column and the test cell) and tried again. This time, the third series quickly achieved holdoff at 201 kV/cm. The fourth series eventually achieved holdoff at 214 kV/cm. But the fifth series could not achieve holdoff at 225 kV/cm.

Because we achieved improvement in holdoff without an extensive standard-conditioning treatment, we feel this proves that IB conditioning does not rely on standard conditioning for its results. Furthermore, while fairly high holdoff (214/kV/cm) was achieved with the short time (15-20 seconds) between breakdown-conditioning shots, we achieved higher holdoff (225 kV/cm) with the longer time duration (one minute) between breakdown-conditioning shots. In fact, since the data collected in Figure 4.13 was collected the next day after Figure 4.12, we expected even higher holdoff values than 225 kV/cm. We believe that this shows the time delay is important for tungsten as well as stainless-steel electrodes. Also, note that when bubbles are in the system (from a malfunctioning purification system), they are the weak link and dominate breakdown behavior.

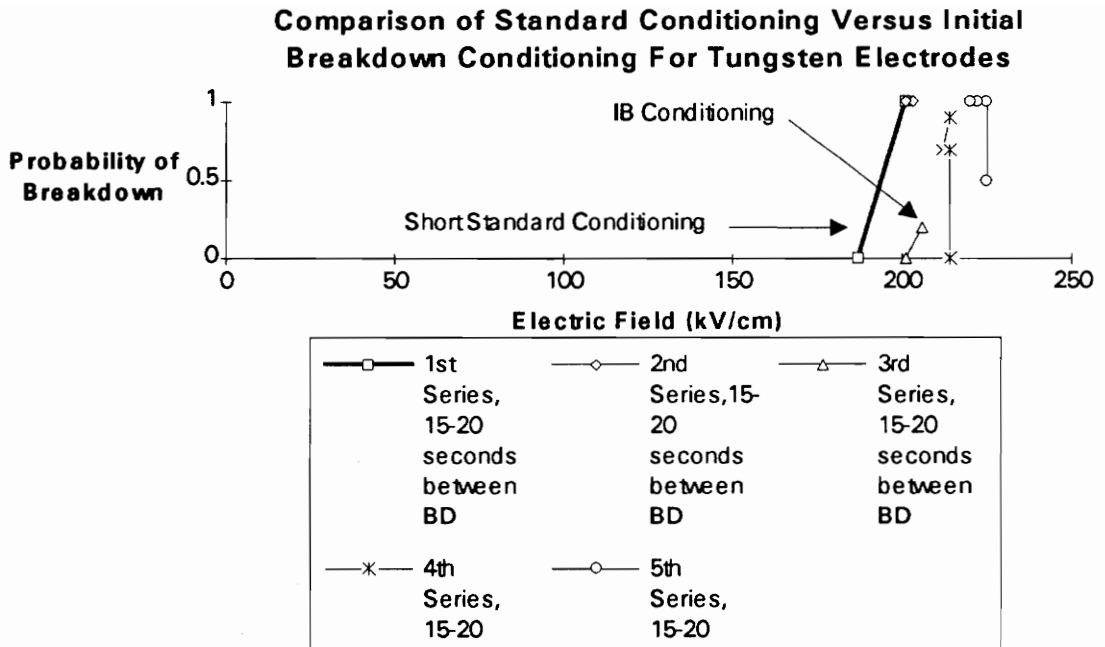


Figure 4.13 Test run of 10/06/93. Note the abbreviated standard-conditioning curve. Also note that only 15-20 seconds was allowed between breakdown for the IB conditioning curves. Some of the lines are not vertical because the applied voltage strays slightly about the set point due to variations in the charging circuitry.

This chapter demonstrates that better filters improve the value and scatter of breakdown strength; our hypothesis (electrical breakdown controlled by contamination in the quasi-static water layer next to the electrodes) is supported by all of our experiments; our predictions on conditioning are correct; and that the time interval between breakdown-conditioning shots does affect electrical breakdown strength.

This chapter is the central part of our thesis on water breakdown. Our hypothesis is supported by the experimental evidence, but the experimental evidence is only indirect. We do not have direct observations in real time of the proposed contamination layers (one at each electrode). It will be a considerable task for some future investigation to provide this direct evidence and correlate it with breakdown behavior because it must be done in the sub-microsecond time regime, within a thin water layer next to the electrode, while high-voltage pulses are present.

Finally, the next chapter reviews previous experimental work to justify some of the assertions made in this chapter.

V. CHAPTER FIVE : CONDITIONING AND DIELECTRIC BREAKDOWN

A. EXPERIMENTAL BASIS FOR A CONDITIONING THEORY OF DIELECTRIC BREAKDOWN IN PURE WATER

We are attempting to explain the impulse breakdown of pure water. Any theory will have to explain valid, pertinent experimental results. This chapter is a brief review of the relevant experimental basis for a breakdown theory as well as a hypothesis (dielectric non-ionic contaminants) that attempts to explain the experiments.

1. EARLY SHORT-TIME-CONSTANT EXPERIMENTS

FIRST OBSERVATION OF CONDITIONING

The early experiments discovered that the probability of breakdown for the next shot depended on the history of the recent shots. Specifically, if recent shots had not resulted in a breakdown, then the next shot was less likely to be a breakdown. Since the probability of breakdown increased with applied electric field, the pattern of testing that resulted in the highest breakdown strengths (which was the goal of the project) was a series of shots at relatively low voltages gradually increasing until a breakdown was encountered.

Another discovery of the short-time-constant experiments was the adherence of the breakdown behavior to "Martin's law". This was an empirical relationship discussed in Chapter II:

$$E_{\max} \times T_{\text{eff}} \times A^{1/10} = M \quad (5.1)$$

where E_{\max} is the maximum value of the electric field in MV/cm, t_{eff} is the time in μs the voltage exceed 63% of the maximum voltage, A is the cross-sectional area of the electrodes in cm^2 , and M is a figure-of-merit called Martin's number (see Chapter II). Martin's number for other investigators of the late 1970's had varied from about 0.2 to 0.3 (bigger is better), but with careful attention to deionization and deaeration, researchers at NSWCCD were able to increase M to values between 0.5 and 0.6.

The area dependence was investigated by Sandia National Laboratories under contract to NSWCCD. The dependence on $A^{1/10}$ was found to be approximately valid out to an electrode area of 10,000 cm^2 .

As investigators increased t_{eff} beyond about 20 μs , they found that Martin's law started to break down. It was finally determined that for t_{eff} greater than about 66 μs there is no time dependence on breakdown strength.

Another significant outcome of the short-time-constant work, which proved to be also important for all water breakdown, was the importance of proper deaeration. Bubbles were the problem. We had a transit with good optics mounted to present a magnified view of the space between the electrodes. Whenever a significant bubble was present on the electrode, the eventual breakdown would occur at that location. Otherwise breakdown location

appeared to be randomly distributed over the electrode surface, with one significant exception. While the breakdown behavior was not significantly affected by highly polished electrode surfaces, the pattern of breakdown pits, which had been random on bead-blasted surfaces, was grouped on the polished surface. Apparently whatever mechanism that had caused the breakdowns to group together had not seriously affected the breakdown strength.

2. ETHYLENE GLYCOL & WATER EXPERIMENTS

The move to experiments with ethylene glycol mixtures with pure water was prompted by the desire to explore liquid dielectrics with large dielectric constants (like water), but with much longer intrinsic time constants. We first discovered the significant effect on breakdown strength of different electrode materials (even between metallurgically similar materials such as 304 versus 310 versus 316 stainless steels) in glycol-water mixtures. While not wanting to focus on these experiments (for the simple reason that we believe the glycol-water system to be even more complex than pure water breakdown), we do want to outline the salient points from these studies that a breakdown theory must eventually consider:

1. There are significant differences in breakdown strength for different materials.

2. The time to recover breakdown strength (i.e., after a breakdown event) is much longer for glycol-water mixtures than for pure water.

3. If observable bubbles are there, the breakdown will occur through the bubble. This suggests that observable bubbles are a weak link.

3. LONG-TIME-CONSTANT WATER EXPERIMENTS

The most important (to the formulation of a breakdown theory) of the experimental results described in Chapter IV for long-time-constant ($> 100 \mu\text{s}$) water experiments are:

1. Conditioning of the water is still required to reach high electric fields.
2. Industrial particulate (30- μm prefilter and 0.5- μm final filter) and organic (activated charcoal) filters improved the breakdown performance.
3. There is a time delay after a breakdown, before the conditioning cycle can be retraced back to the maximum breakdown strength. We are uncertain as to whether the reason for the time delay is related to our non-ionic contaminant theory, or the need for bubbles to dissipate, or some other reason.
4. Different electrode materials will ultimately have different maximum breakdown strengths, after the conditioning cycle is performed.

5. As in the ethylene glycol - water experiments, bubbles must be avoided. Therefore, careful and patient deaeration is required before the experiment starts.

B. OTHER SALIENT EXPERIMENTAL FEATURES THAT THEORY MUST EXPLAIN

In Chapter III, we described the experimental apparatus and procedure to run a typical experiment. We believe the following observations, gathered over a decade of experimentation on water breakdown, are important points that a breakdown theory must address.

1. SPURIOUS BREAKDOWNS

Often during the conditioning procedure, we would encounter a breakdown when we had expected that the electric field would be held off. Sometimes we could see a bubble or piece of dust, but often there was no apparent reason discernible. At that time we assumed that we had merely come up the conditioning curve too quickly. We found that if we waited for a little while (e.g., five to ten minutes), and then restarted at a lower electric field, we could proceed on the conditioning curve without breakdowns.

Now, we wonder if we were encountering small-probability events. It may be important for a breakdown theory to have a long low-probability tail for normally subcritical electric fields.

2. WATER FLOW AND TOTAL LIQUID VOLUME

In the beginning of the water experiments we had an experimental setup with a extra tank of water in the system (see Chapter III). While this water was not in the active flow of the experiment, it was connected to the circulating water by a pipe. Therefore a limited amount of diffusion was possible. The extra tank of water was used as a pressure regulator to handle surges from the pump or other sources. At the same time the height of the water served as a barrier to air infiltration. During this period in the experimental setup about twenty gallons of water were in the active cycle with another twenty or thirty gallons in the reserve tank.

By about 1985 we had improved the design of the water-conditioning system and no longer needed a pressure-surge tank. Then, only about twenty gallons of water were in the system.

The critical point to consider is conditioning of the water. The volume between the two electrode surfaces is only about 81 cm^3 . This means that at least 935 conditioning shots (20 gallons times $3,785.6 \text{ cm}^3$ per gallon divided by 81 cm^3 per conditioning shot) must be made with the Marx generator to hope to have conditioned each cm^3 of water at least one time. We never had that many conditioning shots in these experiments.

Therefore, if we hypothesize that conditioning of the water by non-breakdown shots from the Marx generator affected the breakdown strength, then we must also hypothesize that there is a trapped layer of water near the electrode surfaces in the test cell. This trapped layer of water might be only microns thick (or less) and might not freely interchange with the bulk water. Then, the full effect of all conditioning shots would be concentrated onto a small volume of water (less than or approximately 10^{-3} cm³) near the electrode interface.

Of course, conditioning might also affect only the electrode surface, but this doesn't seem likely because the filters act on the liquid, not the electrode materials, and filters affect breakdown strength. Much more likely is the explanation that filters affect the bulk water, which in turn affects the trapped layer of water next to the electrode surface.

In summary, the conditioning shots were too few in number to have affected the bulk water. The only region that could be affected by the conditioning shots is the region between the electrodes. In between the electrodes, only the water in the stagnant boundary layer next to the electrodes could be continuously exposed to the effects of the conditioning shots, because the bulk water molecules were being constantly swept away by the flow from the pump, to be replaced by unconditioned water. Therefore, we hypothesize that the stagnant region of water next to the electrodes has more of an effect on breakdown probability than the water in the middle of the gap.

3. TIME SCALE OF CONDITIONING SHOTS

There are two types of time scales that we want to discuss in this section. The first type is the length-of-time that conditioning shots affect the breakdown strength. Experimental experience clearly requires new conditioning each day, so eighteen hours (i.e. 4:00 PM on one day until 8:00 AM the next day) is clearly too long for the beneficial effect of conditioning to last. On the other hand, we occasionally take up to three hours to complete an unusually difficult experimental session and we don't need to restart the conditioning cycle. However, if conditioning is starting to fail at that time we might not be able to distinguish that effect from a normal breakdown event. Certainly an hour or two seems to be a valid albeit subjective lower limit for the conditioning effect to last.

The other time scale of interest is the time after a breakdown before electric field can be imposed on the water without an anomalously low breakdown. Experimental experience in glycol/water mixtures indicates that at least five or ten minutes is required after breakdown. In pure water such times could be as short as 45 seconds. Otherwise, breakdown is encountered at very low electric fields. After that time a slight retreat down the conditioning curve will avoid breakdown and the conditioning pattern can be restarted.

4. THERMAL-CYCLING EFFECTS ON BREAKDOWN

We attempted to maintain a constant temperature during most of the experiments, usually because we were trying to maintain a time constant for the

water greater than 100 μ s. Occasionally, our attempts at manual control of the system temperature (e.g., pieces of dry ice in a methanol bath in contact with a metal heat-exchanger plate) went awry, and we had temperature excursions of over five degrees Celsius. During either cooling or warming periods after these temperature excursions, we would observe the ionic purity of the water decrease and occasional notice more anomalously low breakdowns.

C. STATISTICAL TESTS OF AVERAGE BREAKDOWN FIELDS

In the following tables, the statistical analysis of breakdown data sets organized by electrode material is presented. The figure following each table will plot the mean value of the electric field at breakdown for the various electrode configurations. The error bars in the figures are the 95% confidence intervals. The data organized in these tables and figures differs from the presentation we have given in previous papers, because for this thesis we have grouped all the breakdown events into the statistics. In most previous papers, we excluded breakdowns that occurred early in the experimental run and only presented data relevant to establishing a best case threshold for breakdown, and often this was near the end of a run when we had ten shots without a breakdown. Our justification was that earlier breakdowns were not relevant to establishing a breakdown threshold.

Data taken before we discovered the beneficial effect of water filters is given below. Figure 5.2 demonstrates that a significant increase in breakdown strength is observed when a "better" grade of stainless steel than alloy 304 is

used for the electrode material. Similarly, Figure 5.3 demonstrates that 7075 aluminum is slightly inferior to other aluminum alloys. However, Figure 5.4 shows no significant increase in the mean breakdown field for mixed sets of 304 stainless steel and 2024 aluminum, although one polarity has a smaller 95% confidence interval. Similarly, Figure 5.5 shows no significant difference in the mean breakdown strength among gold, lead and mixed gold-lead electrode sets, although one polarity of the mixed set may be slightly different.

We also present below the data taken after we discovered the beneficial effects of water filters. Figure 5.6 shows that the breakdown strength for all of the stainless-steel alloys is approximately the same. This is in contrast to the data before filters in two ways: first, 304 stainless steel is no longer inferior to either 316 or 430 stainless steel, and second, the overall value of the breakdown field is considerably improved. The data is consistent with the following picture: impurities in the water (probably organic but not ionic impurities because the mixed-bed deionizers are effective against ionic impurities down to the parts-per-billion level, while total-organic-carbon [TOC] measurements from independent laboratories indicate a carbon-impurity level in the part-per-million range) were the determining factor for breakdown strength. The fact that pre-filter 304 stainless steel is significantly weaker can be explained if the surface of 304 stainless steel has a different (presumably greater) affinity for drawing suspended particles out of the bulk water to hover close to the electrode surface or perhaps even deposit on it. Unfortunately, we have found no literature support for this hypothesis, probably because the subject area is so unique.

The next set of electrodes of interest are the 5083 aluminum electrodes. The effects of filters are displayed in Figure 5.7. Unfortunately, the results are not as consistent as we'd like with the explanation we devised for the stainless-steel electrodes. Although there is a marked improvement in breakdown performance (i.e., the mean value of the breakdown field increases and the scatter goes down) when particulate filters are added to the water conditioning loop, there are deleterious effects on the breakdown performance (i.e., the mean breakdown field decreases while the scatter increases) when organic filters are added. We discount the possible explanation that the organic filters were contaminated, because these 5083-aluminum tests were performed just after the copper tests described in Figure 5.8, when the copper performance is excellent with filters, and just before the later copper tests depicted in Figure 5.9, when performance again was excellent. We have reviewed the test methodology and can find no flaw. The only explanation that we can think of for these 5083-aluminum results is that the third test set with organic filters was performed on one day (3/18/88) and never repeated. It is possible that organic contamination (which we could not monitor in real time) was introduced to the water system when the organic filter was added on that day.

The previous day was spent collecting data on the 5083-aluminum electrodes with particulate filters. Therefore, there was, at most, one morning for the organic filters to clean up the organic contaminants. If the filters work slowly or if extra contaminants were added during the installation of the filter, this could explain these results. Also, when we did the copper tests following the aluminum electrodes, we allowed at least several days for the organic filters to

condition the water. The fact is that we don't really know what caused the anomalous results with aluminum electrodes and organic filters, but we have pretty good circumstantial evidence that we simply did not allow enough time for the organic filters to function on 3/18/88. That mistake was not repeated on the following electrode set.

The data depicted in Figure 5.8, for copper electrodes with particulate filters and then particulate plus organic filters, once again is consistent with our hypothesis that contaminants affect breakdown strength. Breakdown performance improves (i.e. the mean breakdown field increases while the scatter decreases) when particulate filters or particulate plus organic filters are added to the water-conditioning loop before a copper experiment is performed.

Figure 5.9 depicts the breakdown performance for tungsten electrodes as well as later experiments on copper electrodes. As stated in a previous chapter, tungsten had been the choice material for an earlier breakdown theory because it possesses a high binding energy. Unfortunately, tungsten's breakdown performance is slightly worse than copper's, even with filters. One fact that is not portrayed by the graph is that tungsten's breakdown performance generally gets better as the day's experiments proceed, usually maximizing at about 200 kV/cm. However this is still slightly less than the maximum copper performance.

Also included in Figure 5.9 is later experimental data for copper electrodes. The middle result is for copper experiments run during the four weeks following the data run depicted in Figure 5.8. While the middle column does not equal the

one-day high of 3/11/88 in Figure 5.8, it still reflects the excellent performance of copper with filters. The right column of Figure 5.9 reflects data taken between September 1988 and February 1989 by Dr. Tom Berger and Dr. Bruce Hollmann. They ran experiments in our laboratory while one of us (Victor Gehman) was working on a Ph.D. degree at Virginia Tech, but with our long-range assistance and advice. They have kindly consented to our use of our joint-effort data in this thesis. We later discovered that, during this period, Dr. Hollmann had accidentally substituted the wrong kind of organic filter into our experimental setup. We can find no notation in the data log as to when this occurred and consequently cannot be sure how to interpret six months worth of data. The kind of filter substituted by Dr. Hollmann is designed to be used after a liquid has been cleared of most organic impurities and can be easily "burned out" and rendered ineffective if used in too contaminated an environment. We believe that this may be what happened and this would explain why the latest copper data is significantly reduced from earlier work. Once again, this is only indirect evidence that contaminant density affects breakdown performance.

Figure 5.10 depicts the breakdown performance of three separate electrode materials. The graphite contained binders that may have contributed to the relatively poor performance despite the presence of filters. Both the nickel and silver-coated brass electrodes were measured by Dr. Hollmann or Dr. Berger. While both demonstrate fairly good performance, they are still slightly inferior to copper and do not contribute to a major insight into breakdown performance.

In summary, the statistical evaluation of past breakdown performance yields direct and indirect evidence that contaminants in the water still dominate the breakdown performance of electrode materials. Some materials seem easier to clean-up than others or do not contribute to the contamination of the water as much. Better organic clean up and real-time monitoring of organic contamination seem to be required before we can settle the question of whether different electrode materials have different breakdown strengths and why.

Table 5.1: Stainless steel electrodes, no filters.

SS-NOFLT	Electrodes	304SS-NOFLT	Electrodes	316/430-NOFLT	Electrodes
Statistic	Value	Statistic	Value	Statistic	Value
Mean	137.2	Mean	128.2	Mean	172.0
Standard Error	6.3	Standard Error	5.3	Standard Error	5.9
Median	135.6	Median	134.8	Median	175.8
Mode	134.8	Mode	134.8	Mode	#N/A
Standard Deviation	23.8	Standard Deviation	16.7	Standard Deviation	10.2
Variance	567.8	Variance	279.9	Variance	104.8
Kurtosis	0.66	Kurtosis	2.98	Kurtosis	#DIV/0!
Skewness	0.065	Skewness	-1.76	Skewness	-1.43
Range	91.1	Range	55.9	Range	19.4
Minimum	88.7	Minimum	88.7	Minimum	160.4
Maximum	179.8	Maximum	144.6	Maximum	179.8
Sum	1920.8	Sum	1282.7	Sum	516.0
Count	14	Count	10	Count	3
Confidence Level (95%)	12.5	Confidence Level (95%)	10.4	Confidence Level (95%)	11.6

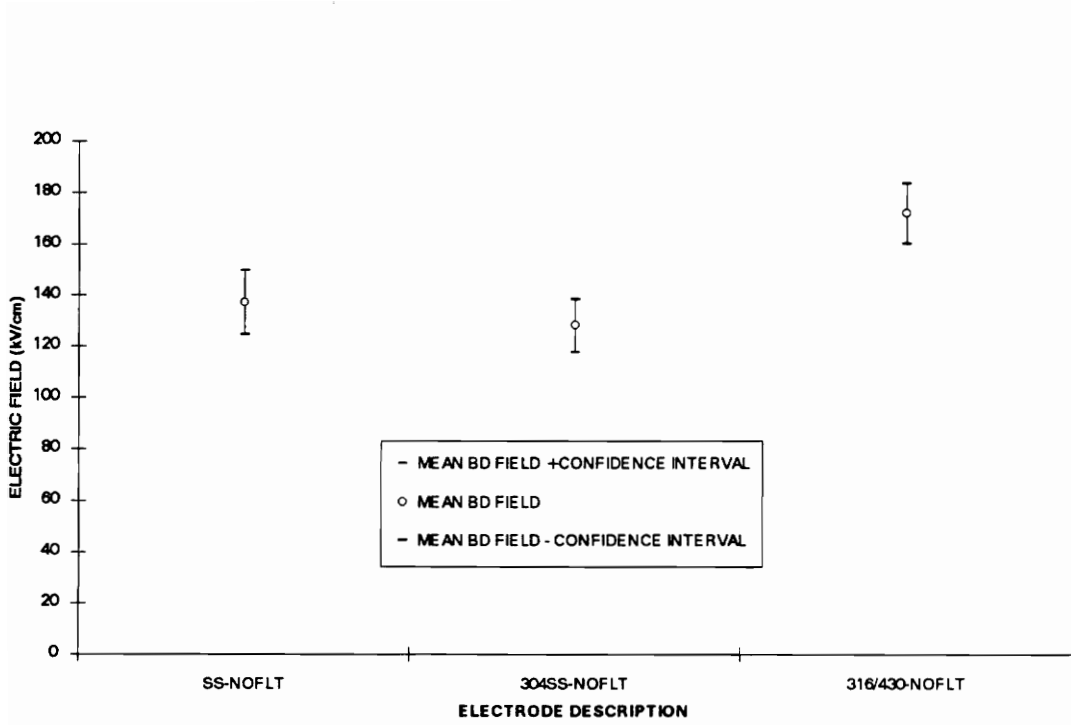


Figure 5.1 Plot of the mean breakdown field plus or minus the 95% confidence interval for stainless-steel electrodes with no filters.

Table 5.2: Aluminum electrodes, no filters.

AL-NOFLT	Electrodes	NOT 7075- NOFLT	Electrodes	7075-NOFLT	Electrodes
Statistic	Value	Statistic	Value	Statistic	Value
Mean	159.5	Mean	173.1	Mean	146.0
Standard Error	4.6	Standard Error	4.3	Standard Error	3.2
Median	158.0	Median	170.3	Median	144.6
Mode	156.9	Mode	#N/A	Mode	156.9
Standard Deviation	17.1	Standard Deviation	11.5	Standard Deviation	8.6
Variance	291.6	Variance	131.4	Variance	73.8
Kurtosis	-0.18	Kurtosis	1.98	Kurtosis	-1.17
Skewness	0.43	Skewness	1.2	Skewness	0.18
Range	60.2	Range	35.8	Range	22.1
Minimum	134.8	Minimum	159.2	Minimum	134.8
Maximum	195	Maximum	195	Maximum	156.9
Sum	2233.4	Sum	1211.4	Sum	1022.1
Count	14	Count	7	Count	7
Confidence Level (95%)	8.9	Confidence Level (95%)	8.5	Confidence Level (95%)	6.4

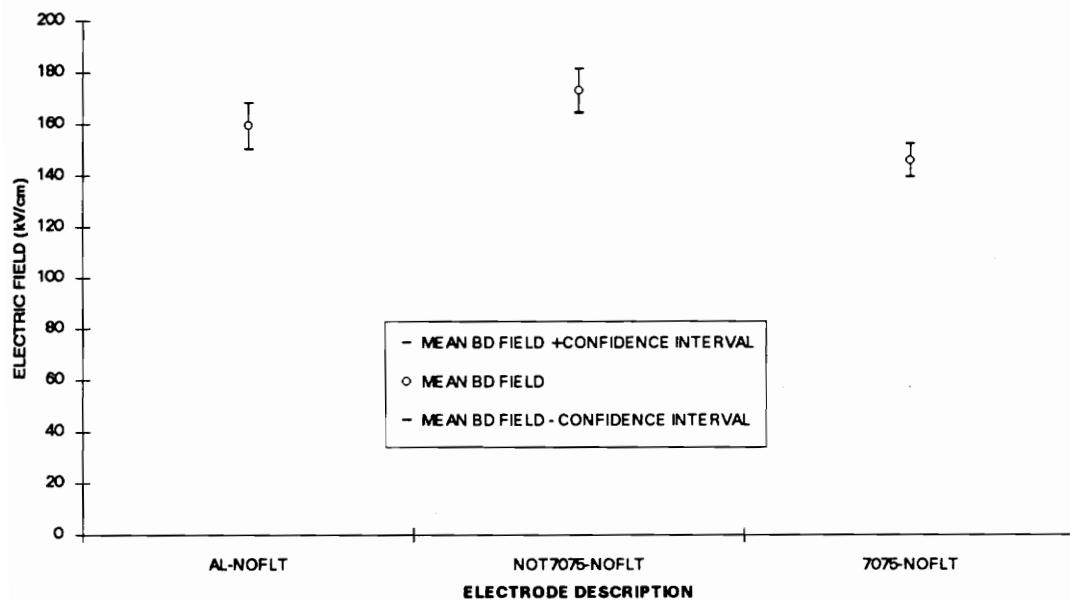


Figure 5.2 Plot of the mean breakdown field plus or minus the 95% confidence interval for aluminum electrodes with no filters.

Table 5.3: Mixed 304 stainless steel, 2024 aluminum electrode sets, with no filters.

304 + ,2024-NOFLT	Electrodes	2024 + 304-NOFLT	Electrodes
Statistic	Value	Statistic	Value
Mean	140.4	Mean	153.8
Standard Error	6.0	Standard Error	3.7
Median	143.1	Median	156.9
Mode	143.1	Mode	156.9
Standard Deviation	19.8	Standard Deviation	13.0
Variance	391.5	Variance	168.4
Kurtosis	-1.1	Kurtosis	0.11
Skewness	-0.23	Skewness	-1.0
Range	55.9	Range	41.2
Minimum	110.8	Minimum	128.4
Maximum	166.7	Maximum	169.6
Sum	1544.0	Sum	1845.4
Count	11	Count	12
Confidence Level (95%)	11.7	Confidence Level (95%)	7.3

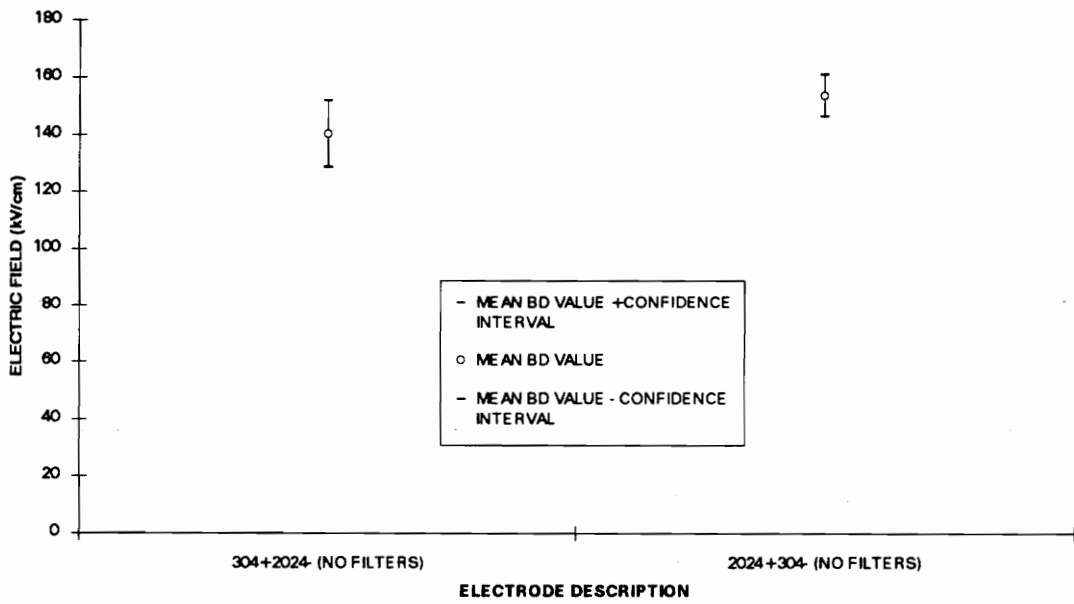


Figure 5.3 Plot of the mean breakdown field plus or minus the 95% confidence interval for 304 stainless steel, 2024 aluminum electrode sets with no filters.

Table 5.4: Pure gold, pure lead and mixed electrodes, no filters

AU - NOFLT	Elec- trodes	AU + ,PB- NOFLT	Elec- trodes	PB + ,AU- NOFLT	Elec- trodes	PB- NOFLT	Elec- trodes
Statistic	Value	Statistic	Value	Statistic	Value	Statistic	Value
Mean	168.8	Mean	164.7	Mean	155.6	Mean	169.3
Standard Error	3.4	Standard Error	2.9	Standard Error	2.9	Standard Error	4.1
Median	174.0	Median	167.6	Median	156.9	Median	169.3
Mode	180.3	Mode	167.6	Mode	147.1	Mode	168.4
Standard Deviation	13.9	Standard Deviation	5.1	Standard Deviation	8.2	Standard Deviation	11.7
Variance	192.9	Variance	26.0	Variance	67.0	Variance	136.7
Kurtosis	1.269	Kurtosis	#DIV/0!	Kurtosis	-1.4	Kurtosis	0.22
Skewnes s	-1.4	Skewnes s	-1.7	Skewnes s	0.28	Skewnes s	-0.32
Range	48.1	Range	8.8	Range	19.6	Range	35.3
Minimum	134.6	Minimum	158.8	Minimum	147.1	Minimum	148.9
Maximum	182.7	Maximum	167.6	Maximum	166.7	Maximum	184.2
Sum	2869.9	Sum	494.1	Sum	1245.1	Sum	1354.2
Count	17	Count	3	Count	8	Count	8
Confiden ce Level (95%)	6.6	Confiden ce Level (95%)	5.8	Confiden ce Level (95%)	5.7	Confiden ce Level (95%)	8.1

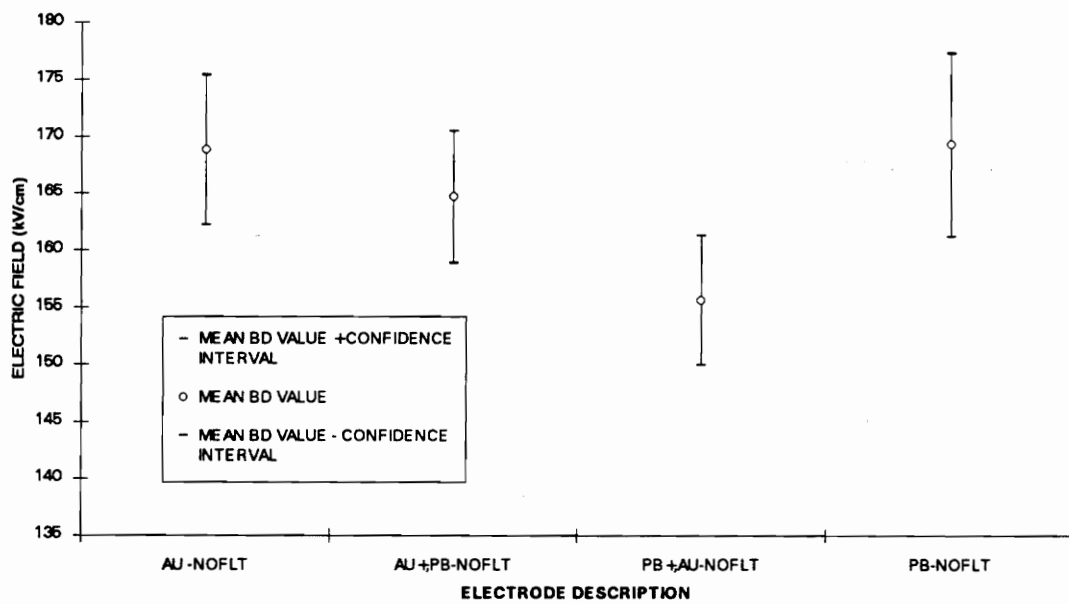


Figure 5.4 Plot of the mean breakdown field plus or minus the 95% confidence interval for pure gold, pure lead and mixed electrodes, with no filters.

Table 5.5: Stainless steel electrodes, with filters.

SS-FLT	Electrodes	304SS-FLT	Electrodes	316,430-FLT	Electrodes
Statistic	Value	Statistic	Value	Statistic	Value
Mean	184.5	Mean	186.7	Mean	181.0
Standard Error	2.3	Standard Error	3.1	Standard Error	2.8
Median	188.1	Median	189.1	Median	179.3
Mode	189.1	Mode	189.1	Mode	#N/A
Standard Deviation	9.1	Standard Deviation	9.9	Standard Deviation	6.9
Variance	83.1	Variance	98.6	Variance	48.2
Kurtosis	-0.63	Kurtosis	0.76	Kurtosis	3.3
Skewness	-0.24	Skewness	-1.0	Skewness	1.7
Range	31.8	Range	31.8	Range	19.4
Minimum	169.2	Minimum	169.2	Minimum	174.8
Maximum	201.0	Maximum	201.0	Maximum	194.2
Sum	2952.8	Sum	1866.6	Sum	1086.2
Count	16	Count	10	Count	6
Confidence Level (95%)	4.5	Confidence Level (95%)	6.2	Confidence Level (95%)	5.6

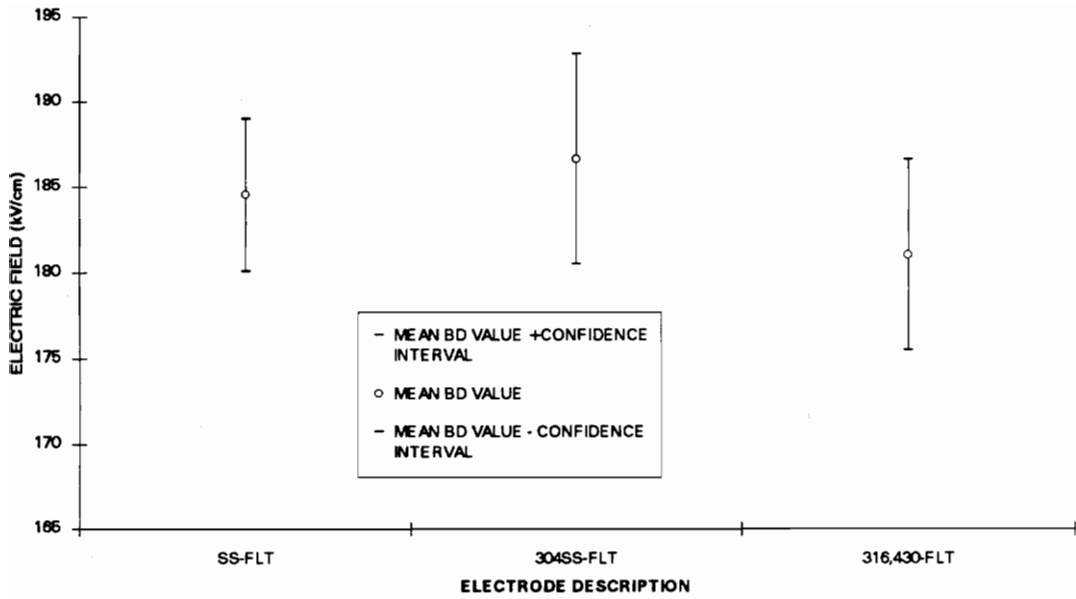


Figure 5.5 Plot of the mean breakdown field plus or minus the 95% confidence interval for stainless steel electrodes, with filters.

Table 5.6: Aluminum 5083-alloy electrodes, with filters.

5083AL&NO FLTR	Electrodes	5083AL & PART. FILTER	Electrodes	5083AL&ALL FLTR	Electrodes
Statistic	Value	Statistic	Value	Statistic	Value
Mean	139.8	Mean	152	Mean	137.5
Standard Error	2.9	Standard Error	1	Standard Error	2.8
Median	135	Median	153	Median	135
Mode	135	Mode	153	Mode	132
Standard Deviation	6.6	Standard Deviation	1.7	Standard Deviation	6.8
Variance	43.2	Variance	3	Variance	46.3
Kurtosis	-3.3	Kurtosis	#DIV/0!	Kurtosis	-1.1
Skewness	0.61	Skewness	-1.7	Skewness	0.79
Range	12	Range	3	Range	16
Minimum	135	Minimum	150	Minimum	132
Maximum	147	Maximum	153	Maximum	148
Sum	699	Sum	456	Sum	825
Count	5	Count	3	Count	6
Confidence Level (95%)	5.8	Confidence Level (95%)	2.0	Confidence Level (95%)	5.4

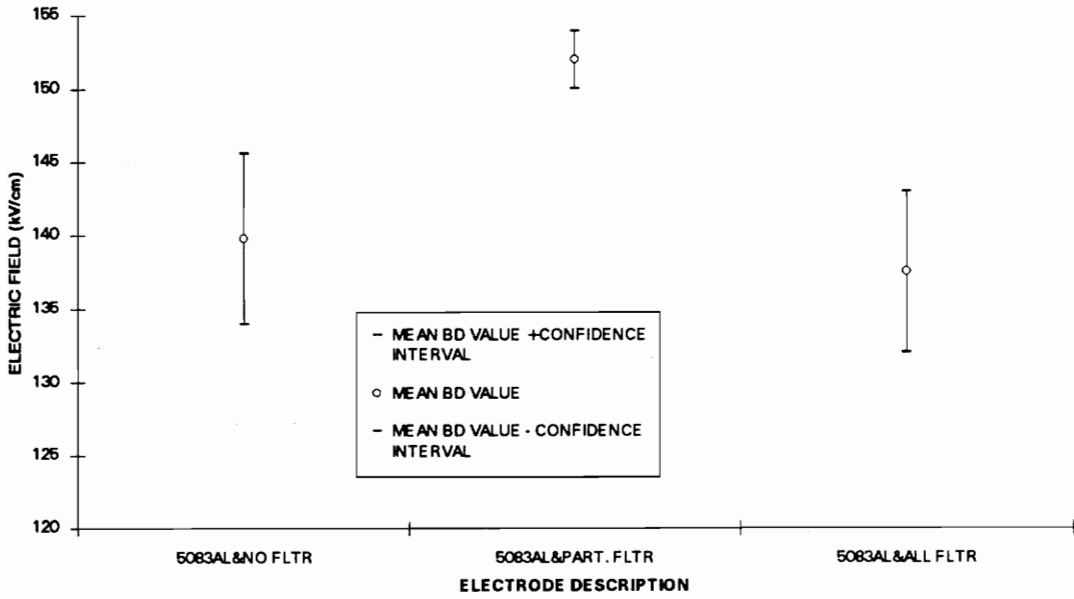


Figure 5.6 Plot of the mean breakdown field plus or minus the 95% confidence interval for aluminum 5083-alloy electrodes, with filters.

Table 5.7: A series of experiments on copper demonstrating the efficacy of various filters.

CU-NOFLT- 3/4/88	Electrodes	CU-P-FLT- 3/10/88	Electrodes	CU-FLT- 3/11/88	Electrodes
Statistic	Value	Statistic	Value	Statistic	Value
Mean	161.1	Mean	186.1	Mean	222.8
Standard Error	8.4	Standard Error	2.0	Standard Error	2.0
Median	162.4	Median	186.1	Median	224.8
Mode	#N/A	Mode	#N/A	Mode	224.8
Standard Deviation	16.8	Standard Deviation	2.8	Standard Deviation	3.4
Variance	281.3	Variance	7.8	Variance	11.8
Kurtosis	-4.4	Kurtosis	#DIV/0!	Kurtosis	#DIV/0!
Skewness	-0.19	Skewness	#DIV/0!	Skewness	-1.7
Range	34.7	Range	4.0	Range	5.9
Minimum	142.6	Minimum	184.2	Minimum	218.8
Maximum	177.2	Maximum	188.1	Maximum	224.8
Sum	644.6	Sum	372.3	Sum	668.3
Count	4	Count	2	Count	3
Confidence Level (95%)	16.4	Confidence Level (95%)	3.9	Confidence Level (95%)	3.9

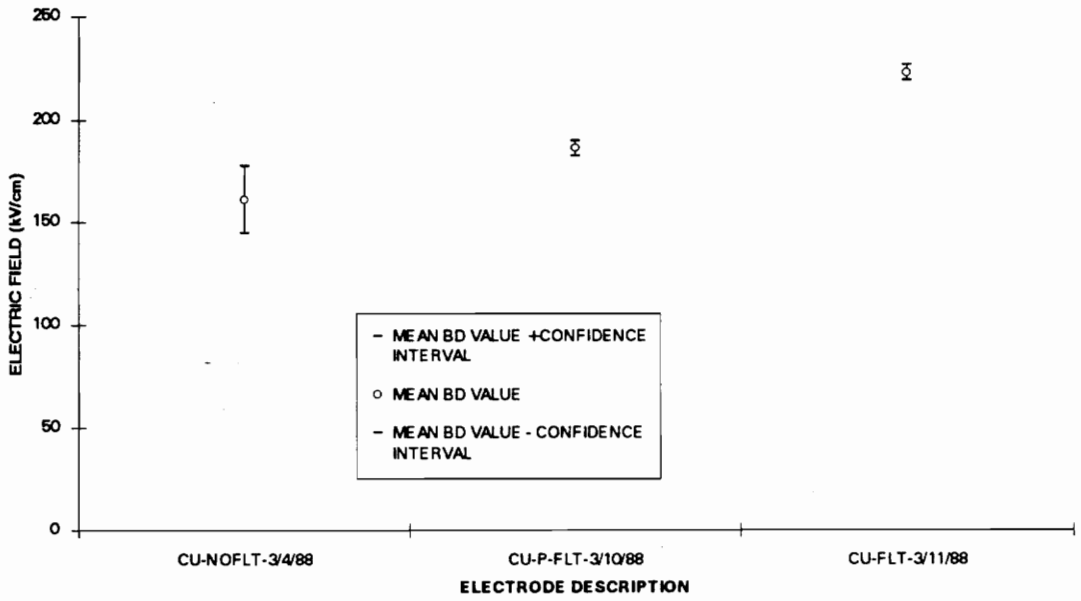


Figure 5.7 Plot of the mean breakdown field plus or minus the 95% confidence interval for a series of experiments on copper demonstrating the efficacy of various filter combinations. On the left is no filters, in the center is only particulate filters, and on the right is the combination of particulate plus organic filter.

Table 5.8: Other miscellaneous copper data and tungsten data, with filters.

W-FLT	Electrodes	CU-FLT-3/23-4/15/88	Electrodes	CU-BZH,TLB	Electrodes
Statistic	Value	Statistic	Value	Statistic	Value
Mean	163.2	Mean	186.6	Mean	168.7
Standard Error	3.0	Standard Error	3.6	Standard Error	2.9
Median	161.2	Median	186.7	Median	172.8
Mode	155.0	Mode	170.4	Mode	179.3
Standard Deviation	20.2	Standard Deviation	21.4	Standard Deviation	20.1
Variance	407.9	Variance	456.8	Variance	403.8
Kurtosis	0.66	Kurtosis	0.14	Kurtosis	-0.29
Skewness	0.099	Skewness	-0.17	Skewness	-0.27
Range	104.3	Range	97.6	Range	93.3
Minimum	107.7	Minimum	133.0	Minimum	123.4
Maximum	212	Maximum	230.6	Maximum	216.7
Sum	7343.0	Sum	6529.5	Sum	8096.4
Count	45	Count	35	Count	48
Confidence Level (95%)	5.9	Confidence Level (95%)	7.1	Confidence Level (95%)	5.7

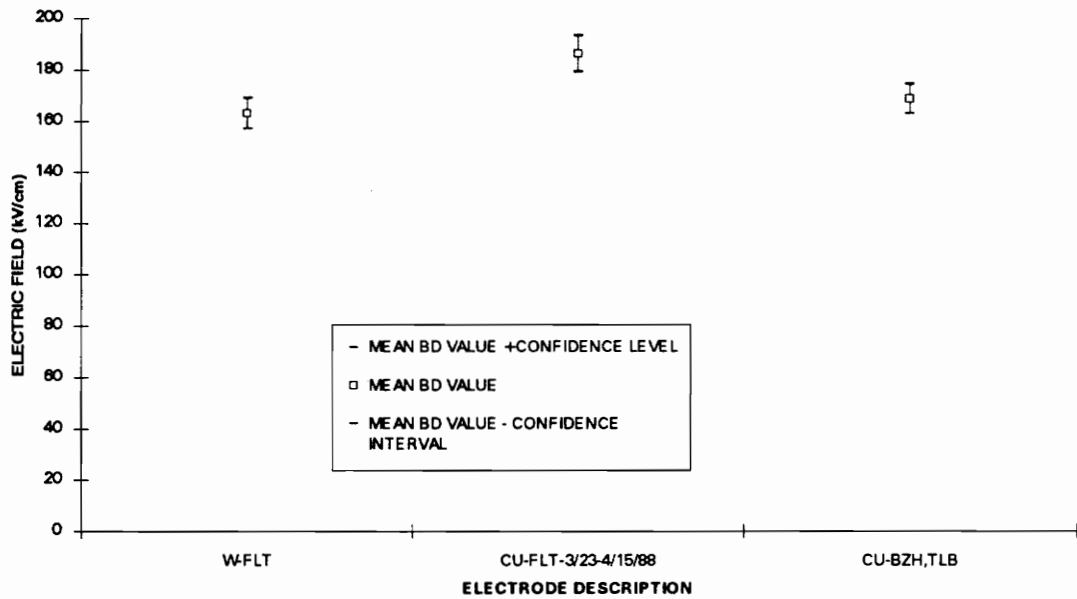


Figure 5.8 Plot of the mean breakdown field plus or minus the 95% confidence interval for tungsten and other copper electrodes, with filters.

Table 5.9: Other electrode sets.

GRAPHITE	Electrodes	NI-TLB,BZH	Electrodes	AG ON	Electrodes
				BRASS-BZH	
Statistic	Value	Statistic	Value	Statistic	Value
Mean	137.2	Mean	191.4	Mean	191.6
Standard Error	5.6	Standard Error	4.3	Standard Error	5.8
Median	147.9	Median	200	Median	197.1
Mode	159.4	Mode	204	Mode	160
Standard Deviation	25.5	Standard Deviation	21.7	Standard Deviation	29.6
Variance	650.3	Variance	468.9	Variance	875.2
Kurtosis	-1.3	Kurtosis	-1.1	Kurtosis	0.40
Skewness	-0.52	Skewness	-0.61	Skewness	-0.84
Range	83.3	Range	68.0	Range	118.6
Minimum	89.6	Minimum	153.3	Minimum	116.7
Maximum	172.9	Maximum	221.3	Maximum	235.3
Sum	2880.2	Sum	4784.7	Sum	4982.0
Count	21	Count	25	Count	26
Confidence Level (95%)	10.9	Confidence Level (95%)	8.5	Confidence Level (95%)	11.4

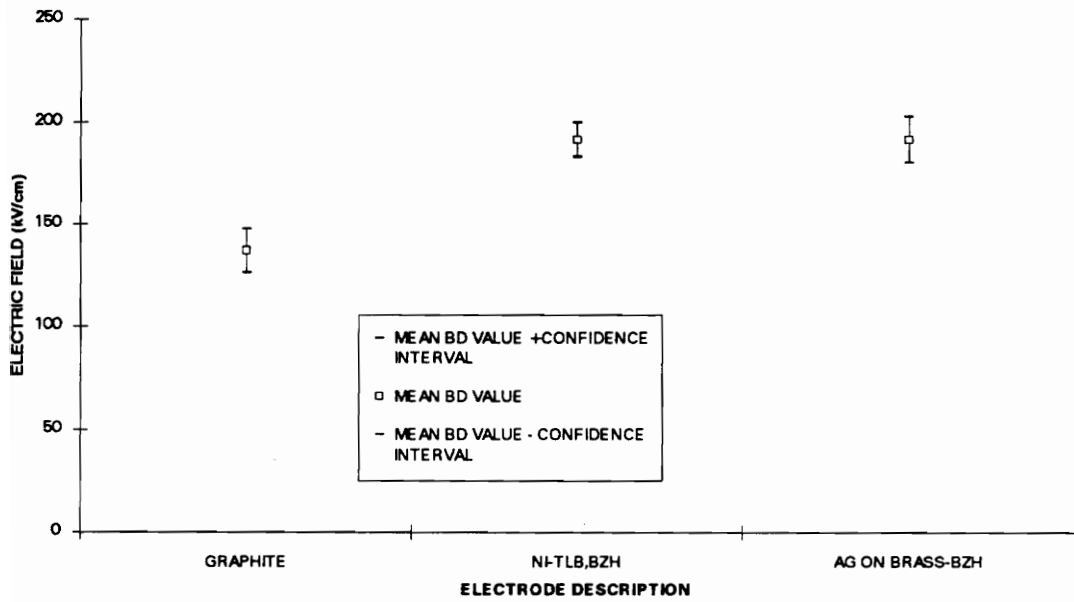


Figure 5.9 Plot of the mean breakdown field plus or minus the 95% confidence interval for graphite, nickel and silver electrodes, with filters.

D. CAN BUBBLES BE A SOURCE OF "CONDITIONING"?

1. HISTORICAL INTEREST

As stated in Chapter 2, researchers have suspected that bubbles in the dielectric, possibly near the electrode surface, could explain some of the breakdown behavior observed in liquids. Bubbles are particularly useful for explaining the effects of pressure on breakdown performance, but these studies are done in low-dielectric-constant insulating liquids like transformer oil and heptane.

We have seen the effects of bubbles in high-purity water in our laboratory. From the late 1970's, Gripshover and Fenneman observed that a bubble sitting on the electrode surface was usually the site for the next breakdown. The larger the bubble the more likely the next breakdown would occur at that spot. When the bubble diameter is much smaller than the electrode gap (i.e., diameter $\ll 0.1 \times$ gap distance), then we can't see the bubbles very well and can not predict where the next breakdown will occur. We have observed these effects in both water and glycol-water mixtures. This is why the deaeration column is always in the conditioning loop for the liquid, the flow of freshly deaered water is aimed at the middle of the gap, and the experiment is not started until there are no readily observable bubbles in the electrode gap and the partial pressure in the deaeration column is close to the partial pressure of water.

2. ELECTRIC FIELD ENHANCEMENT CAUSES BUBBLES

Once we have thoroughly deaired the water, there are few sources of bubbles in the experiment. The only causes we have conjectured are: (1) Ohmic heating caused by locally high current densities, in turn caused by sharp contours or points on the electrode surface, just as posited by the other theorists listed in Chapter 2, and (2) electrolysis of the water.

3. TIME-SCALE AND ENERGY CONSIDERATIONS

The only time there are significant currents being emitted from the electrode surface into the water is during the experiment. Certainly, on the shot when a breakdown actually happens, there is current for at most a few tens of microseconds. When a breakdown doesn't occur, the current pulse can last for hundreds of microseconds. Between each shot, a minimum time of approximately thirty seconds is required to recharge the Marx generator.

If the water capacitor has a planar area (A) of 81 square centimeters (i.e., 8.1×10^{-3} square meters), a gap spacing (d) of 1 centimeter (or 0.01 meters), and a dielectric constant (ϵ_r) of approximately 80, then it has a capacitance, C , given approximately by

$$C = \epsilon_r \epsilon_0 \frac{A}{d} = 5.7 \times 10^{-10} \text{ Farads,} \quad (5.2)$$

where ϵ_0 is the permittivity of free space (8.85×10^{-12} Farads/meter). Therefore, if the charging voltage (V) is approximately 150 kV, then the energy stored in the water capacitor is:

$$E = \frac{1}{2} C V^2 = 6.4 \text{ Joules.} \quad (5.3)$$

This is the energy typically available to vaporize water during a conditioning shot. We calculate that the change in enthalpy for water from a liquid at 0 C to a gas at 100 C is 2,678 kJ/kg. Therefore, we can generate at most (i.e., in the highly unlikely event that all the energy stored in the water capacitor is used to generate water vapor) about $2.4 \times 10^{-3} \text{ cm}^3$ of water vapor per conditioning shot by Ohmic heating. While this may not seem like much, it is sufficient to evenly coat both electrodes with a vapor layer 0.15 microns thick. Our previous theory indicates that this is a thick enough to be a significant factor in breakdown initiation.

Unfortunately, these calculations indicate that increased conditioning shots should weaken the dielectric, but this is exactly the opposite of what we see during experiments. Therefore, we conclude that the bubbles produced during conditioning shots (if any) have an insignificant effect upon breakdown.

It is possible that conditioning shots do shake loose bubbles that adhered to electrode surface and resisted the water current produced by the pumps. However, we have kept careful watch on the dielectric gap over the years with the transit optics. We have occasionally observed bubbles in the gap and, when

we have, the breakdown occurs at that spot. But most of the time during conditioning, we can't see any bubbles. We estimate that the lower limit to the diameter of bubble that we can observe is about 0.1 mm. While this is still large compared to the void-initiation sizes predicted by our previous breakdown theory (in Chapter Two, the theory concerning ions emitted from the electrode to produce voids), we have no evidence that this phenomenon actually occurs. Therefore, we cannot discount the idea that conditioning shots are shaking loose microscopic bubbles from the surface of the electrode, and this mechanism would be consistent with experiment, because it predicts that conditioning shots will improve breakdown performance.

E. CAN AGGREGATED DIELECTRIC INCLUSIONS EXPLAIN "CONDITIONING"?

1. FLOW CLUES TO LOCATION OF CRITICAL INCLUSIONS

The small volume of the dielectric gap compared to the large flow rate and the time between conditioning shots assures that the water in the small volume between the electrodes is exchanged many times between conditioning shots. Therefore, as stated previously in this chapter, we believe that the only location possible for breakdown-causing dielectric inclusions is in the quiescent zone very near each electrode surface. These small volumes will not be greatly disturbed by the bulk flow of the purification system. The inevitable low-level contaminant of the water will reside here for much longer times than in middle of the gap. Because conditioning shots do increase the breakdown strength of the

dielectric gap, we conclude that if the conditioning shots are breaking up dielectric contaminants (i.e., the mechanism which explains the beneficial effect of conditioning on breakdown strength) then the important action takes place in these small volumes near the electrodes. Otherwise, in the rest of the gap fresh contaminants are being constantly swept in, plus the volume of water "treated" with conditioning shots is smaller than the total water volume.

2. ARE LOW ϵ INCLUSIONS ATTRACTED TO THE ELECTRODE SURFACE?

First of all, we know that there are non-ionic contaminants in deionized-water systems. Our impetus to include activated-charcoal filters into the purification system came when a routine commercial analysis revealed that our ionically pure water had a total-organic-carbon content about three times higher than ordinary tap water! The technical representatives at Barnstead Corp. explained that the deionizer tanks were good breeding sites for bacteria. It was probably bacteria and their decaying remains that formed the bulk of our carbon contamination. Another source was the resin beads of the deionizers which broke down and leached long polymer chains into the water. At about the same time, our contacts in the high-power laser community⁵³ told us that the use of Tygon® tubing was being discontinued for the cooling system because Tygon released elastomers into the purified water which later caused problems with the laser heads. At that time we had a considerable amount of Tygon tubing in the water-purification system.

⁵³Copley, John, employee at NSWCCD, private communication circa 1984.

After improving our water piping by: cleaning, including a UV (ultraviolet) sterilizer, removing the Tygon tubing, and using activated-charcoal filters, we found the breakdown strength increase from 120-160 kV/cm up to 180-220 kV/cm depending on the electrode materials used. We considered this to be significant.

While we have no direct observations to support our hypothesis concerning low-dielectric-constant impurities near the electrode surface, there is indirect evidence for this phenomenon. Different electrode materials have different breakdown strength. There are non-ionic contaminants in high-purity water. There is a quiescent zone near the electrode surface where contaminants would be less affected by the water flow than in the bulk of the dielectric. In the literature, high-speed optical recordings of impulse breakdown always find breakdown initiation at an electrode surface. Measurements of ionic purity indicate that ionic contaminants are in the parts-per-billion range while typical organic-contaminant levels are orders-of-magnitude higher. All of these indirect observations are consistent with low- ϵ contaminants (or microscopic bubbles, which could behave like low- ϵ inclusions, electrically) near the electrode surface.

3. VAN DER WAAL FORCES AND BINDING ENERGY FOR INCLUSIONS

There are non-ionic contaminants in the water. Given that it's likely that at least some of the species of contaminants are polar, then there will be Van der Waal forces between at least some of the particles. They will

accumulate or accrete through contact resulting from the random Brownian motion in the water. There should be a population spectrum of different sizes of particles. Conceivably, the longer particles oriented along the impulse electric field should affect breakdown, because they will have a higher voltage across their length than their short counterparts. Thus, the long particles could breakdown in the bulk or along the surface and serve as a source for secondary electrons. Thus, large (i.e., long) contaminant clusters could reduce breakdown strength.

Conditioning is now seen as a means to break up the larger clusters. The more conditioning shots, the more large clusters that will be broken up, hence the lower probability of breakdown for later shots. This agrees with experiment.

4. DISTRIBUTION OF INCLUSION SIZES - GROWTH DYNAMICS

We have considered simulating the growth and dynamics of the non-ionic contaminants (hereafter called dustballs). Basically, our idea is to do a Monte Carlo simulation on the computer of the dustballs life cycle. The program would take a fixed number of dustballs, assign them a random location and initial velocity in the electrode gap, and solve their equations of motion by doing tiny time steps. Brownian motion would be simulated by randomly choosing forces, called η , and applying them to the equations of motion:

$$m_i \ddot{\mathbf{a}}_i = \bar{\mathbf{F}}_i + \bar{\boldsymbol{\eta}} \quad (5.4)$$

where

$$\vec{F}_i = -\vec{\nabla}_i \sum_{j \neq i} V(|\vec{r}_i - \vec{r}_j|) \quad , \text{ and} \quad (5.5)$$

$$V(r) = V_0 \left[\left(\frac{\sigma}{r} \right)^{12} - \left(\frac{\sigma}{r} \right)^6 \right] \quad . \quad (5.6)$$

In equations (5.4) and (5.5), m_i is the mass of the i 'th dustball, a_i is the acceleration of the i 'th dustball, F_i is the force on the i 'th particle due to its Coulombic and/or dielectric interaction with the other dustballs at locations r_j , and η is the random force due to Brownian motion.

The sequence of events in the computer simulation would be as follows:

1. A finite number of dustballs will be assigned random positions and velocities within a three-dimensional grid.
2. Then, a random vector, η , will be added to each dustball to simulate the effects of Brownian motion. Each directional component of η will be randomly chosen from a gaussian distribution. The amplitude or width of the gaussian is not determined, but research into the literature might resolve this issue.
3. Next, an attractive force law, F_i between the dustballs will be formulated for the dustballs. This force law will be calculated from a Lennard-Jones potential (equation 5.6).

4. Then the position and velocity of each dustball will be updated according to equations 5.7 and 5.8:

$$\bar{x}_i(t + \Delta t) = \bar{x}_i(t) + \bar{v}_i(t) \Delta t + \frac{1}{2} \left(\frac{\bar{F}}{m} + \frac{\bar{\eta}}{m} \right) (\Delta t)^2 \quad (5.7)$$

$$\bar{v}_i(t + \Delta t) = \bar{v}_i(t) + \left(\frac{\bar{F}}{m} + \frac{\bar{\eta}}{m} \right) \Delta t \quad (5.8)$$

5. Now the iteration continues as steps 2 through 5 are repeated.

We would then have a model to predict the size of the dustballs as a function of time. However, without a more physically grounded justification for the size and form of the attractive potentials or any firm knowledge of forces that would breakup the dustballs (other than conditioning shots), we would be engaging in curve fitting. That is, we would adjust the size of the parameters until the answer agreed with our estimates for the dustball size. This would not increase our understanding of the mechanism for water breakdown. Until we have high-quality physical parameters for low-concentration, non-ionic contaminants in water, we can't do meaningful computer simulation.

5. CONDITIONING BREAKUP OF INCLUSIONS

What can break up clusters of dustballs? Filters can and we observed improved breakdown performance when we use filters. Conditioning shots could also break up dustballs.

As we condition the gap, we are dumping energy into the water. Equation 5.9 specifies that amount of energy,

$$\text{Energy} = k \sum_n E_n^2 \quad (5.9)$$

where k is the proportionality constant containing the capacitance of the water gap and E_n is the electric field in the water on the n^{th} conditioning shot.

Unfortunately, we don't keep a record of each conditioning shot in the Excel database, because the data is too unwieldy. We do keep a record of the first conditioning shot and electric field, E_0 . We also have followed a conditioning pattern of ten shots at one voltage and then a small increment in voltage and then another ten shots, and so on. Therefore, we should be able to make a good estimate of E_n using equation 5.10,

$$E_n = E_0 + \left[\frac{E_f - E_0}{n_f} \right] \times n \quad (5.10)$$

where n_f is the number of the final conditioning shot. We can use equations 5.9 and 5.10 to estimate the amount of energy dumped into the water before a given breakdown event. Presumably, some part of the conditioning energy breaks up

dustballs (probably breaking large dustballs into greater numbers of smaller dustballs) and contributes to a higher probability of larger breakdown strength. Another natural prediction of this hypothesis is that there would be a diminishing effect of conditioning. That is, after breaking up the really large dustballs requiring a certain amount of energy, continued conditioning will not appreciably affect breakdown strength. Furthermore, if an actual breakdown event would be required to break up particularly tough dustballs, then we could be in a situation where the second (or subsequent) breakdown might be due to the electrode surface. Figure 5.11 is a schematic summary of these ideas.

Because of the typical pattern of the conditioning shots, the first breakdown value (for the electric field) will be related to the amount of energy dumped into the water during conditioning. Therefore, the size of the largest dustball that could be broken up by conditioning should be related to the inverse of the value of the electric field at the first breakdown, as in equation 5.11:

$$L_{\max} \propto \frac{1}{E} \quad (5.11)$$

The amount of conditioning energy required for a breakdown should depend on the size of the maximum dustball. Thus, plotting an estimate for the conditioning energy versus $(1/E)$ should reveal the exponential dependence of breakdown on L_{\max} .

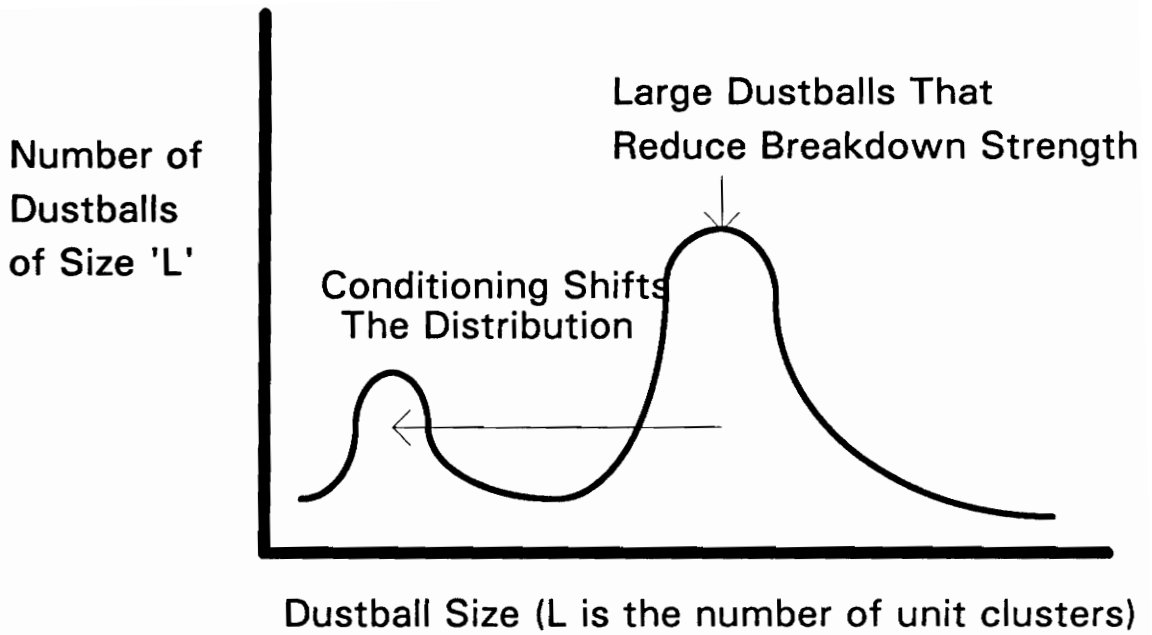


Figure 5.10. Schematic of the general idea of dustball size distributions and conditioning effects.

We have organized the data in a database (see the appendix) with regard to: electrode material, immersion time, temperature, filters, and ionic purity of water. Estimated conditioning energy (called approximate energy) is plotted versus $(1/E)$ in the following figures. We were trying to analyze the data and look for trends, such as the highest breakdown strength corresponds to the greatest conditioning energy. This is the general trend in the data and supports our breakdown model that concludes that contaminants near the electrode control breakdown behavior. We could not deduce any further conclusions from the these graphs, but the log-log plots (later in the chapter) were more interesting.

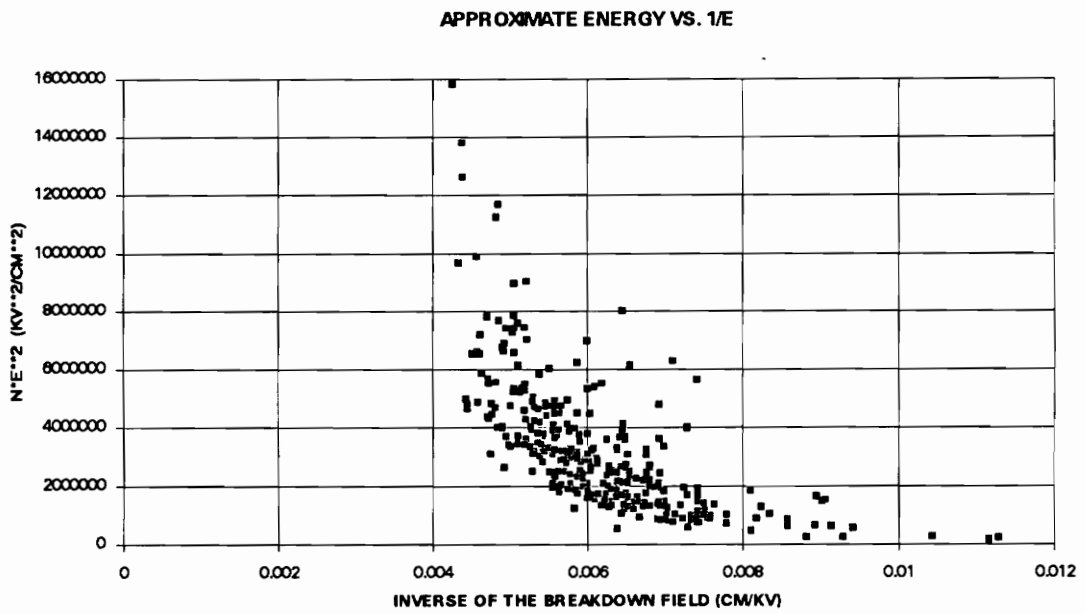


Figure 5.11. The plot of approximate energy (arbitrary units) versus $1/E$ for all the experiments in the database.

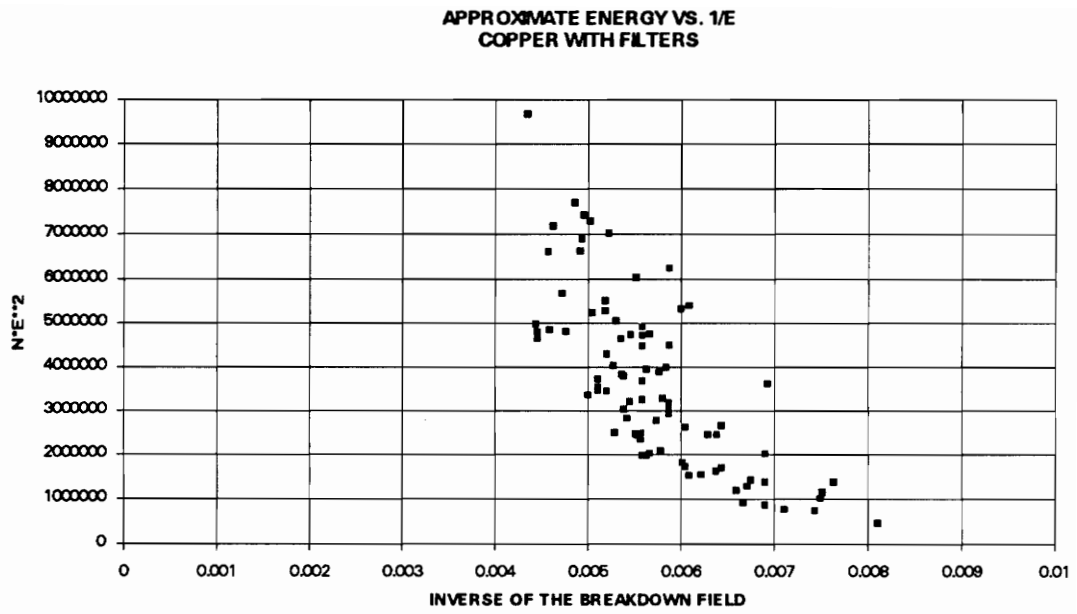


Figure 5.12. Same plot for copper electrodes with filters.

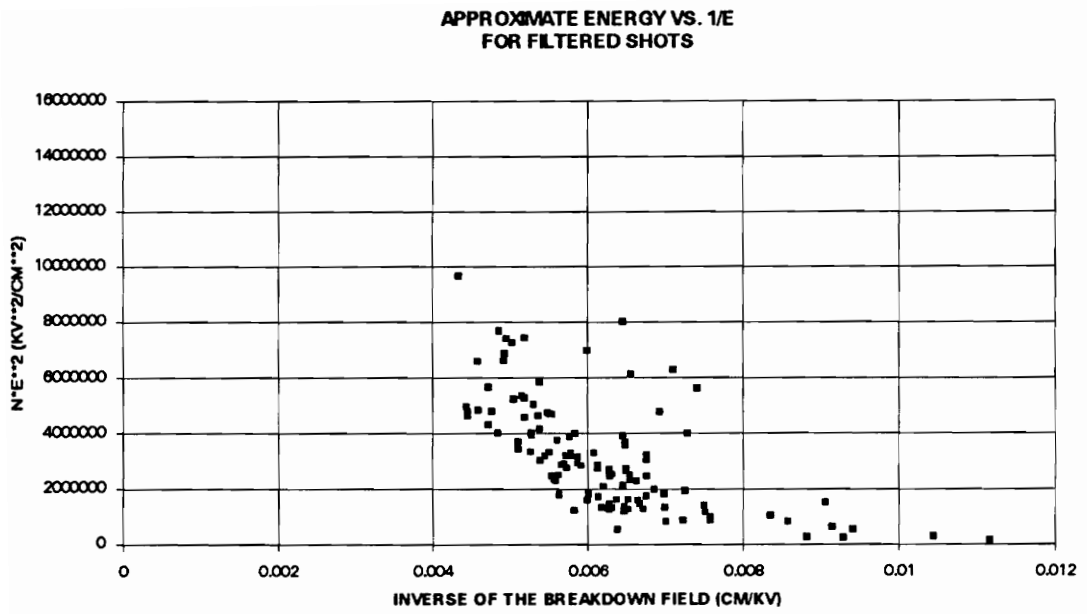


Figure 5.13. Same plot with filters for all electrode materials.

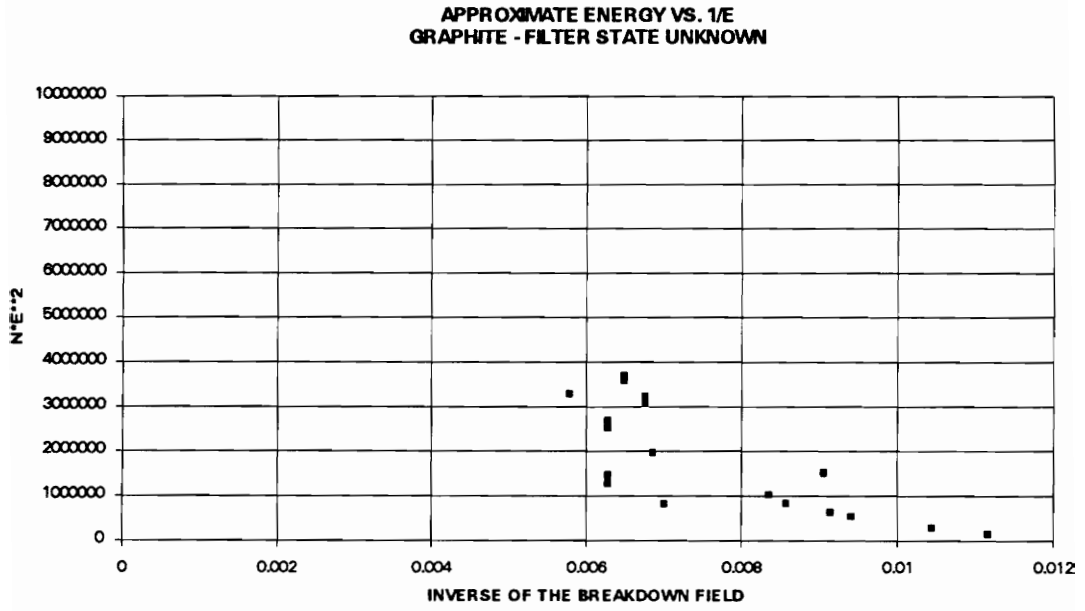


Figure 5.14. Same plot for filters and graphite electrodes.

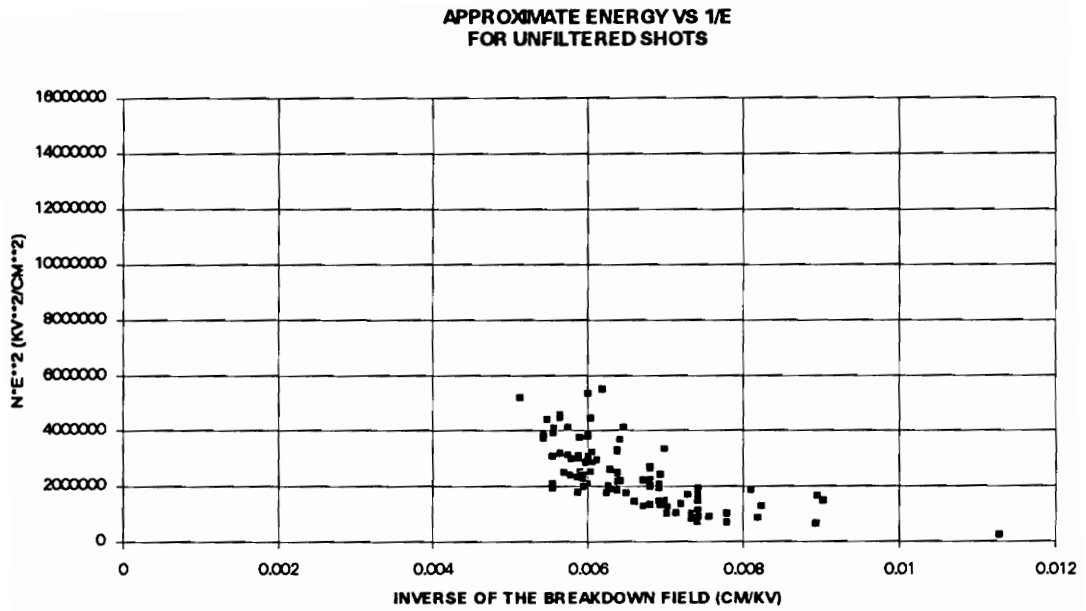


Figure 5.15. Same plot for all unfiltered breakdown experiments.

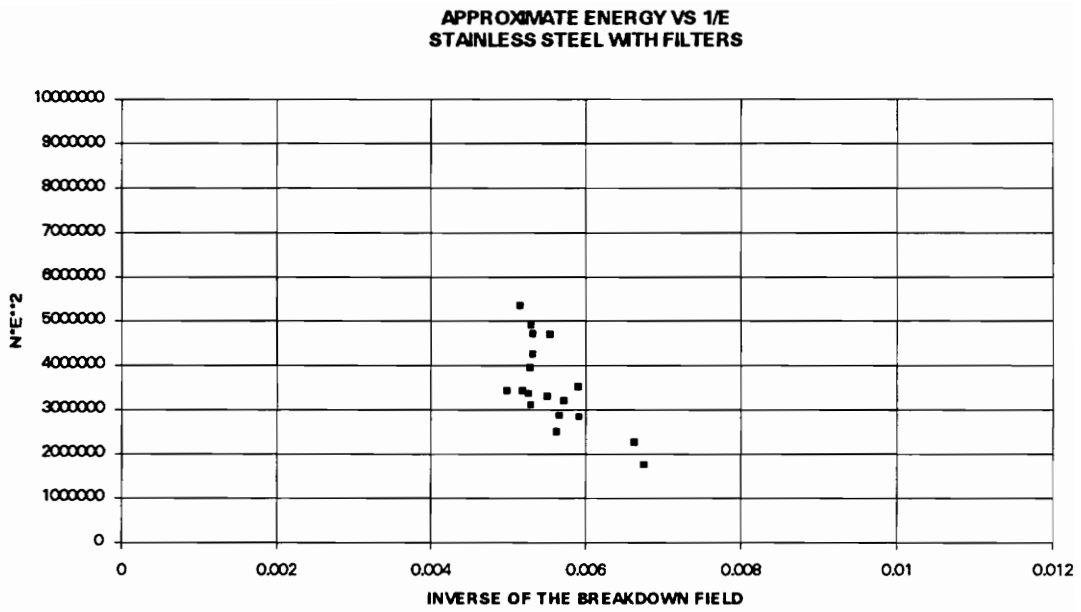


Figure 5.16. Same plot for filters and stainless steel electrodes.

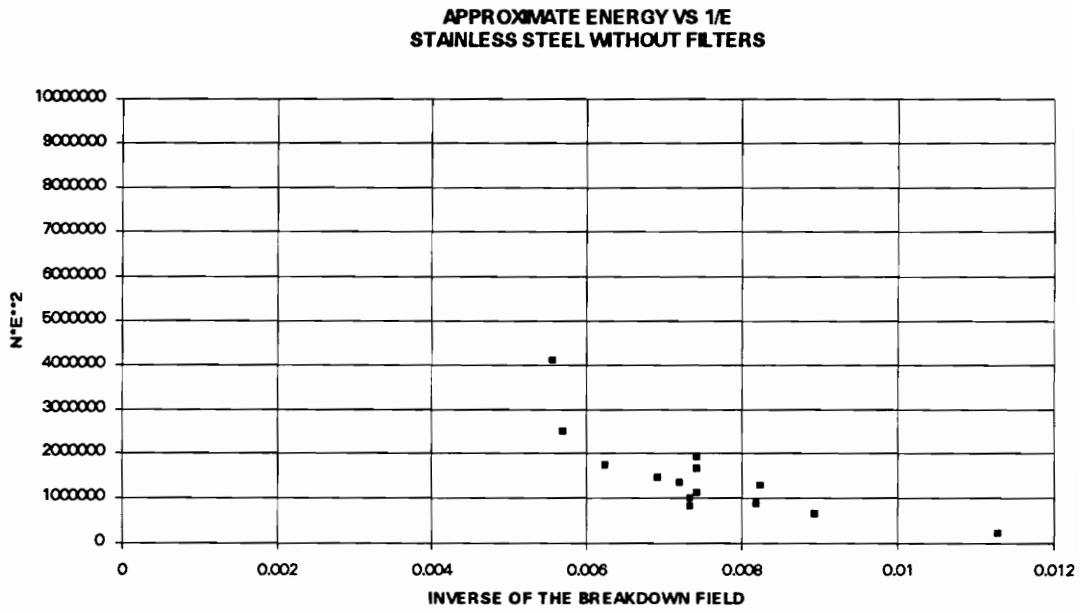


Figure 5.17. Same plot for no filters and stainless steel electrodes.

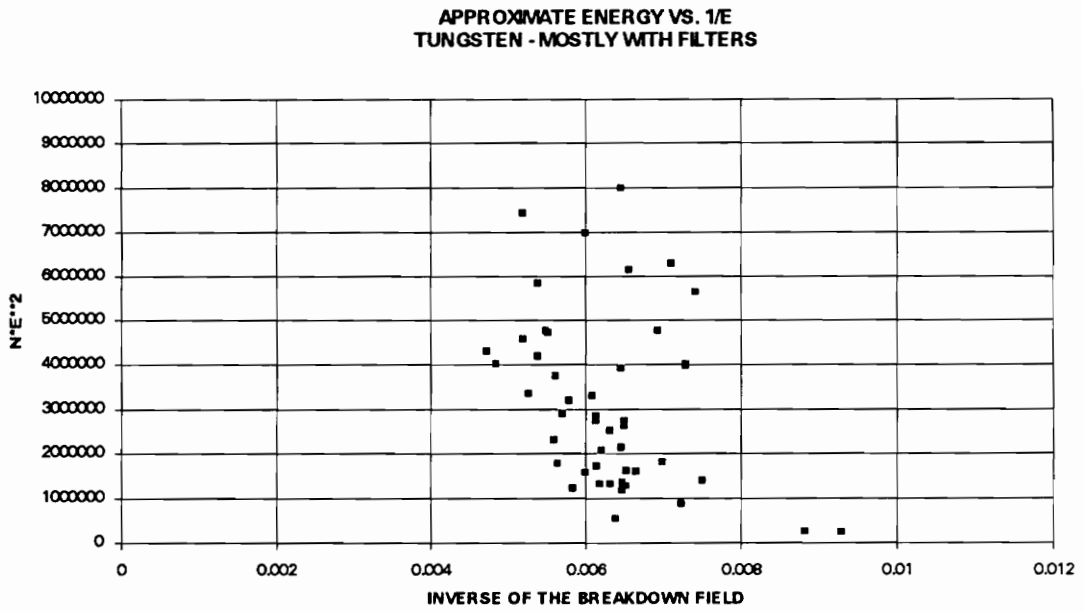


Figure 5.18. Same plot for tungsten electrodes.

After looking at these and other graphs, we tried to do log-log plots to determine the power in the relationship:

$$\text{Conditioning Energy} \propto \left(\frac{1}{E}\right)^{-x} \quad (5.12)$$

Since the conditioning energy is proportional to E^2 , we'd expect the exponent to be at least -2. And if the conditioning energy is also proportional to a volume of the dustball mass that needed to be disrupted, then the conditioning energy is proportional to L^3_{max} , and hence to $(1/E)^{-3}$. Therefore, the total exponent should be -5. But the energy function we were examining was only approximately the conditioning energy, and other problems with the experiments could be expected to affect the statistics. The first figure we looked at did indeed have an exponent of -5 (see Figure 5.20), but others did not. For example, see Figure 5.21.

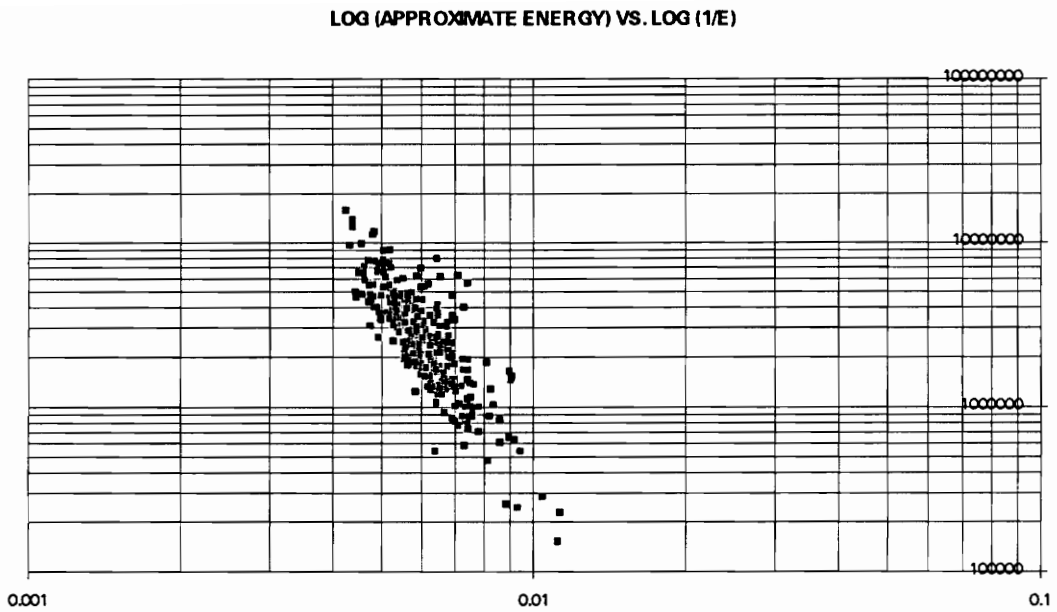


Figure 5.19. Log-log plot of the approximate energy vs. $1/E$. The exponent measured from a blowup of the graph was -4.88 . This is in excellent agreement with some thoughts we have on dustballs.

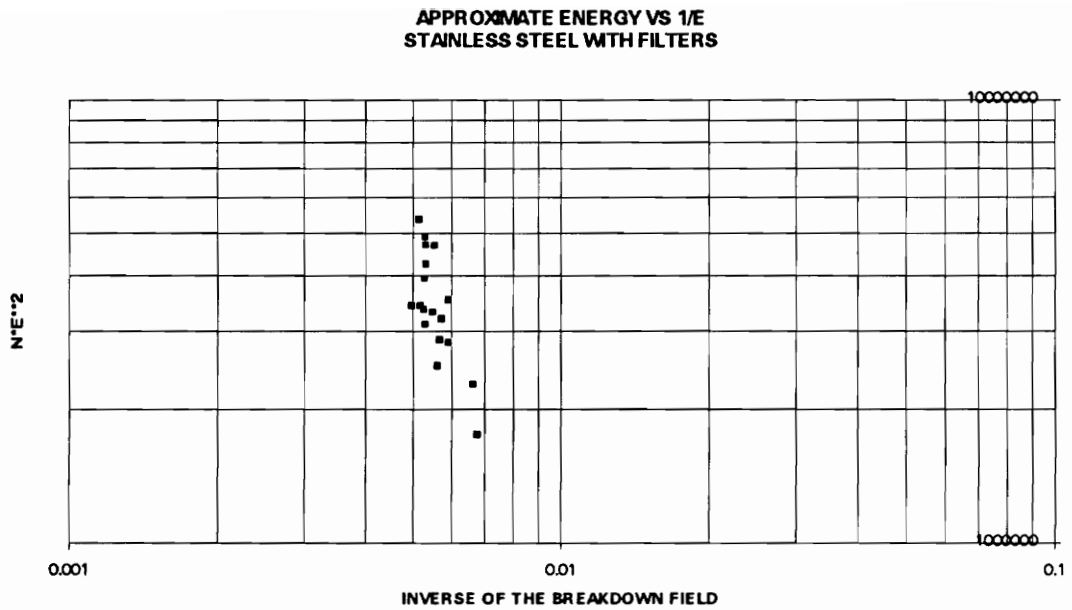


Figure 5.20. Same plot, but for filters with stainless steel electrodes. There are fewer data points here, which may help explain the poor agreement of the exponent with the expected value of -5. The exponent measured on a blown-up graph was -3.17.

Conclusions: At this time, we can't directly prove that our hypothesis (i.e., conditioning shots break up non-ionic contaminants which improves breakdown strength), but we do have semi-quantitative agreement with experimental results.

We recalculated the conditioning energy according to equations 5.9 and 5.10. For the starting n and the starting E , we used the values at the start of each breakdown cycle, not just the initial values for the day, to calculate a more accurate estimate for the conditioning energy called "true energy". The following graphs are plots of "true energy" versus $1/E$.

In Figure 5.22, we plot the log of the "true" energy (as defined above) versus $1/E$. Interestingly, we find the appearance of many straight lines of data points, all with about the same slope. Unfortunately, the obviously hoped-for correlation that these lines are different electrode sets does not seem to be true, at least as far as we've been able to deconvolute the data from the Excel spreadsheet.

To demonstrate this lack of correlation, we present Figure 5.23, which is a subset of Figure 5.22, for the tungsten electrodes only. As you can see, the data points range over the entire graph and do not just comprise one or two lines of the data points seen in Figure 5.2.

At the top of the graph, where conditioning energy is greatest, we measured a slope of ~ -3.5 . We repeated the above procedure for Figure 5.24. Along the top of the graph, we could measure a distinct line with a slope of ~ -4.4 . This is significant, because the slope for large values of conditioning energy is close to

the -5 exponent we had theorized previously to be indicative that the conditioning energy depended on the volume of the largest dustballs. Of course, agreement for the tungsten subset is better than for the complete set. We believe that this result reflects the fact that the original data was not gathered for the express purpose of determining this relationship, and that we may have introduced some error into the data by condensing tens of thousands of data points into less than 700 entries in an Excel spreadsheet.

We can only conclude, as before, that there is a semi-quantitative agreement between theory and experiment for our hypothesis.

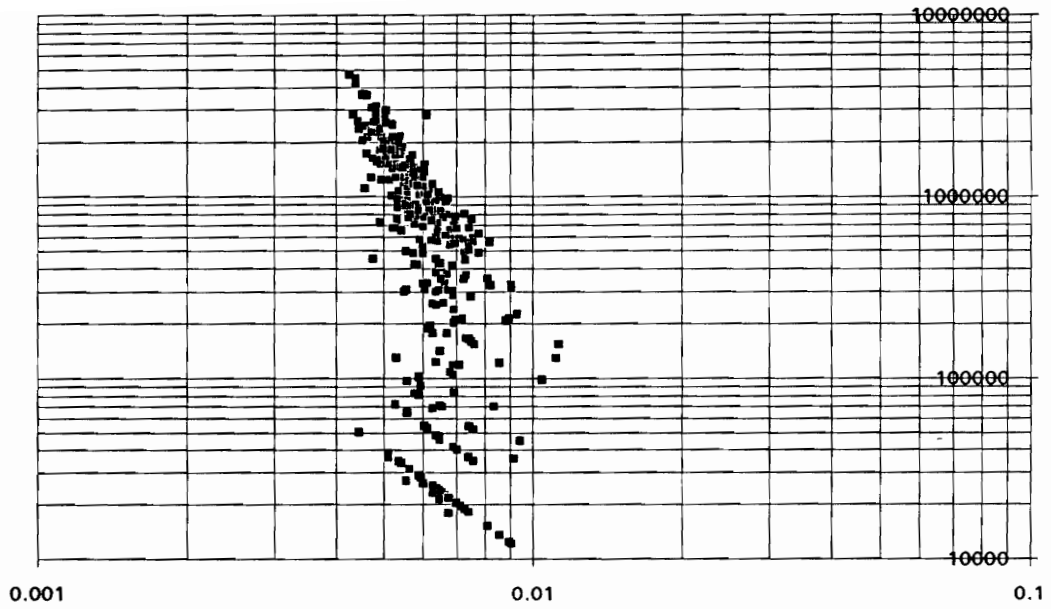


Figure 5.21. Plot of "true" energy (as defined above) versus $1/E$ for all shots in the water database.

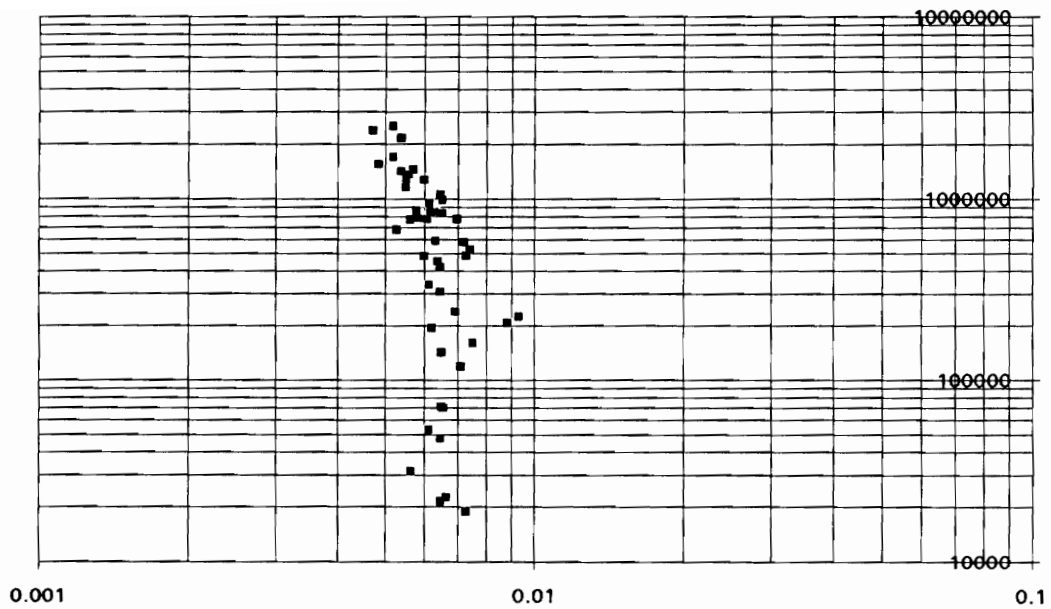


Figure 5.22. Plot of the log of "true" energy versus $1/E$ for tungsten electrodes.

Conditioning Modeling

Now we'll discuss the next level of sophistication in our effort to build a conditioning model for water breakdown. As stated in previous chapters, the conditioning process starts at a very low value of electric field. A conditioning pulse with a small electric-field value would require a large dustball to initiate a breakdown. In Figure 5.24, we represent this small-electric-field pulse as a vertical line plotted well to the right of most of the dustball-size distribution. Thus, we map the conditioning pulse to a dustball size, specifically the minimum dustball size that could initiate a breakdown given the conditioning pulse. Because the initial conditioning pulse has a low electric field, it maps to the far right of the graph where the chance of "encountering" or "interacting" with such a large dustball is very small and the probability of breakdown is small. At the same time, we hypothesize that the conditioning pulses are breaking up the large dustballs into more numerous but smaller dustballs. Thus breakdown conditioning proceeds as low-probability-of-breakdown pulses move the dustball distribution toward more numerous but smaller dustballs. The smaller dustballs are less likely to cause breakdown when acted upon by an electric field.

We think of this process, in terms of Figure 5.24, as the steady march to the left of the vertical line. Another way to explain this is that in standard conditioning the electric-field magnitude of the pulses get larger as time goes on. All the while, the dustball distribution moves slowly to the left as well. Eventually, the vertical line (which is the map of the conditioning pulse) catches up with a significant-enough portion of the distribution to cause a breakdown.

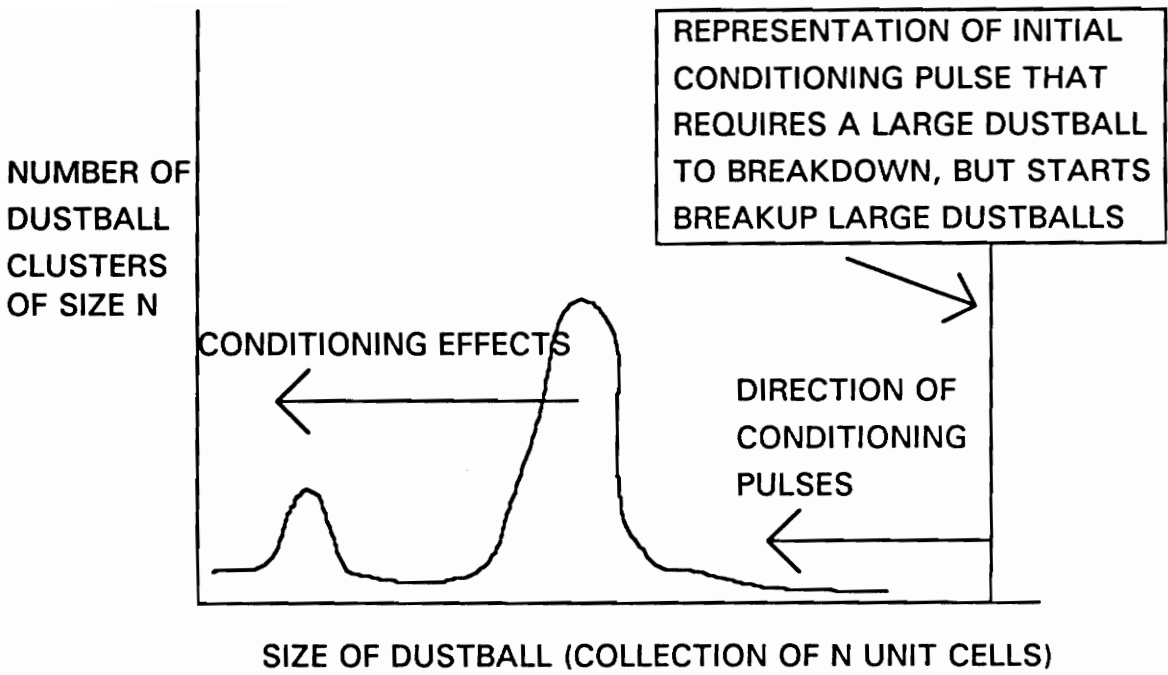


Figure 5.23. Schematic representation of a more developed idea about the mechanism of conditioning.

Experimentally, we find that after a breakdown, we must wait for a time and restart conditioning at a low electric field, else we'll get another breakdown. As a separate idea, we believe that the volume of dielectric liquid involved with a typical experiment dictates that the dustball population of most concern is the one that exists in a trapped layer close to the electrode surfaces. Combining this observation and idea with the mechanism proposed above, leads to our next hypothesis that the breakdown event disturbs the stagnant boundary layer, introducing a new, but limited, population of dustballs into the stagnant boundary layer from the bulk water. This is the reason that conditioning must be restarted after breakdown, but not at as low values as originally needed at the start of the day.

This breakdown mechanism also qualitatively explains the effect of filters on breakdown (e.g., for copper electrodes the 10% breakdown threshold increases from ~135 kV/cm for unfiltered water to ~200-220 kV/cm for 0.5- μ m-filtered water). We hypothesize that the filters greatly reduce the population of the dustballs sized greater than 0.5 μ m. Then the conditioning pulses have fewer large dustballs to pulverize and can push the distribution farther to the left before catching up to it and causing a breakdown.

The proposed breakdown mechanism predict that conditioning shots breakup large impurities into smaller ones. Presumably, as the number of smaller impurities grows, it will require more conditioning shots to reduce the upper limit on the size of the impurities. Thus. later conditioning shots should not be as effective, and a limit to the increase in breakdown strength will be reached

We summarize these qualitative arguments with the following equations, where P_{BD} is the probability of breakdown

$$P_{BD} \propto n_V^\alpha, \quad (5.13)$$

where P_{BD} is the probability of breakdown, n_V is the total number of voids (bubbles) in the water and α is a positive exponent.

$$P_{BD} \propto n_c^{\beta(n_c)}, \quad (5.14)$$

where n_c is the number of conditioning shots and is greater than one and β is initially a negative coefficient but becomes less significant as n_c becomes large.

$$P_{BD} \propto N^\delta, \quad (5.15)$$

where N is a size parameter of the non-ionic contaminants (dustballs) and δ is positive.

VI. CHAPTER SIX : SUMMARY AND OUTLOOK

In the previous chapters, we presented details of a difficult and ambiguous project to study the breakdown of water as a dielectric at high electric fields. We attempted to understand the mechanisms of breakdown in the context of the pre-existing development project and to determine the largest field strength that can be achieved without breakdown. A number of different factors and mechanisms have been studied in relation to their role in dielectric breakdown in water. These will be briefly summarized here. A number of factors would seem to be physically relevant. These include:

- Ionic conductivity
- Temperature
- Bubbles and deaeration of the liquid dielectric
- Electrode materials
- Electrode surface conditions and treatments
- Filters and water quality
- Nature of conditioning of the system

A summary of the findings for each of these aspects will be given below.

- Ionic conductivity

Ionic conductivity is clearly a dominant mechanism for the relaxation of the charge placed on the capacitor plates in these experiments. In order to study long-time-scale experiments almost all of the experiments in this study

were carried out with water of extremely low ionic impurities. For all of these experiments the resistivity was close to the intrinsic ionic limit for water.

- Temperature

The temperature of the water was kept very low and constant in almost all of the experiments. On those occasions where the temperature was not controlled, spurious breakdowns were observed to occur. These were often associated with temperature changes and thus expansion or contraction of the system which would flush material out into the circulating water. For the most part, temperature was well controlled to keep the intrinsic time constant of the system in the range of 300 microseconds.

- Bubbles and deaeration of the liquid dielectric

Bubbles are a clear and well known source of breakdowns. If there are observable bubbles on the surface of the plates of the capacitor, the breakdown is overwhelmingly likely to initiate at the bubble. In order to suppress the formation of bubbles, the water was deaerated and kept at low temperatures. Under these conditions bubbles would not form spontaneously or, if formed, would collapse fairly quickly. For the bulk of the data reported here there were no observable bubbles.

- Electrode materials

Optical data in the literature and observations in this study indicate that the breakdown initiates at the electrode surface. Accordingly, a major part of the early efforts focused on the study of a variety of electrodes and surface

treatments of these. For the most part, these investigations were carried out before the importance of filters was understood. With *unfiltered* water, breakdown fields by material were:

Table 6.1 Electric-field breakdown results by material for unfiltered water.

Material	Breakdown (kV/cm)	Standard Deviation
Graphite	137	25
Stainless Steel	145	16
Aluminum	159	8
Copper	161	16
Gold	168	13
Lead	169	8

The overall average breakdown field for all of the electrode materials was 157 kV/cm. The order of the breakdown fields by material is not rationalized by any simple idea. Furthermore, the relatively large standard deviations for the breakdown fields among the materials does not really suggest a clear separation by materials.

- Electrode surface conditions and treatments

A large number of surface treatments (electropolishing, passivating, bead blasting, oxide layers) were tried in a long search to increase the breakdown fields. No consistent physical picture arises from these studies, except that breakdown can be somewhat affected by the surface treatment and that polished surfaces are not better than bead-blasted surfaces, which is unexpected

because it is assumed that smooth surfaces would have a higher breakdown strength than rough surfaces. Cuprous oxide layers on copper gave rise to significantly lower breakdown fields (96-105 kV/cm). This work was carried out without filters.

- Filters and water quality

One of the last experimental treatments was the inclusion of both particulate filters (down to 0.2 microns) and organic filters (activated charcoal). With these filters in place, the overall average breakdown field changes from 156 kV/cm to 186 kV/cm. Electrodes of only three different materials were used here. In the following summary table, the average breakdown field and the standard error of the mean are quoted for both filtered and unfiltered conditions and for the combinations of filters.

Table 6.2 Comparison of electric-field breakdown results for filtered versus unfiltered water.

Material	Breakdown without Filters (kV/cm)	Breakdown with Filters (kV/cm)
304SS	128 ± 5	174 ± 8 (Particulate only)
304SS	128 ± 5	190 ± 3 (Both)
Copper	161 ± 8	186 ± 2 (Particulate only)
Copper	161 ± 8	222 ± 2 (Both)
Tungsten	N.A.	163 ± 3 (Both)

In Table 6.2, (Both) refers to using activated charcoal as well as the particulate filters. We assume that activated charcoal binds organic fragments smaller than 0.5 (and later 0.2) microns as well as organic molecules themselves. Efficiency of the filters and the concentration of non-ionic contaminants were not monitored. Yet, the large increase of the breakdown field with the inclusion of the organic filters is striking evidence of the effect of organic-based impurities in the system. The water quality for these samples was kept as high as possible and these data were taken after the Tygon hoses were taken out of the system. Thus, these data should be the closest to representing the measurement of the pure electrode-breakdown effect. Tungsten was measured with the complete set of filters, though there was no reliable data, with no filters, for comparison.

- Nature of conditioning of the system

The last aspect of this study to summarize is the lore of conditioning of the water/electrode system. These experiments delineate a hysteresis of the probability of breakdown function versus the electric field. Many of the simple ideas of magnetic hysteresis appear to be useful here.

The first comment is that these water-breakdown phenomena have some parallels with high-voltage experience in air. With spark gaps it is commonly known that a new spark gap will break down with less repeatability than a spark gap with large number of breakdowns. At that point it is usually said that the gap has been aged, or conditioned. If the spark gap is enclosed, this aging is long lived and the gap is stable for a long time. The usual explanation of this aging phenomena is that all sharp edges or points on the gap electrodes have been

blasted or melted and the only remaining breakdown mechanisms are related to the dielectric and not some peculiarity of the electrodes. For water-dielectric breakdown, there is one major difference from the air gap. In our case the aging or conditioning is short-lived and must be repeated at the beginning of each experimental session.

The standard conditioning process begins at a low field and determines the breakdown probability on the basis of 10-shot episodes in which the capacitor is charged at each shot. At any field value, E , the probability of breakdown $P_{BD}(E)$ is estimated on the basis of 10 shots repeated every 15 seconds to 1 or 2 minutes. By increasing the voltage across the capacitor at each step $P_{BD}(E)$ is determined. The result curve is zero for fields a little below the field E_{50} (which is the field at which the probability of breakdown is 0.5) and is one for fields a little above E_{50} (i.e., the transition from zero to one is sharp but finite, usually the width is about 20- or 30 kV/cm). The region in which $P_{BD}(E)$ changes from 0 to 1 is often narrow while strong hysteresis is displayed. In order to characterize the observations of this work it is useful to define a hysteresis region for the probability-of-breakdown function. We have defined E_{50} as the 50% field for a standard monotonically increasing sampled-conditioning curve. If this process were to be reversed and the field was decreased monotonically from high fields, there is expected to be a smaller 50% field (denoted by E_{50}^-). This lower 50% field has been observed in several measurements carried out earlier than this study. No direct determination of this parameter is made here, though the hysteretic region below E_{50} was observed. To complete the phenomenological descriptors, we now define a new 50% field value that represents the upper limit of the hysteresis region and represents the

boundary between the “conditioning” region and the complete breakdown region where $P_{BD}(E) = 1$ for all larger fields. Let us define this field with the symbol E_{50}^+ . This parameter is estimated through the experiments of Chapter 4. Figure 6.1 exhibits these three quantities and the variation of the probability of breakdown $P_{BD}(E)$.

Probability of Breakdown

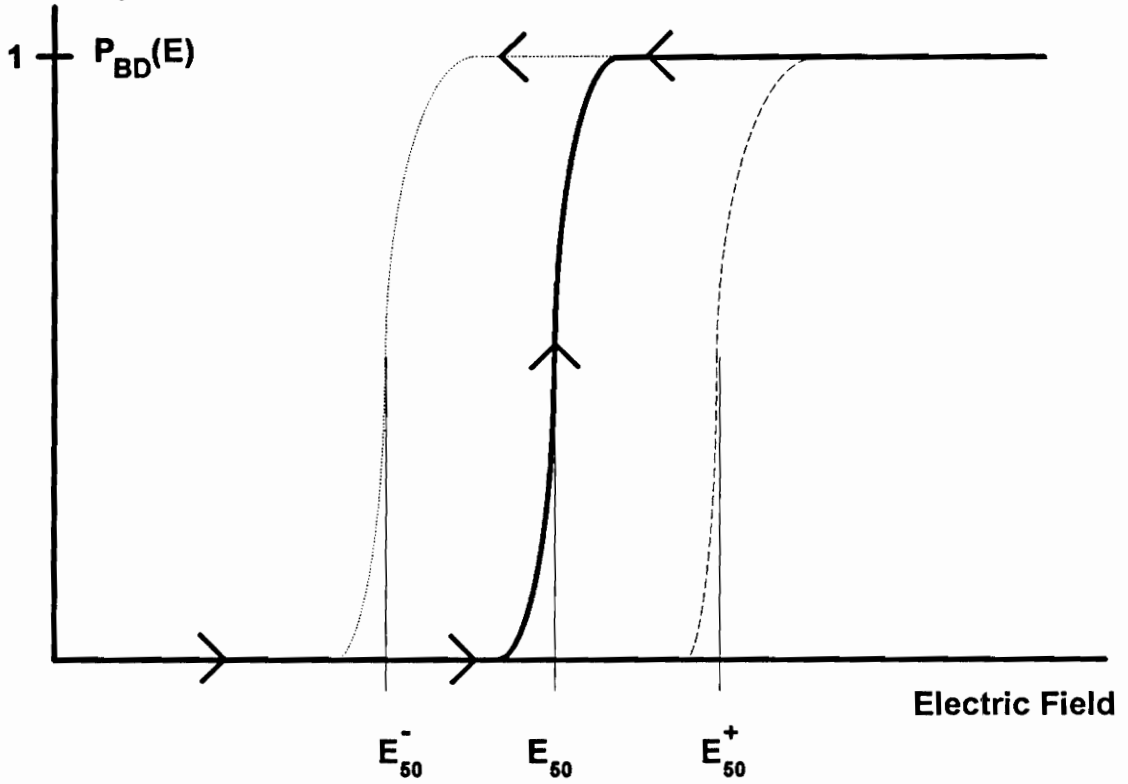


Figure 6.1 Conceptual diagram of the hysteresis region for the breakdown probability as a function of electric field.

Using this language several simple summary statements can be made.

1. The standard 50% field, E_{50} , as determined by the standard monotonically increasing sequence is mildly hysteretic. The initial measurements are smaller than subsequent values and the series of values were used to determine the reported breakdown fields for any electrode. It would appear that a sequence of standard-conditioning procedures would have the E_{50} values converge to E_{50}^+ as the sequence continues. As was shown in Chapter 4, there are other conditioning sequences that can estimate E_{50}^+ .

2. In Chapter 4 a process called Initial Breakdown Conditioning (IB), was defined to be a sequence of shots at a fixed field. The essential observations of that chapter were that successive 10-shot estimates of $P_{BD}(E)$ started at 1 and then decreased to zero for fields between E_{50}^- and E_{50}^+ . While there are no good estimates of the lower field, E_{50}^- there were good observations of the initial value of $P_{BD}(E) = 1$ for fields below the initial E_{50} . These constant field sequences seemed to drive $P_{BD}(E)$ to 0 for fields larger than the initial E_{50} and less than E_{50}^+ . The values of E_{50}^+ estimated from the several different sequences in Chapter 4 (figures 4.7 to 4.11) were roughly the same value of about 200 kV/cm for Cu and 225 kV/cm for W. These values are not very precisely determined, but suggest this phenomenological picture is consistent.

3. The process observed above, in which a constant-field conditioning sequence was able to drive the breakdown probability to zero, was found to depend on the repetition rate of the shots. If the conditioning shots were as

close as 15 seconds, it was not possible to drive $P_{BD}(E)$ to 0 . The zero value was easily obtained when the time interval between conditioning shots was lengthened to 1 minute. This observation suggests that something is not able to be healed or swept away if the time between conditioning shots is too short.

This summary of conditioning data is consistent with the hysteresis region being determined by some sort of impurity (most probably organic) that is dislodged from the stagnant-water region close to the electrode surface. The nature of the more intrinsic 50% field E_{50}^+ has not been determined by this study, but may reflect properties of the electrodes more than anything else. It could be studied by a wide variety of different conditioning sequences.

Suggestions for future experiments

Clearly, the next experimental step would involve construction of a new breakdown apparatus using only the best materials for high-purity water systems; namely, polyvinylidene fluoride (PVDF) or polypropylene (PPP) for non-metallic components, and metallic components that match the electrodes under test. Perhaps this set-up could finally observe the breakdown of pure water. Then we could proceed with the investigation into the effects of electrode surface on breakdown. This system could be built for tens of thousands of dollars and is quite feasible within the scope of today's technology.

To directly ascertain the cause for the breakdown initiation, we would need an in-situ instrument, capable of microscopic examination (nanometer by

nanometer) of the electrode surface under high-field conditions with a time resolution of a few tens of picoseconds. Then we could observe the proto-streamers and determine the conditions under which they grow into breakdowns. Unfortunately, this device is impractical at this time and we will have to content ourselves with indirect evidence as to the nature of high-purity-water electrical breakdown for the indefinite future.

APPENDIX A: WATER-BREAKDOWN DATABASE

Throughout the thesis, we've produced graphs and tables drawn from a database of electrical-breakdown results. The database was itself distilled from over 25,000 shots in the water-dielectric laboratory; we reproduce now the Excel file that contains the database.. Note: non-breakdown is designated as a 0, a breakdown is a 1.

Table A.1 Database of Experiments on Electrical Breakdown in Water

Date	Time	Shot No.	BD	kV	cm	Electrode	Tau (us)	Temp (C)	Days Immersion or since system was opened	Who	E (kV/cm)
5/3/85	15:30	11066	0	69.2	0.99	310 SS	584	2	-	VHG	70
5/3/85	16:28	11125	1	121	0.99	310 SS	522	3.6	-	VHG	122
6/20/85	13:50	11159	0	70	0.98	5083 AL	476	4.6	-	VHG	71
6/20/85	15:20	11247	1	166	0.98	5083 AL	423	4.7	-	VHG	169
9/5/85	14:00	11265	0	84.4	1	2024 AL	241	5.7	8	VHG	84
9/5/85	15:03	11340	1	167	1	2024 AL	269	4.2	8	VHG	167
9/5/85	15:08	11342	0	147	1	2024 AL	-	-	8	VHG	147
9/5/85	16:38	11402	1	195	1	2024 AL	301	6.7	8	VHG	195
9/11/85	13:55	11406	0	89.5	1.01	316 SS	280	5.1	-	VHG	89
9/11/85	15:22	11474	1	162	1.01	316 SS	52	4	-	VHG	160
9/26/85	13:35	11483	0	92.1	1.01	2024 AL	430	4.2	14	VHG	91
9/26/85	14:38	11544	1	172	1.01	2024 AL	300	4.5	14	VHG	170
8/13/86	12:56	11668	0	88	0.99	430 SS	453	5.7	14	VHG + ARM	89
8/13/86	14:13	11749	1	174	0.99	430 SS	436	5.4	14	VHG + ARM	176
8/13/86	14:35	11760	0	145	0.99	430 SS	442	5.5	14	VHG + ARM	146
8/13/86	14:56	11795	1	178	0.99	430 SS	406	6.7	14	VHG + ARM	180
8/27/86	14:24	11800	0	70	0.98	6061 AL	398	6.2	8	VHG + ARM	71

8/27/86	15:16	11880	1	167	0.98	6061 AL	-	6.3	8	VHG + ARM	170
8/27/86	15:40	11891	0	144	0.98	6061 AL	-	5.5	8	VHG + ARM	147
8/27/86	15:46	11902	1	156	0.98	6061 AL	-	5.5	8	VHG + ARM	159
8/27/86	15:52	11911	0	167	0.98	6061 AL	-	5.5	8	VHG + ARM	170
8/27/86	16:02	11921	1	176.5	0.98	6061 AL	-	6.2	8	VHG + ARM	180
9/12/86	13:19	11931	0	37.5	0.99	304 SS	445	6.1	8	VHG + ARM	38
9/12/86	13:56	11975	1	135	0.99	304 SS	-	6.4	8	VHG + ARM	136
9/12/86	13:58	11976	0	135	0.99	304 SS	-	6.5	8	VHG + ARM	136
9/12/86	14:00	11985	1	135	0.99	304 SS	-	6.5	8	VHG + ARM	136
9/12/86	14:15	11989	0	126	0.99	304 SS	390	6.6	8	VHG + ARM	127
9/12/86	14:23	12001	1	137.5	0.99	304 SS	390	6.7	8	VHG + ARM	139
9/19/86	13:10	12010	0	85	1.02	304SS+ 2024AL-	320	7	5	VHG + ARM	83
9/19/86	13:35	12053	1	131	1.02	304SS+ 2024AL-	311	6.9	5	VHG + ARM	128
9/19/86	13:41	12062	0	143	1.02	304SS+ 2024AL-	311	6.9	5	VHG + ARM	140
9/19/86	13:42	12063	1	143	1.02	304SS+ 2024AL-	311	6.9	5	VHG + ARM	140
9/19/86	14:00	12071	0	135	1.02	304SS+ 2024AL-	339	6.9	5	VHG + ARM	132
9/19/86	14:02	12082	1	146	1.02	304SS+ 2024AL-	339	6.9	5	VHG + ARM	143
9/19/86	14:18	12091	0	72	1.02	304SS+ 2024AL-	-	7.4	5	VHG + ARM	71
9/19/86	14:30	12130	1	113	1.02	304SS+ 2024AL-	-	-	5	VHG + ARM	111
9/19/86	14:33	12131	0	126	1.02	304SS+ 2024AL-	-	-	5	VHG + ARM	124
9/19/86	14:34	12132	1	126	1.02	304SS+ 2024AL-	-	-	5	VHG + ARM	124
9/19/86	14:37	12141	0	114	1.02	304SS+ 2024AL-	-	-	5	VHG + ARM	112

9/19/86	14:38	12142	1	114	1.02	304SS+ 2024AL-	322	6.7	5	VHG + ARM	112
9/24/86	13:19	12161	0	82.5	1.02	2024AL+ 304SS-	254	6.9	10	VHG + ARM	81
9/24/86	13:35	12212	1	135	1.02	2024AL+ 304SS-	-	-	10	VHG + ARM	132
9/24/86	13:39	12221	0	145	1.02	2024AL+ 304SS-	-	-	10	VHG + ARM	142
9/24/86	13:42	12223	1	145	1.02	2024AL+ 304SS-	-	-	10	VHG + ARM	142
9/24/86	13:49	12233	0	157	1.02	2024AL+ 304SS-	-	-	10	VHG + ARM	154
9/24/86	13:50	12235	1	157	1.02	2024AL+ 304SS-	251	6.7	10	VHG + ARM	154
9/24/86	13:59	12241	0	81	1.02	2024AL+ 304SS-	251	6.7	10	VHG + ARM	79
9/24/86	14:30	12313	1	159	1.02	2024AL+ 304SS-	-	-	10	VHG + ARM	156
9/24/86	14:34	12322	0	169	1.02	2024AL+ 304SS-	-	-	10	VHG + ARM	166
9/24/86	14:43	12324	1	169	1.02	2024AL+ 304SS-	292	7.1	10	VHG + ARM	166
10/1/86	13:08	12332	0	87	1.02	304SS+ 2024AL-	300	6.3	17	VHG + ARM	85
10/1/86	13:48	12424	1	169	1.02	304SS+ 2024AL-	-	7.2	17	VHG + ARM	166
10/1/86	13:59	12433	0	64	1.02	304SS+ 2024AL-	-	7.4	17	VHG + ARM	63
10/1/86	14:28	12496	1	146	1.02	304SS+ 2024AL-	-	-	17	VHG + ARM	143
10/1/86	14:32	12503	0	158	1.02	304SS+ 2024AL-	-	-	17	VHG + ARM	155
10/1/86	14:33	12504	1	158	1.02	304SS+ 2024AL-	-	-	17	VHG + ARM	155
10/1/86	14:40	12513	0	170	1.02	304SS+ 2024AL-	-	-	17	VHG + ARM	167
10/1/86	15:00	12525	1	170	1.02	304SS+ 2024AL-	250	7.6	17	VHG + ARM	167
10/8/86	13:40	12555	0	72.5	1.02	2024AL+ 304SS-	300	6.5	24	VHG + ARM	71
10/8/86	14:03	12616	1	131	1.02	2024AL+ 304SS-	-	-	24	VHG + ARM	128
10/8/86	14:10	12626	0	149	1.02	2024AL+ 304SS-	-	-	24	VHG + ARM	146

10/8/86	14:31	12637	1	160	1.02	2024AL+ 304SS-	-	6.5	24	VHG + ARM	157
10/8/86	14:33	12639	0	160	1.02	2024AL+ 304SS-	-	-	24	VHG + ARM	157
10/8/86	14:34	12640	1	160	1.02	2024AL+ 304SS-	-	-	24	VHG + ARM	157
10/8/86	14:35	12641	0	158	1.02	2024AL+ 304SS-	-	-	24	VHG + ARM	155
10/8/86	14:36	12643	1	160	1.02	2024AL+ 304SS-	-	-	24	VHG + ARM	157
10/8/86	14:37	12645	0	150	1.02	2024AL+ 304SS-	-	-	24	VHG + ARM	147
10/8/86	15:00	12686	1	173	1.02	2024AL+ 304SS-	-	-	24	VHG + ARM	170
10/8/86	15:17	12696	0	86	1.02	2024AL+ 304SS-	-	5.8	24	VHG + ARM	84
10/8/86	15:52	12766	1	165	1.02	2024AL+ 304SS-	200	6.6	24	VHG + ARM	162
5/27/87	13:50	12776	0	55	1.03	304SS+ 2024AL-	514	6.5	-	VHG + LA	53
5/27/87	15:00	12866	1	160.4	1.03	304SS+ 2024AL-	445	6.11	-	VHG + LA	156
5/28/87	13:00	12876	0	55	1.03	304SS- 2024AL+	542	5.8	-	VHG + LA	53
5/28/87	14:35	12981	1	170	1.03	304SS- 2024AL+	413	6.6	-	VHG + LA	165
6/4/87	13:00	13005	0	40	1.02	7075 AL	591	4	3	VHG + LA	39
6/4/87	13:45	13086	1	137.5	1.02	7075 AL	-	-	3	VHG + LA	135
6/4/87	13:46	13087	0	137.5	1.02	7075 AL	-	-	3	VHG + LA	135
6/4/87	14:00	13105	1	160	1.02	7075 AL	-	-	3	VHG + LA	157
6/4/87	14:01	13106	0	160	1.02	7075 AL	-	-	3	VHG + LA	157
6/4/87	14:02	13107	1	160	1.02	7075 AL	-	-	3	VHG + LA	157
6/10/87	12:45	13114	0	45	1.02	7075 AL	446	8.4	10	VHG + LA	44
6/10/87	13:00	13204	1	140	1.02	7075 AL	-	-	10	VHG + LA	137
6/10/87	13:05	13205	0	147.5	1.02	7075 AL	-	-	10	VHG + LA	145
6/10/87	13:06	13207	1	147.5	1.02	7075 AL	-	-	10	VHG + LA	145
6/10/87	13:07	13209	0	147.5	1.02	7075 AL	-	-	10	VHG + LA	145
6/10/87	13:09	13214	1	147.5	1.02	7075 AL	-	-	10	VHG + LA	145
6/10/87	13:10	13216	0	150	1.02	7075 AL	-	-	10	VHG + LA	147

6/10/87	13:11	13217	1	150	1.02	7075 AL	-	-	10	VHG + LA	147
6/24/87	13:00	13225	0	57	1.02	304 SS	317	6.64	-	VHG + LA	56
6/24/87	13:20	13254	1	90.44	1.02	304 SS	-	-	-	VHG + LA	89
6/24/87	13:50	13256	0	90.44	1.02	304 SS	-	-	-	VHG + LA	89
6/24/87	14:10	13277	1	114.24	1.02	304 SS	-	-	-	VHG + LA	112
6/24/87	14:20	13286	0	104.5	1.02	304 SS	-	-	-	VHG + LA	102
6/24/87	14:40	13312	1	123.8	1.02	304 SS	-	-	-	VHG + LA	121
6/26/87	13:30	13317	0	45	1.02	304 SS	478	5.1	-	VHG + LA	44
6/26/87	14:30	13379	1	137.5	1.02	304 SS	-	-	-	VHG + LA	135
6/26/87	14:31	13381	0	137.5	1.02	304 SS	-	-	-	VHG + LA	135
6/26/87	14:40	13387	1	147.5	1.02	304 SS	-	-	-	VHG + LA	145
6/26/87	15:10	13399	0	125	1.02	304 SS	-	-	-	VHG + LA	123
6/26/87	15:20	13409	1	137.5	1.02	304 SS	-	-	-	VHG + LA	135
6/26/87	15:49	13420	0	137.5	1.02	304 SS	-	-	-	VHG + LA	135
6/26/87	15:52	13423	1	137.5	1.02	304 SS	-	-	-	VHG + LA	135
7/8/87	12:27	13431	0	61.88	0.99	Au Plating	287	5.91	-	VHG + LA	63
7/8/87	13:27	13494	1	142.8	0.99	Au Plating	-	-	-	VHG + LA	144
7/8/87	13:47	13501	0	133.28	0.99	Au Plating	-	-	-	VHG + LA	135
7/8/87	14:17	13531	1	171.36	0.99	Au Plating	-	-	-	VHG + LA	173
7/8/87	14:32	13534	0	161.84	0.99	Au Plating	-	-	-	VHG + LA	163
7/8/87	14:39	13541	1	161.84	0.99	Au Plating	-	-	-	VHG + LA	163
7/8/87	14:52	13544	0	142.8	0.99	Au Plating	-	-	-	VHG + LA	144
7/8/87	14:56	13548	1	142.8	0.99	Au Plating	-	-	-	VHG + LA	144
7/9/87	12:25	13554	0	61.88	0.99	Au Plating	563.2	5.05	-	VHG + LA	63
7/9/87	13:45	13640	1	166.6	0.99	Au Plating	-	-	-	VHG + LA	168
7/9/87	14:10	13649	0	142.8	0.99	Au Plating	-	-	-	VHG + LA	144
7/9/87	14:40	13686	1	180.88	0.99	Au Plating	-	-	-	VHG + LA	183
7/10/87	13:30	13689	0	76.16	0.99	Au Plating	-	-	-	VHG + LA	77
7/10/87	14:10	13738	1	133.28	0.99	Au Plating	-	-	-	VHG + LA	135
7/10/87	14:20	13739	0	147.56	0.99	Au Plating	-	-	-	VHG + LA	149
7/10/87	14:28	13747	1	147.56	0.99	Au Plating	-	-	-	VHG + LA	149

7/10/87	14:29	13748	0	147.56	0.99	Au Plating	-	-	-	VHG + LA	149
7/10/87	14:35	13749	1	178.5	0.99	Au Plating	-	-	-	VHG + LA	180
7/10/87	14:36	13750	0	178.5	0.99	Au Plating	-	-	-	VHG + LA	180
7/10/87	14:39	13753	1	178.5	0.99	Au Plating	-	-	-	VHG + LA	180
7/10/87	14:42	13756	0	178.5	0.99	Au Plating	-	-	-	VHG + LA	180
7/10/87	14:45	13759	1	166.6	0.99	Au Plating	-	-	-	VHG + LA	168
7/10/87	15:10	13764	0	133.28	0.99	Au Plating	-	-	-	VHG + LA	135
7/10/87	15:30	13784	1	178.5	0.99	Au Plating deteriorated	-	-	-	VHG + LA	180
8/6/87	13:00	13789	0	57.12	1.02	Replated Au	433.3	5.26	-	VHG + LA	56
8/6/87	14:40	13891	1	180.9	1.02	Replated Au	-	-	-	VHG + LA	177
8/6/87	15:20	13900	0	142.8	1.02	Replated Au	-	-	-	VHG + LA	140
8/6/87	15:53	13933	1	180.9	1.02	Replated Au	-	-	-	VHG + LA	177
8/6/87	15:54	13934	0	180.9	1.02	Replated Au	-	-	-	VHG + LA	177
8/6/87	15:55	13935	1	180.9	1.02	Replated Au	397	5.8	-	VHG + LA	177
8/7/87	12:30	13940	0	54.6	1.02	Replated Au with reversed polarity	457.4	5.55	-	VHG + LA	54
8/7/87	14:10	14043	1	177.5	1.02	Replated Au with reversed polarity	-	-	-	VHG + LA	174
8/7/87	14:30	14046	0	159.3	1.02	Replated Au with reversed polarity	-	-	-	VHG + LA	156
8/7/87	14:40	14058	1	168.4	1.02	Replated Au with reversed polarity	-	-	-	VHG + LA	165
8/7/87	15:00	14059	0	168.4	1.02	Replated Au with reversed polarity	-	-	-	VHG + LA	165
8/7/87	15:10	14076	1	177.5	1.02	Replated Au with reversed polarity	371.1	6.12	-	VHG + LA	174
8/13/87	12:30	14088	0	38.3	1.02	Lead - & Au +	373.3	5.82	-	VHG + LA	38
8/13/87	13:50	14163	1	162	1.02	Lead - & Au +	-	-	-	VHG + LA	159

8/13/87	14:10	14169	0	152	1.02	Lead - & Au +	-	-	-	VHG + LA	149
8/13/87	14:30	14189	1	171	1.02	Lead - & Au +	-	-	-	VHG + LA	168
8/13/87	14:31	14190	0	171	1.02	Lead - & Au +	-	-	-	VHG + LA	168
8/13/87	14:32	14191	1	171	1.02	Lead - & Au +	270	6.52	-	VHG + LA	168
8/14/87	13:30	14205	0	55	1.02	Lead + & Au -	320	5.68	-	VHG + LA	54
8/14/87	14:40	14266	1	150	1.02	Lead + & Au -	-	-	-	VHG + LA	147
8/14/87	14:41	14267	0	150	1.02	Lead + & Au -	-	-	-	VHG + LA	147
8/14/87	14:50	14280	1	160	1.02	Lead + & Au -	-	-	-	VHG + LA	157
8/14/87	15:10	14286	0	138	1.02	Lead + & Au -	-	-	-	VHG + LA	135
8/14/87	15:40	14316	1	170	1.02	Lead + & Au -	-	-	-	VHG + LA	167
8/14/87	16:00	14322	0	150	1.02	Lead + & Au -	-	-	-	VHG + LA	147
8/14/87	16:05	14327	1	150	1.02	Lead + & Au -	-	-	-	VHG + LA	147
8/14/87	16:07	14329	0	150	1.02	Lead + & Au -	-	-	-	VHG + LA	147
8/14/87	16:08	14330	1	150	1.02	Lead + & Au -	-	-	-	VHG + LA	147
8/14/87	16:10	14332	0	160	1.02	Lead + & Au -	-	-	-	VHG + LA	157
8/14/87	16:15	14337	1	160	1.02	Lead + & Au -	-	-	-	VHG + LA	157
8/14/87	16:17	14339	0	160	1.02	Lead + & Au -	-	-	-	VHG + LA	157
8/14/87	16:18	14340	1	160	1.02	Lead + & Au -	-	-	-	VHG + LA	157
8/14/87	16:19	14341	0	160	1.02	Lead + & Au -	-	-	-	VHG + LA	157
8/14/87	16:20	14342	1	170	1.02	Lead + & Au -	240	5.9	-	VHG + LA	167
8/20/87	13:00	14346	0	57.5	0.95	Lead + & Lead -	181.9	5.91	-	VHG + LA	61
8/20/87	14:20	14426	1	160	0.95	Lead + & Lead -	-	-	-	VHG + LA	168

8/20/87	14:24	14430	0	160	0.95	Lead + & Lead -	-	-	-	VHG + LA	168
8/20/87	14:25	14431	1	160	0.95	Lead + & Lead -	-	-	-	VHG + LA	168
8/20/87	14:29	14435	0	160	0.95	Lead + & Lead -	-	-	-	VHG + LA	168
8/20/87	14:55	14456	1	175	0.95	Lead + & Lead -	-	-	-	VHG + LA	184
8/20/87	14:56	14457	0	175	0.95	Lead + & Lead -	-	-	-	VHG + LA	184
8/20/87	14:57	14458	1	175	0.95	Lead + & Lead -	-	-	-	VHG + LA	184
8/21/87	13:40	14460	0	75	0.94	Lead - & Lead +	147.7	5.8	-	VHG + LA	80
8/21/87	14:50	14539	1	150	0.94	Lead - & Lead +	-	-	-	VHG + LA	160
8/21/87	15:30	14542	0	140	0.94	Lead - & Lead +	-	-	-	VHG + LA	149
8/21/87	15:47	14559	1	140	0.94	Lead - & Lead +	-	-	-	VHG + LA	149
8/21/87	15:48	14560	0	140	0.94	Lead - & Lead +	-	-	-	VHG + LA	149
8/21/87	15:52	14564	1	160	0.94	Lead - & Lead +	-	-	-	VHG + LA	170
8/21/87	15:54	14566	0	160	0.94	Lead - & Lead +	-	-	-	VHG + LA	170
8/21/87	15:55	14567	1	160	0.94	Lead - & Lead +	-	-	-	VHG + LA	170
1/15/88	14:08	14572	0	73	1.08	304SS & 30um & 0.5um with partial bypass on	351	9	-	VHG	68
1/15/88	14:34	14652	1	160	1.08	304SS & 30um & 0.5um	344	9.2	-	VHG	148
1/15/88	14:39	14657	0	160	1.08	304SS & 30um & 0.5um	344	9.2	-	VHG	148
1/15/88	14:54	14672	1	163	1.08	304SS & 30um & 0.5um	-	-	-	VHG	151
1/27/88	13:52	14682	0	61.6	1.04	304SS & 30um & 0.5um always in-line	277	10.5	-	VHG	59

1/27/88	15:04	14792	1	197	1.04	304SS & 30um & 0.5um always in-line	-	-	-	VHG	189
1/28/88	13:36	14803	0	62	1.04	304SS & 30um & 0.5um always in-line	274	12.1	-	VHG	60
1/28/88	14:23	14902	1	176	1.04	304SS & 30um & 0.5um always in-line	267	14.3	-	VHG	169
2/8/88	13:32	14906	0	85	1.03	430 SS & 30 um & 0.5 um filters always in-line	313	13.2	-	VHG	83
2/8/88	14:24	14998	1	182	1.03	430 SS & 30 um & 0.5 um filters always in-line	297	14.7	-	VHG	177
2/8/88	14:47	15006	0	153	1.03	430 SS & 30 um & 0.5 um filters always in-line	300	14	-	VHG	149
2/8/88	15:09	15048	1	200	1.03	430 SS & 30 um & 0.5 um filters always in-line	257	15.5	-	VHG	194
2/17/88	13:20	15066	0	75	1.03	430 SS & 30 um & 0.5 um filters always in-line	343	12	-	VHG	73
2/17/88	14:11	15171	1	180	1.03	430 SS & 30 um & 0.5 um filters always in-line	279	13.9	-	VHG	175
2/17/88	14:39	15176	0	152	1.03	430 SS & 30 um & 0.5 um filters always in-line	317	13.2	-	VHG	148
2/17/88	14:55	15210	1	186	1.03	430 SS & 30 um & 0.5 um filters always in-line	314	12.4	-	VHG	181
2/26/88	13:49	15216	0	85	1.03	W & 30 um & 0.5 um & charcoal filters	302	13.4	-	VHG	83

2/26/88	14:12	15285	1	158	1.03	W & 30 um & 0.5 um & charcoal filters	-	-	-	VHG	153
2/26/88	14:16	15286	0	155	1.03	W & 30 um & 0.5 um & charcoal filters	-	-	-	VHG	150
2/26/88	14:17	15287	1	155	1.03	W & 30 um & 0.5 um & charcoal filters	-	-	-	VHG	150
2/26/88	14:18	15288	0	155	1.03	W & 30 um & 0.5 um & charcoal filters	-	-	-	VHG	150
2/26/88	14:22	15296	1	166	1.03	W & 30 um & 0.5 um & charcoal filters	262	14.6	-	VHG	161
2/26/88	14:40	15306	0	131	1.03	W & 30 um & 0.5 um & charcoal filters	272	14.9	-	VHG	127
2/26/88	15:02	15359	1	187	1.03	W & 30 um & 0.5 um & charcoal filters	248	15.8	-	VHG	182
2/29/88	13:34	15366	0	66	1.03	W & 30 um & 0.5 um & no charcoal filters	302	13.4	-	VHG	64
2/29/88	14:10	15460	1	181	1.03	W & 30 um & 0.5 um & no charcoal filters	240	13.5	-	VHG	176
2/29/88	14:46	15466	0	150	1.03	W & 30 um & 0.5 um & no charcoal filters	306	12.8	-	VHG	146
2/29/88	15:04	15509	1	188	1.03	W & 30 um & 0.5 um & no charcoal filters	269	13.4	-	VHG	183
3/4/88	14:12	15518	0	88	1.01	Cu - Freshly bead-blasted, no filters	266	12.2	5	VHG & DD	87
3/4/88	14:35	15568	1	144	1.01	Cu - Freshly bead-blasted, no filters	-	-	5	VHG & DD	143

3/4/88	14:36	15569	0	144	1.01	Cu - Freshly bead-blasted, no filters	-	-	5	VHG & DD	143
3/4/88	14:39	15581	1	153	1.01	Cu - Freshly bead-blasted, no filters	-	-	5	VHG & DD	151
3/4/88	14:40	15582	0	153	1.01	Cu - Freshly bead-blasted, no filters	-	-	5	VHG & DD	151
3/4/88	14:49	15598	1	175	1.01	Cu - Freshly bead-blasted, no filters	239	17.3	5	VHG & DD	173
3/4/88	15:08	15608	0	120	1.01	Cu - Freshly bead-blasted, no filters	290	17.3	5	VHG & DD	119
3/4/88	15:32	15661	1	179	1.01	Cu - Freshly bead-blasted, no filters	-	-	5	VHG & DD	177
3/10/88	13:30	15678	0	83	1.01	Cu & Particulate filters only, no organic filters	264	17.1	11	VHG & DD	82
3/10/88	14:13	15774	1	186	1.01	Cu & Particulate filters only, no organic filters	-	-	11	VHG & DD	184
3/10/88	14:32	15788	0	166	1.01	Cu & Particulate filters only, no organic filters	-	-	11	VHG & DD	164
3/10/88	14:44	15812	1	190	1.01	Cu & Particulate filters only, no organic filters	-	-	11	VHG & DD	188
3/11/88	13:10	15828	0	87	1.01	Cu & All filters in (particulate and organic filters)	312	17.3	12	VHG & DD	86
3/11/88	13:57	15920	1	227	1.01	Cu & All filters in (particulate and organic filters)	-	-	12	VHG & DD	225
3/11/88	13:58	15922	0	227	1.01	Cu & All filters in (particulate and organic filters)	-	-	12	VHG & DD	225
3/11/88	13:59	15923	1	227	1.01	Cu & All filters in (particulate and organic filters)	-	-	12	VHG & DD	225

3/11/88	14:14	15938	0	181	1.01	Cu & All filters in (particulate and organic filters)	-	-	12	VHG & DD	179
3/11/88	14:24	15966	1	221	1.01	Cu & All filters in (particulate and organic filters)	234	14.4	12	VHG & DD	219
3/16/88	13:51	15978	0	88	1	5083 AI & no filters	273	11.64	2	VHG & DD	88
3/16/88	14:05	16018	1	135	1	5083 AI & no filters	-	-	2	VHG & DD	135
3/16/88	14:05	16022	0	135	1	5083 AI & no filters	-	-	2	VHG & DD	135
3/16/88	14:06	16023	1	135	1	5083 AI & no filters	-	-	2	VHG & DD	135
3/16/88	14:06	16024	0	135	1	5083 AI & no filters	-	-	2	VHG & DD	135
3/16/88	14:07	16026	1	135	1	5083 AI & no filters	-	-	2	VHG & DD	135
3/16/88	14:15	16038	0	113	1	5083 AI & no filters	247	11.7	2	VHG & DD	113
3/16/88	14:25	16070	1	147	1	5083 AI & no filters	-	-	2	VHG & DD	147
3/16/88	14:26	16071	0	147	1	5083 AI & no filters	-	-	2	VHG & DD	147
3/16/88	14:26	16072	1	147	1	5083 AI & no filters	271	11.7	2	VHG & DD	147
3/17/88	13:09	16088	0	86	1	5083 AI & 30 um & 0.5 um filters	268	12.75	3	VHG & DD	86
3/17/88	13:33	16154	1	150	1	5083 AI & 30 um & 0.5 um filters	-	-	3	VHG & DD	150
3/17/88	13:43	16168	0	133	1	5083 AI & 30 um & 0.5 um filters	259	11.5	3	VHG & DD	133
3/17/88	13:51	16188	1	153	1	5083 AI & 30 um & 0.5 um filters	-	-	3	VHG & DD	153
3/17/88	13:53	16194	0	153	1	5083 AI & 30 um & 0.5 um filters	-	-	3	VHG & DD	153
3/17/88	13:54	16195	1	153	1	5083 AI & 30 um & 0.5 um filters	259	11.84	3	VHG & DD	153

3/18/88	10:36	16208	0	78	1	5083 AI & all filters (30 um & 0.5 um filters & organic filters)	313	11.38	4	VHG & DD	78
3/18/88	10:50	16258	1	132	1	5083 AI & all filters (30 um & 0.5 um filters & organic filters)	-	-	4	VHG & DD	132
3/18/88	10:50	16259	0	132	1	5083 AI & all filters (30 um & 0.5 um filters & organic filters)	-	-	4	VHG & DD	132
3/18/88	10:51	16261	1	132	1	5083 AI & all filters (30 um & 0.5 um filters & organic filters)	-	-	4	VHG & DD	132
3/18/88	10:51	16262	0	132	1	5083 AI & all filters (30 um & 0.5 um filters & organic filters)	-	-	4	VHG & DD	132
3/18/88	10:52	16265	1	132	1	5083 AI & all filters (30 um & 0.5 um filters & organic filters)	-	-	4	VHG & DD	132
3/18/88	10:53	16272	0	143	1	5083 AI & all filters (30 um & 0.5 um filters & organic filters)	-	-	4	VHG & DD	143
3/18/88	10:54	16273	1	143	1	5083 AI & all filters (30 um & 0.5 um filters & organic filters)	288	11.4	4	VHG & DD	143
3/18/88	11:31	16288	0	115	1	5083 AI & all filters (30 um & 0.5 um filters & organic filters)	321	11.3	4	VHG & DD	115
3/18/88	11:36	16310	1	138	1	5083 AI & all filters (30 um & 0.5 um filters & organic filters)	-	-	4	VHG & DD	138

3/18/88	11:39	16319	0	148	1	5083 Al & all filters (30 um & 0.5 um filters & organic filters)	-	-	4	VHG & DD	148
3/18/88	11:40	16320	1	148	1	5083 Al & all filters (30 um & 0.5 um filters & organic filters)	-	-	4	VHG & DD	148
3/22/88	13:50	16338	0	82	1.03	Cu & all filters (30 um & 0.5 um filters & organic filters)	308	11.45	-	VHG & DD	80
3/22/88	14:15	16403	1	137	1.03	Cu & all filters (30 um & 0.5 um filters & organic filters) but lost vacuum here.	-	-	-	VHG & DD	133
3/23/88	13:23	16418	0	79	0.988	Cu & all filters (30 um & 0.5 um filters & organic filters)	338	10.32	-	VHG & DD	80
3/23/88	13:44	16484	1	155	0.988	Cu & all filters (30 um & 0.5 um filters & organic filters)	-	-	-	VHG & DD	157
3/23/88	14:00	16498	0	137	0.988	Cu & all filters (30 um & 0.5 um filters & organic filters)	312	10.51	-	VHG & DD	139
3/23/88	14:21	16551	1	196	0.988	Cu & all filters (30 um & 0.5 um filters & organic filters)	-	-	-	VHG & DD	198
3/23/88	14:49	16558	0	175	0.988	Cu & all filters (30 um & 0.5 um filters & organic filters)	306	11.75	-	VHG & DD	177
3/23/88	14:59	16578	1	201	0.988	Cu & all filters (30 um & 0.5 um filters & organic filters)	303	11.22	-	VHG & DD	203
3/29/88	12:15	16588	0	81	0.98	Cu & all filters (30 um & 0.5 um filters & organic filters)	337	10.73	-	VHG & DD	83

3/29/88	12:28	16646	1	146	0.98	Cu & all filters (30 um & 0.5 um filters & organic filters)	-	-	6	VHG & DD	149
3/29/88	12:35	16660	0	112	0.98	Cu & all filters (30 um & 0.5 um filters & organic filters)	-	-	6	VHG & DD	114
3/29/88	12:50	16717	1	170	0.98	Cu & all filters (30 um & 0.5 um filters & organic filters)	-	-	6	VHG & DD	173
3/29/88	12:56	16720	0	183	0.98	Cu & all filters (30 um & 0.5 um filters & organic filters)	-	-	6	VHG & DD	187
3/29/88	12:57	16721	1	183	0.98	Cu & all filters (30 um & 0.5 um filters & organic filters)	291	11.83	6	VHG & DD	187
3/31/88	13:36	16740	0	86	0.98	Cu & all filters (30 um & 0.5 um filters & organic filters)	325	11.7	8	VHG & DD	88
3/31/88	14:15	16828	1	182	0.98	Cu & all filters (30 um & 0.5 um filters & organic filters)	-	-	8	VHG & DD	186
3/31/88	14:15	16829	0	182	0.98	Cu & all filters (30 um & 0.5 um filters & organic filters)	-	-	8	VHG & DD	186
3/31/88	14:20	16830	1	192	0.98	Cu & all filters (30 um & 0.5 um filters & organic filters)	-	-	8	VHG & DD	196
3/31/88	14:21	16831	0	192	0.98	Cu & all filters (30 um & 0.5 um filters & organic filters)	-	-	8	VHG & DD	196
3/31/88	14:22	16832	1	192	0.98	Cu & all filters (30 um & 0.5 um filters & organic filters)	-	-	8	VHG & DD	196
3/31/88	14:26	16836	0	192	0.98	Cu & all filters (30 um & 0.5 um filters & organic filters)	-	-	8	VHG & DD	196

3/31/88	14:27	16837	1	192	0.98	Cu & all filters (30 um & 0.5 um filters & organic filters)	-	-	8	VHG & DD	196
3/31/88	14:28	16838	0	192	0.98	Cu & all filters (30 um & 0.5 um filters & organic filters)	-	-	8	VHG & DD	196
3/31/88	14:35	16849	1	206	0.98	Cu & all filters (30 um & 0.5 um filters & organic filters)	-	-	8	VHG & DD	210
3/31/88	14:45	16860	0	152	0.98	Cu & all filters (30 um & 0.5 um filters & organic filters)	271	13.02	8	VHG & DD	155
3/31/88	15:09	16907	1	199	0.98	Cu & all filters (30 um & 0.5 um filters & organic filters)	-	-	8	VHG & DD	203
4/5/88	13:53	16930	0	38	0.98	Cu & all filters (30 um & 0.5 um filters & organic filters)	340	10.74	13	VHG & DD	39
4/5/88	14:47	17021	1	171	0.98	Cu & all filters (30 um & 0.5 um filters & organic filters)	-	-	13	VHG & DD	174
4/5/88	14:47	17022	0	171	0.98	Cu & all filters (30 um & 0.5 um filters & organic filters)	-	-	13	VHG & DD	174
4/5/88	15:10	17056	1	208	0.98	Cu & all filters (30 um & 0.5 um filters & organic filters)	-	-	13	VHG & DD	212
4/5/88	15:30	17067	0	168	0.98	Cu & all filters (30 um & 0.5 um filters & organic filters)	304	-	13	VHG & DD	171
4/5/88	15:54	17111	1	202	0.98	Cu & all filters (30 um & 0.5 um filters & organic filters)	-	-	13	VHG & DD	206
4/6/88	12:50	17126	0	90	0.98	Cu & all filters (30 um & 0.5 um filters & organic filters)	324	11.65	14	VHG & DD	92

4/6/88	13:26	17221	1	180	0.98	Cu & all filters (30 um & 0.5 um filters & organic filters)	-	-	14	VHG & DD	184
4/6/88	13:53	17236	0	162	0.98	Cu & all filters (30 um & 0.5 um filters & organic filters)	291	12.1	14	VHG & DD	165
4/6/88	14:05	17268	1	189	0.98	Cu & all filters (30 um & 0.5 um filters & organic filters)	267	13.05	14	VHG & DD	193
4/7/88	13:28	17286	0	86	0.98	Cu & all filters (30 um & 0.5 um filters & organic filters)	314	11.69	15	VHG & DD	88
4/7/88	13:48	17361	1	177	0.98	Cu & all filters (30 um & 0.5 um filters & organic filters)	-	-	15	VHG & DD	181
4/7/88	13:59	17376	0	156	0.98	Cu & all filters (30 um & 0.5 um filters & organic filters)	323	10.45	15	VHG & DD	159
4/7/88	14:00	17383	1	156	0.98	Cu & all filters (30 um & 0.5 um filters & organic filters)	-	-	15	VHG & DD	159
4/7/88	14:01	17384	0	156	0.98	Cu & all filters (30 um & 0.5 um filters & organic filters)	-	-	15	VHG & DD	159
4/7/88	14:02	17387	1	167	0.98	Cu & all filters (30 um & 0.5 um filters & organic filters)	-	-	15	VHG & DD	170
4/7/88	14:02	17389	0	167	0.98	Cu & all filters (30 um & 0.5 um filters & organic filters)	-	-	15	VHG & DD	170
4/7/88	14:03	17390	1	167	0.98	Cu & all filters (30 um & 0.5 um filters & organic filters)	-	-	15	VHG & DD	170
4/7/88	14:03	17392	0	167	0.98	Cu & all filters (30 um & 0.5 um filters & organic filters)	-	-	15	VHG & DD	170

4/7/88	14:04	17393	1	167	0.98	Cu & all filters (30 um & 0.5 um filters & organic filters)	-	-	15	VHG & DD	170
4/7/88	14:04	17394	0	167	0.98	Cu & all filters (30 um & 0.5 um filters & organic filters)	-	-	15	VHG & DD	170
4/7/88	14:05	17395	1	167	0.98	Cu & all filters (30 um & 0.5 um filters & organic filters)	-	-	15	VHG & DD	170
4/8/88	13:15	17406	0	89	0.98	Cu & all filters (30 um & 0.5 um filters & organic filters)	360	10.25	16	VHG & DD	91
4/8/88	13:33	17472	1	163	0.98	Cu & all filters (30 um & 0.5 um filters & organic filters)	-	-	16	VHG & DD	166
4/8/88	13:37	17477	0	176	0.98	Cu & all filters (30 um & 0.5 um filters & organic filters)	-	-	16	VHG & DD	180
4/8/88	13:38	17479	1	176	0.98	Cu & all filters (30 um & 0.5 um filters & organic filters)	-	-	16	VHG & DD	180
4/8/88	13:38	17480	0	176	0.98	Cu & all filters (30 um & 0.5 um filters & organic filters)	-	-	16	VHG & DD	180
4/8/88	13:39	17483	1	176	0.98	Cu & all filters (30 um & 0.5 um filters & organic filters)	-	-	16	VHG & DD	180
4/8/88	13:48	17496	0	142	0.98	Cu & all filters (30 um & 0.5 um filters & organic filters)	301	11.75	16	VHG & DD	145
4/8/88	14:22	17590	1	195	0.98	Cu & all filters (30 um & 0.5 um filters & organic filters)	315	10.69	16	VHG & DD	199
4/14/88	13:43	17606	0	89	0.98	Cu & all filters (30 um & 0.5 um filters & organic filters)	329	11.22	22	VHG & DD	91

4/14/88	14:13	17704	1	221	0.98	Cu & all filters (30 um & 0.5 um filters & organic filters)	-	-	22	VHG & DD	226
4/14/88	14:26	17716	0	186	0.98	Cu & all filters (30 um & 0.5 um filters & organic filters)	322	10.74	22	VHG & DD	190
4/14/88	14:27	17718	1	186	0.98	Cu & all filters (30 um & 0.5 um filters & organic filters)	-	-	22	VHG & DD	190
4/14/88	14:29	17720	0	172	0.98	Cu & all filters (30 um & 0.5 um filters & organic filters)	-	-	22	VHG & DD	176
4/14/88	14:55	17788	1	226	0.98	Cu & all filters (30 um & 0.5 um filters & organic filters)	291	11.9	22	VHG & DD	231
4/15/88	13:24	17800	0	80	0.98	Cu & all filters (30 um & 0.5 um filters & organic filters)	325	11.63	23	VHG & DD	82
4/15/88	14:01	17902	1	214	0.98	Cu & all filters (30 um & 0.5 um filters & organic filters)	-	-	23	VHG & DD	218
4/15/88	14:16	17920	0	150	0.98	Cu & all filters (30 um & 0.5 um filters & organic filters)	265	13.59	23	VHG & DD	153
4/15/88	14:24	17936	1	168	0.98	Cu & all filters (30 um & 0.5 um filters & organic filters)	-	-	23	VHG & DD	171
4/15/88	14:25	17938	0	168	0.98	Cu & all filters (30 um & 0.5 um filters & organic filters)	-	-	23	VHG & DD	171
4/15/88	14:27	17942	1	185	0.98	Cu & all filters (30 um & 0.5 um filters & organic filters)	-	-	23	VHG & DD	189
4/15/88	14:41	17945	0	160	0.98	Cu & all filters (30 um & 0.5 um filters & organic filters)	-	-	23	VHG & DD	163

4/15/88	14:55	17982	1	198	0.98	Cu & all filters (30 um & 0.5 um filters & organic filters)	-	-	23	VHG & DD	202
4/19/88	13:21	17995	0	84	0.845	W & all filters (30 um & 0.5 um filters & organic filters)	312	10.83	1	VHG & DD	99
4/19/88	13:26	18016	1	91	0.845	W & all filters (30 um & 0.5 um filters & organic filters)	-	-	1	VHG & DD	108
4/19/88	13:57	18035	0	91	0.845	W & all filters (30 um & 0.5 um filters & organic filters)	310	-	1	VHG & DD	108
4/19/88	14:11	18084	1	121	0.845	W & all filters (30 um & 0.5 um filters & organic filters)	-	-	1	VHG & DD	143
4/19/88	16:23	18095	0	87	0.845	W & all filters (30 um & 0.5 um filters & organic filters)	360	10.9	1	VHG & DD & SB	103
4/19/88	17:08	18158	1	131	0.845	W & all filters (30 um & 0.5 um filters & organic filters)	333	10.4	1	VHG & DD & SB	155
4/19/88	17:52	18176	0	99	0.845	W & all filters (30 um & 0.5 um filters & organic filters)	-	-	1	VHG & DD & SB	117
4/19/88	18:10	18206	1	116	0.845	W & all filters (30 um & 0.5 um filters & organic filters)	-	-	1	VHG & DD & SB	137
4/19/88	18:11	18207	0	116	0.845	W & all filters (30 um & 0.5 um filters & organic filters)	-	-	1	VHG & DD & SB	137
4/19/88	18:12	18208	1	116	0.845	W & all filters (30 um & 0.5 um filters & organic filters)	-	330	1	VHG & DD & SB	137
4/19/88	18:13	18212	0	116	0.845	W & all filters (30 um & 0.5 um filters & organic filters)	-	-	1	VHG & DD & SB	137

4/19/88	18:17	18224	1	122	0.845	W & all filters (30 um & 0.5 um filters & organic filters)	-	-	1	VHG & DD & SB	144
4/19/88	18:23	18227	0	129	0.845	W & all filters (30 um & 0.5 um filters & organic filters)	-	-	1	VHG & DD & SB	153
4/19/88	18:39	18246	1	141	0.845	W & all filters (30 um & 0.5 um filters & organic filters)	-	-	1	VHG & DD & SB	167
4/19/88	18:47	18256	0	129	0.845	W & all filters (30 um & 0.5 um filters & organic filters)	296	12.3	1	VHG & DD & SB	153
4/19/88	18:48	18259	1	129	0.845	W & all filters (30 um & 0.5 um filters & organic filters)	296	12.3	1	VHG & DD & SB	153
4/19/88	23:17	18266	0	82	0.845	W & all filters (30 um & 0.5 um filters & organic filters)	360	10.7	1	VHG & DD & SB	97
4/19/88	23:35	18305	1	114	0.845	W & all filters (30 um & 0.5 um filters & organic filters)	-	-	1	VHG & DD & SB	135
4/19/88	23:42	18306	0	119	0.845	W & all filters (30 um & 0.5 um filters & organic filters)	-	-	1	VHG & DD & SB	141
4/19/88	23:44	18312	1	119	0.845	W & all filters (30 um & 0.5 um filters & organic filters)	-	-	1	VHG & DD & SB	141
4/19/88	23:45	18314	0	119	0.845	W & all filters (30 um & 0.5 um filters & organic filters)	-	-	1	VHG & DD & SB	141
4/19/88	23:54	18328	1	131	0.845	W & all filters (30 um & 0.5 um filters & organic filters)	-	-	1	VHG & DD & SB	155
4/20/88	0:22	18346	0	111	0.845	W & all filters (30 um & 0.5 um filters & organic filters)	401	8.6	2	VHG & DD & SB	131

4/20/88	0:48	18403	1	141	0.845	W & all filters (30 um & 0.5 um filters & organic filters)	325	10.6	2	VHG & DD & SB	167
4/20/88	10:54	18426	0	89	0.845	W & all filters (30 um & 0.5 um filters & organic filters)	340	11.55	2	VHG & DD	105
4/20/88	11:11	18468	1	139	0.845	W & all filters (30 um & 0.5 um filters & organic filters)	-	-	2	VHG & DD	164
4/20/88	11:29	18486	0	120	0.845	W & all filters (30 um & 0.5 um filters & organic filters)	285	12	2	VHG & DD	142
4/20/88	11:54	18546	1	163	0.845	W & all filters (30 um & 0.5 um filters & organic filters)	289	11.72	2	VHG & DD	193
4/21/88	13:14	18556	0	84	0.845	W & all filters (30 um & 0.5 um filters & organic filters)	342	11.17	3	VHG & DD	99
4/21/88	13:29	18598	1	145	0.845	W & all filters (30 um & 0.5 um filters & organic filters)	-	-	3	VHG & DD	172
4/21/88	13:34	18612	0	150	0.845	W & all filters (30 um & 0.5 um filters & organic filters)	-	-	3	VHG & DD	178
4/21/88	13:35	18613	1	150	0.845	W & all filters (30 um & 0.5 um filters & organic filters)	-	-	3	VHG & DD	178
4/21/88	13:42	18626	0	121	0.845	W & all filters (30 um & 0.5 um filters & organic filters)	300	-	3	VHG & DD	143
4/21/88	13:46	18645	1	131	0.845	W & all filters (30 um & 0.5 um filters & organic filters)	-	-	3	VHG & DD	155
4/21/88	13:47	18646	0	133	0.845	W & all filters (30 um & 0.5 um filters & organic filters)	-	-	3	VHG & DD	157

4/21/88	13:49	18659	1	138	0.845	W & all filters (30 um & 0.5 um filters & organic filters)	-	-	3	VHG & DD	163
4/21/88	13:50	18661	0	138	0.845	W & all filters (30 um & 0.5 um filters & organic filters)	-	-	3	VHG & DD	163
4/21/88	13:51	18663	1	138	0.845	W & all filters (30 um & 0.5 um filters & organic filters)	-	-	3	VHG & DD	163
4/27/88	13:36	18676	0	72	0.96	Graphite	344	11.66	-	VHG & DD	75
4/27/88	13:40	18695	1	86	0.96	Graphite	-	-	-	VHG & DD	90
4/27/88	13:41	18696	0	89	0.96	Graphite	-	-	-	VHG & DD	93
4/27/88	13:44	18707	1	92	0.96	Graphite	-	-	-	VHG & DD	96
4/27/88	13:45	18720	0	102	0.96	Graphite	-	-	-	VHG & DD	106
4/27/88	13:47	18724	1	102	0.96	Graphite	-	-	-	VHG & DD	106
4/27/88	13:48	18726	0	105	0.96	Graphite	-	-	-	VHG & DD	109
4/27/88	13:49	18729	1	105	0.96	Graphite	-	-	-	VHG & DD	109
4/27/88	13:51	18736	0	112	0.96	Graphite	-	-	-	VHG & DD	117
4/27/88	13:52	18737	1	112	0.96	Graphite	-	-	-	VHG & DD	117
4/27/88	13:54	18743	0	112	0.96	Graphite	-	-	-	VHG & DD	117
4/27/88	14:05	18748	1	115	0.96	Graphite	-	-	-	VHG & DD	120
4/27/88	14:13	18766	0	78	0.96	Graphite	276	-	-	VHG & DD	81
4/27/88	14:19	18800	1	106	0.96	Graphite	-	-	-	VHG & DD	110
4/27/88	14:19	18801	0	106	0.96	Graphite	-	-	-	VHG & DD	110
4/27/88	14:20	18802	1	106	0.96	Graphite	-	-	-	VHG & DD	110
4/27/88	14:23	18815	0	115	0.96	Graphite	-	-	-	VHG & DD	120
4/27/88	14:24	18816	1	142	0.96	Graphite	-	-	-	VHG & DD	148

4/27/88	14:25	18823	0	142	0.96	Graphite	-	-	-	VHG & DD	148
4/27/88	14:26	18824	1	142	0.96	Graphite	-	-	-	VHG & DD	148
4/27/88	14:27	18825	0	142	0.96	Graphite	-	-	-	VHG & DD	148
4/27/88	14:28	18827	1	148	0.96	Graphite	-	-	-	VHG & DD	154
4/27/88	14:29	18830	0	148	0.96	Graphite	-	-	-	VHG & DD	154
4/27/88	14:30	18831	1	148	0.96	Graphite	-	-	-	VHG & DD	154
6/6/88	13:25	18846	0	90	0.96	Graphite	320	11.96	-	VHG & DD	94
6/6/88	13:39	18886	1	137	0.96	Graphite	-	-	-	VHG & DD	143
6/6/88	13:40	18893	0	137	0.96	Graphite	-	-	-	VHG & DD	143
6/6/88	13:42	18896	1	153	0.96	Graphite	-	-	-	VHG & DD	159
6/6/88	13:43	18901	0	153	0.96	Graphite	-	-	-	VHG & DD	159
6/6/88	13:44	18902	1	153	0.96	Graphite	-	-	-	VHG & DD	159
6/6/88	13:44	18903	0	153	0.96	Graphite	-	-	-	VHG & DD	159
6/6/88	13:45	18904	1	153	0.96	Graphite	-	-	-	VHG & DD	159
6/6/88	14:00	18916	0	118	0.96	Graphite	290	12.65	-	VHG & DD	123
6/6/88	14:06	18939	1	140	0.96	Graphite	-	-	-	VHG & DD	146
6/6/88	14:07	18945	0	140	0.96	Graphite	-	-	-	VHG & DD	146
6/6/88	14:09	18946	1	153	0.96	Graphite	-	-	-	VHG & DD	159
6/6/88	14:09	18948	0	153	0.96	Graphite	-	-	-	VHG & DD	159
6/6/88	14:10	18949	1	153	0.96	Graphite	-	-	-	VHG & DD	159
6/6/88	14:10	18951	0	153	0.96	Graphite	-	-	-	VHG & DD	159
6/6/88	14:11	18952	1	153	0.96	Graphite	-	-	-	VHG & DD	159
6/6/88	14:12	18953	0	153	0.96	Graphite	-	-	-	VHG & DD	159
6/6/88	14:13	18956	1	166	0.96	Graphite	-	-	-	VHG & DD	173

6/9/88	13:17	18966	0	83	0.99	W	338	11.86	2	VHG & DD	84
6/9/88	13:29	19012	1	137	0.99	W	-	-	2	VHG & DD	138
6/9/88	13:31	19015	0	137	0.99	W	-	-	2	VHG & DD	138
6/9/88	13:32	19016	1	153	0.99	W	-	-	2	VHG & DD	155
6/9/88	13:33	19021	0	153	0.99	W	-	-	2	VHG & DD	155
6/9/88	13:34	19023	1	153	0.99	W	-	-	2	VHG & DD	155
6/9/88	14:53	19036	0	120	0.99	W	304	12.97	2	VHG & DD	121
6/9/88	15:02	19066	1	157	0.99	W	308	-	2	VHG & DD	159
6/10/88	11:13	19076	0	92	0.99	W	310	11.95	3	VHG & DD	93
6/10/88	11:30	19129	1	157	0.99	W	-	-	3	VHG & DD	159
6/10/88	11:47	19146	0	132	0.99	W	307	11.46	3	VHG & DD	133
6/10/88	11:50	19155	1	132	0.99	W	296	12.43	3	VHG & DD	133
6/22/88	13:12	19256	0	83	1	316 SS	363	11.2	-	VHG & SG	83
6/22/88	13:46	19335	1	178	1	316 SS	-	-	-	VHG & SG	178
6/22/88	14:17	19346	0	165	1	316 SS	-	-	-	VHG & SG	165
6/22/88	14:23	19356	1	182	1	316 SS	-	-	-	VHG & SG	182
6/28/88	13:26	19366	0	73	1	W	357	11.7	5	VHG & KC	73
6/28/88	13:50	19431	1	163	1	W	302	12.9	5	VHG & KC	163
6/29/88	13:22	19455	0	72	1	W	175	23.71	6	VHG & DD	72
6/29/88	14:15	19576	1	186	1	W	-	-	6	VHG & DD	186
6/30/88	14:06	19605	0	86	1	W	112	23.3	7	VHG & KC	86
6/30/88	14:59	19728	1	193	1	W	-	-	7	VHG & KC	193
7/7/88	13:13	19739	0	92	1	W	341	12.05	14	VHG & KC	92
7/7/88	13:43	19811	1	179	1	W	-	-	14	VHG & KC	179

7/7/88	13:44	19812	0	179	1	W	-	-	14	VHG & KC	179
7/7/88	14:00	19832	1	190	1	W	307	12.03	14	VHG & KC	190
7/7/88	14:21	19844	0	154	1	W	-	-	14	VHG & KC	154
7/7/88	14:22	19850	1	154	1	W	-	-	14	VHG & KC	154
7/7/88	14:23	19851	0	154	1	W	-	-	14	VHG & KC	154
7/7/88	14:24	19854	1	154	1	W	-	-	14	VHG & KC	154
7/13/88	13:38	19855	0	95	1	W	329	12.4	20	VHG & KC	95
7/13/88	14:21	19951	1	212	1	W	279	13.3	20	VHG & KC	212
7/13/88	14:46	19965	0	122	1	W	316	12.7	20	VHG & KC	122
7/13/88	15:13	20024	1	186	1	W	319	11.6	20	VHG & KC	186
8/4/88	14:25	20025	0	93	1	W	354	11.3	42	TB	93
8/4/88	14:47	20076	1	162	1	W	354	11.3	42	TB	162
8/4/88	15:10	20095	0	132	1	W	317	12.6	42	TB	132
8/4/88	15:30	20132	1	173	1	W	286	13.3	42	TB	173
8/18/88	13:35	20165	0	130	1	W	375	11.1	56	TB	130
8/18/88	13:46	20187	1	156.7	1	W	375	11.1	56	TB	156.7
8/18/88	14:38	20205	0	130	1	W	323	12.2	56	TB	130
8/18/88	15:00	20259	1	206.8	1	W	323	12.2	56	TB	206.8
8/24/88	13:30	20265	0	90	1	W	368	-	62	TB	90
8/24/88	13:53	20320	1	153.4	1	W	368	-	62	TB	153.4
8/24/88	14:50	20355	0	153.4	1	W	368	-	62	TB	153.4
8/24/88	15:00	20383	1	178.4	1	W	368	-	62	TB	178.4
9/3/88	13:55	20386	0	90	1	W	386	10.8	9	TB	90
9/3/88	14:09	20406	1	113.4	1	W	386	10.8	9	TB	113.4
9/22/88	13:40	20516	0	90	1	Cu	206	11.3	7	TB	90
9/22/88	13:53	20547	1	123.4	1	Cu	206	11.3	7	TB	123.4
9/22/88	14:10	20556	0	123.4	1	Cu	206	11.3	7	TB	123.4
9/22/88	14:12	20573	1	133.4	1	Cu	206	11.3	7	TB	133.4
9/28/88	14:05	20596	0	86.7	1	Cu	321	11.5	13	TB	86.7
9/28/88	14:32	20656	1	160.8	1	Cu	321	11.5	13	TB	160.8
9/28/88	14:58	20666	0	126.7	1	Cu	321	11.5	13	TB	126.7
9/28/88	15:12	20696	1	156.7	1	Cu	321	11.5	13	TB	156.7
10/6/88	12:36	20706	0	89.29	1	Cu	387	10.5	21	BZH	89.29
10/6/88	12:57	20763	1	164.29	1	Cu	387	10.5	21	BZH	164.29
10/6/88	13:45	20776	0	128.57	1	Cu	349	10.4	21	BZH	128.57
10/6/88	14:00	20906	1	164.29	1	Cu	345	10.4	21	BZH	164.29

10/14/88	12:48	20926	0	86.21	1	Cu	333	10.9	27	BZH	86.21
10/14/88	13:09	20967	1	134.49	1	Cu	315	11.4	27	BZH	134.49
10/14/88	13:45	20976	0	137.94	1	Cu	315	11.4	27	BZH	137.94
10/14/88	13:50	20991	1	148.29	1	Cu	315	11.4	27	BZH	148.29
10/14/88	14:46	20996	0	127.59	1	Cu	300	12.3	27	BZH	127.59
10/14/88	15:11	21036	1	172.43	1	Cu	277	-	27	BZH	172.43
10/19/88	12:57	21046	0	93.11	1	Cu	269	11.6	2	BZH	93.11
10/19/88	13:10	21087	1	144.84	1	Cu	269	11.6	2	BZH	144.84
10/19/88	13:56	21096	0	131.04	1	Cu	274	-	2	BZH	131.04
10/19/88	14:00	21112	1	144.84	1	Cu	274	-	2	BZH	144.84
10/19/88	14:37	21116	0	117.25	1	Cu	271	-	2	BZH	117.25
10/19/88	14:39	21126	1	131.04	1	Cu	271	-	2	BZH	131.04
10/19/88	14:39	21127	0	131.04	1	Cu	271	-	2	BZH	131.04
10/19/88	14:44	21142	1	144.84	1	Cu	271	-	2	BZH	144.84
10/20/88	12:43	21146	0	89.66	1	Cu	306	11.8	3	BZH	89.66
10/20/88	13:09	21209	1	165.53	1	Cu	306	11.8	3	BZH	165.53
10/20/88	14:02	21216	0	127.59	1	Cu	279	13.4	3	BZH	127.59
10/20/88	14:20	21260	1	179.32	1	Cu	279	13.4	3	BZH	179.32
10/20/88	14:46	21266	0	141.39	1	Cu	300	-	3	BZH	141.39
10/20/88	15:03	21299	1	179.32	1	Cu	300	-	3	BZH	179.32
10/26/88	12:49	21306	0	89.66	1	Cu	327	12.8	9	BZH	89.66
10/26/88	13:13	21358	1	151.73	1	Cu	306	-	9	BZH	151.73
10/26/88	13:40	21366	0	127.59	1	Cu	332	12.5	9	BZH	127.59
10/26/88	13:54	21402	1	165.53	1	Cu	309	-	9	BZH	165.53
10/26/88	14:25	21406	0	131.04	1	Cu	330	12.6	9	BZH	131.04
10/26/88	14:48	21453	1	179.32	1	Cu	330	12.6	9	BZH	179.32
10/27/88	12:40	21456	0	100	1	Cu	324	12.2	10	BZH	100
10/27/88	13:24	21526	1	189.29	1	Cu	296	11.9	10	BZH	189.29
10/27/88	14:18	21531	0	146.43	1	Cu	317	12.5	10	BZH	146.43
10/27/88	14:34	21566	1	185.72	1	Cu	316	11.7	10	BZH	185.72
10/27/88	14:48	21571	0	157.15	1	Cu	328	11.7	10	BZH	157.15
10/27/88	15:07	21604	1	192.86	1	Cu	302	12.8	10	BZH	192.86
11/2/88	12:42	21611	0	103.46	1	Cu	310	11.8	16	BZH	103.46
11/2/88	13:21	21673	1	179.32	1	Cu	289	11.1	16	BZH	179.32
11/2/88	14:17	21676	0	144.84	1	Cu	301	12	16	BZH	144.84
11/2/88	14:31	21712	1	179.32	1	Cu	286	12	16	BZH	179.32
11/2/88	14:52	21716	0	144.84	1	Cu	295	11.7	16	BZH	144.84
11/2/88	15:04	21750	1	179.32	1	Cu	299	11.4	16	BZH	179.32
11/3/88	12:58	21756	0	106.67	1	Cu	319	9.8	17	BZH	106.67
11/3/88	13:25	21821	1	176.68	1	Cu	324	10.4	17	BZH	176.68
11/3/88	13:34	21826	0	140.01	1	Cu	-	9.8	17	BZH	140.01
11/3/88	14:00	21866	1	186.68	1	Cu	332	9.7	17	BZH	186.68
11/3/88	14:27	21876	0	140.01	1	Cu	333	9.8	17	BZH	140.01
11/3/88	14:42	21908	1	176.68	1	Cu	-	-	17	BZH	176.68

11/3/88	14:52	21926	0	143.34	1	Cu	-	-	17	BZH	143.34
11/3/88	15:00	21948	1	166.68	1	Cu	294	10.2	17	BZH	166.68
11/16/88	12:38	21966	0	103.7	1	Cu	552	4.1	7	BZH	103.7
11/16/88	12:58	22005	1	140.73	1	Cu	513	4.6	7	BZH	140.73
11/16/88	13:03	22006	0	118.51	1	Cu	-	-	7	BZH	118.51
11/16/88	13:16	22036	1	155.55	1	Cu	511	4.8	7	BZH	155.55
11/16/88	13:26	22041	0	118.51	1	Cu	-	-	7	BZH	118.51
11/16/88	13:39	22076	1	155.55	1	Cu	483	4.9	7	BZH	155.55
11/16/88	14:18	22081	0	118.51	1	Cu	576	4.9	7	BZH	118.51
11/16/88	14:38	22121	1	170.36	1	Cu	486	4.8	7	BZH	170.36
11/16/88	14:45	22126	0	103.7	1	Cu	-	-	7	BZH	103.7
11/16/88	14:49	22139	1	144.44	1	Cu	-	-	7	BZH	144.44
11/16/88	14:52	22141	0	122.22	1	Cu	-	-	7	BZH	122.22
11/16/88	15:10	22181	1	170.36	1	Cu	450	4.9	7	BZH	170.36
11/17/88	12:50	21186	0	103.7	1	Cu	342	11.4	8	BZH	103.7
11/17/88	13:21	21249	1	177.77	1	Cu	298	10.9	8	BZH	177.77
11/17/88	13:36	21256	0	118.51	1	Cu	317	11.8	8	BZH	118.51
11/17/88	14:08	21311	1	177.77	1	Cu	297	12	8	BZH	177.77
2/1/89	13:26	21336	0	92.31	1	Cu	260	12	10	BZH	92.31
2/1/89	13:54	21377	1	149.99	1	Cu	274	-	10	BZH	149.99
2/1/89	14:03	21391	0	111.53	1	Cu	-	-	10	BZH	111.53
2/1/89	14:40	21452	1	192.3	1	Cu	274	12.1	10	BZH	192.3
2/3/89	14:04	21466	0	92.31	1	Cu	244	11.6	12	BZH	92.31
2/3/89	14:45	21559	1	192.31	1	Cu	225	12.7	12	BZH	192.31
2/7/89	14:16	21566	0	92.31	1	Cu	253	11.9	16	BZH	92.31
2/7/89	14:44	21636	1	173.08	1	Cu	250	11.9	16	BZH	173.08
2/8/89	12:14	21646	0	73.08	1	Cu	358	11	17	BZH	73.08
2/8/89	12:56	21729	1	184.62	1	Cu	176	11.6	17	BZH	184.62
2/9/89	12:35	21776	0	95.83	1	Cu	295	11	18	BZH	95.83
2/9/89	13:16	21860	1	200	1	Cu	247	11.7	18	BZH	200
2/9/89	13:28	21866	0	108.33	1	Cu	256	-	18	BZH	108.33
2/9/89	14:06	21929	1	216.67	1	Cu	249	11.6	18	BZH	216.67
2/9/89	14:25	21946	0	166.67	1	Cu	249	11.6	18	BZH	166.67
2/9/89	14:35	21967	1	191.67	1	Cu	245	11.6	18	BZH	191.67
2/14/89	13:00	21971	0	96.3	1	Cu	280	12.1	23	BZH	96.3
2/14/89	13:30	22046	1	181.48	1	Cu	260	12.9	23	BZH	181.48
2/14/89	13:52	22051	0	122.22	1	Cu	277	12.8	23	BZH	122.22
2/14/89	14:32	22112	1	183.33	1	Cu	250	13.4	23	BZH	183.33
2/14/89	14:50	22121	0	148.15	1	Cu	251	13.5	23	BZH	148.15
2/14/89	15:02	22154	1	181.48	1	Cu	255	12.4	23	BZH	181.48
3/29/89	12:41	22206	0	93.33	1	Ni	280	11.5	7	BZH	93.33
3/29/89	13:14	22272	1	166.67	1	Ni	239	11.7	7	BZH	166.67
3/29/89	13:43	22276	0	131.67	1	Ni	264	11.9	7	BZH	131.67
3/29/89	14:21	22297	1	153.33	1	Ni	264	11.9	7	BZH	153.33

3/29/89	14:22	22299	0	153.33	1	Ni	264	11.9	7	BZH	153.33
3/29/89	14:32	22318	1	166.67	1	Ni	238	11.8	7	BZH	166.67
3/29/89	14:53	22321	0	143.33	1	Ni	260	11.8	7	BZH	143.33
3/29/89	15:00	22337	1	153.33	1	Ni	254	12	7	BZH	153.33
3/30/89	12:47	22341	0	96.3	1	Ni	318	11.5	8	BZH	96.3
3/30/89	13:49	22404	1	174.07	1	Ni	310	11.8	8	BZH	174.07
3/30/89	14:10	22411	0	135.19	1	Ni	315	11.7	8	BZH	135.19
3/30/89	14:33	22447	1	170.37	1	Ni	320	11.9	8	BZH	170.37
3/30/89	14:45	22451	0	144.44	1	Ni	320	11.9	8	BZH	144.44
3/30/89	15:03	22485	1	183.33	1	Ni	296	12.4	8	BZH	183.33
4/5/89	13:50	22486	0	104	1	Ni	314	10.6	14	TLB	104
4/5/89	14:30	22582	1	204	1	Ni	263	11.1	14	TLB	204
4/5/89	14:45	22586	0	119	1	Ni	272	11.1	14	TLB	119
4/5/89	15:08	22646	1	196	1	Ni	258	11.1	14	TLB	196
4/6/89	13:30	22656	0	108	1	Ni	276	11	15	TLB	108
4/6/89	14:06	22720	1	203	1	Ni	249	10	15	TLB	203
4/6/89	14:30	22716	0	141	1	Ni	260	10.4	15	TLB	141
4/6/89	14:50	22782	1	216	1	Ni	231	11.6	15	TLB	216
4/11/89	12:58	22786	0	85.11	1	Ni	237	11.4	20	BZH	85.11
4/11/89	13:26	22856	1	210.64	1	Ni	216	11.5	20	BZH	210.64
4/11/89	14:03	22861	0	148.94	1	Ni	240	11.4	20	BZH	148.94
4/11/89	14:24	22920	1	221.28	1	Ni	226	11	20	BZH	221.28
4/12/89	12:47	22931	0	87.5	1	Ni	349	11.5	21	BZH	87.5
4/12/89	13:36	23028	1	212.5	1	Ni	261	11.5	21	BZH	212.5
4/12/89	14:24	23031	0	137.5	1	Ni	276	11.8	21	BZH	137.5
4/12/89	14:56	23104	1	212.5	1	Ni	265	11.8	21	BZH	212.5
4/13/89	12:58	21006	0	100	1	Ni	319	10.6	22	BZH	100
4/13/89	13:39	21097	1	202.08	1	Ni	307	11.2	22	BZH	202.08
4/13/89	13:43	21201	0	127.08	1	Ni	-	-	22	BZH	127.08
4/13/89	14:38	21281	1	206.25	1	Ni	286	11.6	22	BZH	206.25
4/18/89	12:50	21286	0	98.15	1	Ni	309	10.8	27	BZH	98.15
4/18/89	13:16	21330	1	155.56	1	Ni	301	11	27	BZH	155.56
4/18/89	13:28	21331	0	127.78	1	Ni	301	11	27	BZH	127.78
4/18/89	14:00	21405	1	200	1	Ni	264	10.5	27	BZH	200
4/18/89	14:32	21416	0	137.04	1	Ni	338	10.5	27	BZH	137.04
4/18/89	14:56	21475	1	198.15	1	Ni	251	10.7	27	BZH	198.15
4/19/89	13:22	21475	0	104	1	Ni	288	10.3	28	BZH	104
4/19/89	14:10	21572	1	204	1	Ni	222	11.3	28	BZH	204
4/19/89	14:30	21576	0	138	1	Ni	250	11.2	28	BZH	138
4/19/89	14:56	21637	1	204	1	Ni	240	11.5	28	BZH	204
4/20/89	13:07	21641	0	104	1	Ni	270	11.5	29	BZH	104
4/20/89	14:06	21742	1	210	1	Ni	196	11.8	29	BZH	210
4/20/89	14:45	21746	0	136	1	Ni	258	11.8	29	BZH	136
4/20/89	15:12	21809	1	198	1	Ni	171	11.7	29	BZH	198

5/2/89	13:00	21811	0	101.85	1	Ag/Brass	311	11.4	12	BZH	101.85
5/2/89	13:12	21842	1	137.04	1	Ag/Brass	318	11.2	12	BZH	137.04
5/2/89	13:27	21246	0	103.7	1	Ag/Brass	323	11.4	12	BZH	103.7
5/2/89	14:26	21256	1	116.67	1	Ag/Brass	310	11	12	BZH	116.67
5/2/89	14:26	21257	0	116.67	1	Ag/Brass	310	11	12	BZH	116.67
5/2/89	14:48	21312	1	185.19	1	Ag/Brass	298	11.7	12	BZH	185.19
5/3/89	12:48	21316	0	88	1	Ag/Brass	274	10.4	13	BZH	88
5/3/89	13:13	21356	1	144	1	Ag/Brass	236	11.3	13	BZH	144
5/3/89	13:46	21366	0	104	1	Ag/Brass	305	11	13	BZH	104
5/3/89	14:01	21408	1	160	1	Ag/Brass	282	10.1	13	BZH	160
5/3/89	14:25	21411	0	106	1	Ag/Brass	313	10.8	13	BZH	106
5/3/89	14:51	21479	1	174	1	Ag/Brass	278	11.6	13	BZH	174
5/4/89	12:41	21481	0	90.2	1	Ag/Brass	195	11.5	14	BZH	90.2
5/4/89	13:16	21571	1	188.24	1	Ag/Brass	181	11.4	14	BZH	188.24
5/4/89	14:12	21576	0	109.8	1	Ag/Brass	241	13.2	14	BZH	109.8
5/4/89	14:59	21681	1	198.04	1	Ag/Brass	230	13.9	14	BZH	198.04
5/9/89	12:52	21686	0	98	1	Ag/Brass	326	10.7	19	BZH	98
5/9/89	13:43	21794	1	208	1	Ag/Brass	294	10.7	19	BZH	208
5/9/89	14:01	21796	0	116	1	Ag/Brass	302	10.1	19	BZH	116
5/9/89	14:13	21826	1	160	1	Ag/Brass	302	10.8	19	BZH	160
5/9/89	14:21	21831	0	104	1	Ag/Brass	307	11	19	BZH	104
5/9/89	14:50	21915	1	198	1	Ag/Brass	288	11	19	BZH	198
5/10/89	13:37	21921	0	96.15	1	Ag/Brass	262	10.8	20	BZH	96.15
5/10/89	14:22	22050	1	207.69	1	Ag/Brass	240	10.5	20	BZH	207.69
5/10/89	14:32	22051	0	134.62	1	Ag/Brass	241	10.8	20	BZH	134.62
5/10/89	14:56	22118	1	196.15	1	Ag/Brass	231	10.7	20	BZH	196.15
5/11/89	13:12	22121	0	98	1	Ag/Brass	240	10.9	21	BZH	98
5/11/89	13:51	22219	1	192	1	Ag/Brass	205	10.9	21	BZH	192
5/11/89	14:22	22221	0	108	1	Ag/Brass	230	11	21	BZH	108
5/11/89	15:16	22364	1	228	1	Ag/Brass	202	11.6	21	BZH	228
5/16/89	12:51	22366	0	98.04	1	Ag/Brass	268	10.4	26	BZH	98.04
5/16/89	13:34	22489	1	211.76	1	Ag/Brass	228	11.3	26	BZH	211.76
5/16/89	14:02	22491	0	98.04	1	Ag/Brass	273	9.8	26	BZH	98.04
5/16/89	15:06	22652	1	235.29	1	Ag/Brass	231	11.1	26	BZH	235.29
5/17/89	12:53	21654	0	101.96	1	Ag/Brass	250	10.5	27	BZH	101.96
5/17/89	13:46	21787	1	221.57	1	Ag/Brass	239	10.4	27	BZH	221.57
5/17/89	14:08	21788	0	101.96	1	Ag/Brass	247	11	27	BZH	101.96
5/17/89	14:47	21899	1	192.16	1	Ag/Brass	219	11	27	BZH	192.16
5/18/89	14:17	21901	0	90.91	1	Ag/Brass	201	13.6	28	BZH	90.91
5/18/89	15:03	22037	1	198.18	1	Ag/Brass	187	14.5	28	BZH	198.18
5/23/89	13:14	22038	0	94.23	1	Ag/Brass	265	10.1	33	BZH	94.23
5/23/89	13:39	22102	1	171.15	1	Ag/Brass	221	10.6	33	BZH	171.15
5/23/89	14:02	22103	0	96.15	1	Ag/Brass	243	10.4	33	BZH	96.15
5/23/89	15:04	22244	1	219.23	1	Ag/Brass	213	11.6	33	BZH	219.23

5/24/89	12:56	22246	0	88.68	1	Ag/Brass	226	9	34	BZH	88.68
5/24/89	13:40	22346	1	186.79	1	Ag/Brass	214	10.4	34	BZH	186.79
5/24/89	14:10	22348	0	94.34	1	Ag/Brass	232	10.5	34	BZH	94.34
5/24/89	15:13	22511	1	228.3	1	Ag/Brass	213	10.7	34	BZH	228.3
5/25/89	12:55	22512	0	98.11	1	Ag/Brass	213	10.1	35	BZH	98.11
5/25/89	13:45	22651	1	216.98	1	Ag/Brass	173	11.6	35	BZH	216.98
5/25/89	14:09	22652	0	94.34	1	Ag/Brass	184	12.4	35	BZH	94.34
5/25/89	14:54	22773	1	207.55	1	Ag/Brass	163	14.8	35	BZH	207.55
10/18/89	13:45	22805	0	84	1	Ni	352	12	-	VHG	84
10/18/89	14:16	22870	1	163	1	Ni	369	11.4	-	VHG	163
11/2/89	13:10	22902	0	85	1.01	304 SS	360	11.7	-	VHG	84
11/2/89	13:34	22989	1	191	1.01	304 SS	368	11.4	-	VHG	189
11/2/89	14:27	22992	0	141	1.01	304 SS	368	11.4	-	VHG	140
11/2/89	14:40	23039	1	191	1.01	304 SS	368	11.4	-	VHG	189
11/14/89	14:25	23063	0	84	1.01	304 SS	315	13.9	-	VHG	83
11/14/89	14:53	23156	1	192	1.01	304 SS	329	13.3	-	VHG	190
11/14/89	15:03	23163	0	155	1.01	304 SS	329	13.3	-	VHG	153
11/14/89	15:11	23196	1	190	1.01	304 SS	329	13.3	-	VHG	188
11/16/89	14:11	23203	0	81	1.01	304 SS	331	13.3	-	VHG	80
11/16/89	14:37	23295	1	195	1.01	304 SS	344	12.7	-	VHG	193
11/16/89	14:48	23304	0	157	1.01	304 SS	347	12.6	-	VHG	155
11/16/89	14:54	23326	1	171	1.01	304 SS	347	12.6	-	VHG	169
11/27/89	13:46	23356	0	87	1.01	304 SS	412	18.2	-	VHG	86
11/27/89	14:08	23441	1	203	1.01	304SS	423	9.7	-	VHG	201
11/27/89	14:19	23446	0	154	1.01	304 SS	423	9.7	-	VHG	152
11/27/89	14:27	23476	1	190	1.01	304 SS	423	9.7	-	VHG	188

Vita

Victor Herbert Gehman, Jr. was born March 24, 1955 in Lancaster, Pennsylvania. He was raised there, attending St. Anthony's Parochial School and then Lancaster Catholic High School. He attended Virginia Tech in 1973. While still an undergraduate, he worked in the Neutron Activation Analysis Laboratory in Robeson Hall, eventually earning a Nuclear Regulatory Commission license to operate the nuclear reactor at Virginia Tech. He graduated from Virginia Tech in 1977 with a B.S. in Physics. While earning the B.S., he met, became engaged and married Sharon Todd. They then started a family and had five children: starting with Victor Michael in 1977, then Thomas Todd in 1979, Matthew Jonathan in 1982, James Robert in 1985, and Molly Elizabeth in 1988. He transferred to the Materials Science Department and earned an M.S. in Materials Engineering in 1979 working on nucleation and growth of titanium thin films on single-crystal silicon. In October 1979, he accepted a position at the Naval Surface Weapons Center in Dahlgren, Virginia, which later became the Naval Surface Warfare Center, Dahlgren Division (NSWCDD). While employed at Dahlgren, he earned another M.S., this time in Physics, from Virginia Tech in 1987, and started to pursue (also while employed full time) a Ph.D. degree in Physics, again at Virginia Tech, on the impulse electrical breakdown of high-purity water. After graduation in 1995, he will continue with his duties at NSWCDD.